COLD FLOW PERFORMANCE OF A RAMJET ENGINE

A Thesis

Presented to

the Faculty of California Polytechnic State University

San Luis Obispo

In Partial Fulfillment

of the Requirements for the Degree

Master of Science in Aerospace Engineering

by

Harrison G. Sykes

December 2014

COMMITTEE MEMBERSHIP

TITLE:	Cold Flow Performance of a Ramjet Engine
AUTHOR:	Harrison G. Sykes
DATE SUBMITTED:	December 2014
COMMITTEE CHAIR:	Eric Mehiel, Ph.D. Associate Professor Aerospace Engineering Department
COMMITTEE MEMBER:	Patrick Lemieux, Ph.D. Associate Professor, Mechanical Engineering Department
COMMITTEE MEMBER:	Daniel J. Wait, M.S. Systems Engineer, Tyvak Nano-Satelite Systems LLC

ABSTRACT

Cold Flow Performance of a Ramjet Engine

Harrison G. Sykes

The design process and construction of the initial modular ramjet attachment to the Cal Poly supersonic wind tunnel is presented. The design of a modular inlet, combustor, and nozzle are studied in depth with the intentions of testing in the modular ramjet. The efforts undertaken to characterize the Cal Poly supersonic wind tunnel and the individual component testing of this attachment are also discussed. The data gathered will be used as a base model for future expansion of the ramjet facility and eventual hot fire testing of the initial components. Modularity of the inlet, combustion chamber, and nozzle will allow for easier modification of the initial design and the designs ability to incorporate clear walls will allow for flow and combustion visualization once the performance of the hot flow ramjet is determined. The testing of the blank ramjet duct resulted in an error of less than 10% from predicted results. The duct was also tested with the modular inlet installed and resulted in between a 13-30% error based on the predicted results. Hot flow characteristics of the ramjet were not achieved, and the final cold flow test with the nozzle installed was a failure due to improper configuration of the nozzle. The errors associated with this testing can largely be placed on the poor performance of the Cal Poly supersonic wind tunnel and the alterations made to the testing in an attempt to accommodate these flaws. The final tests were halted for safety concerns and could continue after a thorough safety review.

ACKNOWLEDGMENTS

I would Like to thank the following people for their contributions in completing my thesis:

Dr. Mehiel for his help and guidance during several difficult events, Dr. Dianne DeTurris for her expertise in both combustion and supersonics, Dr. Patrick Lemieux for having the insight to point the project down the right path, Cody Thompson for his help with the construction of the ramjet, Kelsey Selin for help with the fuel system design and the early ramjet designs, Andrew Carter for designing the variable geometry inlet, Paul Stone for the design of the combustion chamber, Clinton Humphreys for his work on the variable geometry nozzle and Dr. John Chen for his help with the high speed camera.

I would especially like to thank Sal Estéves for his help with construction and making the project his own. You not only help me with the physical construction but you made the time I spent in the lab more enjoyable. I had an easier time with this project than I would've had I not had your help. I also want to thank you for the mattress you lent me on some of those late weekend nights when I didn't have a place to stay.

I want to thank Dan Wait for all he has done for this project. You always gave me sound advice and always had the broader picture in your mind when I was getting dirty with minor details. You always knew the right course of action whether it was to spend the night at the wind tunnel or to take the night to blow off steam. I appreciate every piece of knowledge and best practice you passed on to me, even if I didn't follow it exactly at the time. This project has come a long way from when Kelsey and I originally approached you about making an after burner and it is largely because of your help. I was very lucky to have you as an advisor on this project.

I would also like to thank my parents for the financial and emotion support you've given me throughout my years in the undergraduate and graduate programs at Cal Poly. I would also like to thank my brother Sam Sykes and my good friend Joe Bauer for spending an entire weekend machining my plates for me and showing me what can be accomplished with a hand mill. I want to thank my sister Chelsea for her help with setting up the picture of the oblique shock. Finally, I would like to thank my girlfriend Maya who as helped me out since before this thesis had even begun to take shape in my head. I could not have completed this without the help of every one of you.

–Harrison G. Sykes

TABLE OF CONTENTS

LIST OF TABLES

LIST OF FIGURES

Chapter 1

Introduction

1.1 Demand for Ramjet Propulsion

Ramjet engines have been highly prevalent in the search for efficient propulsion at high speeds. [22] Using the ram pressure of forward motion as the compression stage of a propulsion system was first discussed in an article in 1913. Without the understanding of supersonic flight, it was concluded that the efficiency would be very low in comparison to modern propulsion systems. [10] The basic ramjet compresses air using supersonic speeds and inlet geometry, and has no compressor or turbine, often utilizing no moving parts at all. [22] This meant that it had no way to start up without already being moving, and cannot produce static thrust like gas turbines can. This insight into the low-speed performance of the ramjet would be the first of many discussions on the matter as the ramjet continued to evolve.

The ramjet was in use in guided missiles, small helicopters, and research airplanes by the late 1950s but there were already plans in the works to broaden its use. With the success of the commercial jet transports, aircraft companies began looking for ways to increase speed with supersonic aircraft, and made bold predictions of future hypersonic aircraft, powered by the ramjet engine. Despite limitations of the technology of the time, it was predicted that ramjets would reach optimum efficiency between Mach 6 and Mach 8, and would allow a transport aircraft to travel 6000 miles in 2 hours. It was even reasoned that the ramjets efficiency at this speed would make the direct operating costs of such an aircraft comparable with subsonic aircraft of the time. Even with the bold predictions of the ramjets future, an even greater discovery was being pursued by the late 1950s, supersonic combustion and the hypersonic air breathing engines. [18]

The kerosene fueled ramjet was seen as the likely contender so long as fossil fuels were available, but in 1965, NASA began the Hypersonic Research Engine Project which relied on hydrogen fuel for a Supersonic Combustion Ramjet (scramjet) which would be flight tested on the X-15 research

plane. [18] [29] After successes with this project, although no flight testing was completed, NASA began to integrate the engine into a vehicle instead of a standalone engine. Considering the entire underside of the vehicle as part of the propulsion system allowed for increases in propulsion system efficiency. The entire fore body of the vehicle acted as part of the inlet expansion and the aft body acted as part of the nozzle expansion, allowing the scramjet to ingest the majority of the air affected by the bow shock. The NASA scramjet was also modular, in the sense that it was made of small, ground test sized modules, that were of a rectangular cross section. [29] The rectangular cross section would be a common feature among later scramjet vehicles like the X-43 and X-51 experimental hypersonic aircraft.

Although the scramjet has taken the search for greater speed to a new level, the ramjet has remained prominent in the realm of efficient propulsion. In 2006, a Ukrainian study found that a ramjet based solution for small payload insertion into low earth orbit would be more efficient than a jet engine based system, like the ones employed by Virgin Galactic's SpaceShipOne/White knight and SpaceShipTwo/White Knight 2. [6] [33] The SR-71 reconnaissance aircraft, designed during the height of the ramjet development, utilized a jet engine to over come the ramjets lack of static thrust and at higher Mach numbers ducted air around the jet engine directly to the afterburner. [13] This idea is still present today, although taking different form, in the combined engine. An example of the combined engine is the "over-under" turbo-ramjet, a ramjet and a jet engine mounted one on top of the other and integrated into a craft like the scramjet. [16] Another example is the Synergistic Air-Breathing Rocket Engine (SABRE) concept which utilizes a ramjet style inlet to compress air for its hybrid air breathing rocket engine during atmospheric flight. The SABRE stops using the inlet at higher Mach numbers and switches to a liquid oxygen and liquid hydrogen closed cycle rocket engine to achieve single-stage-to-orbit capabilities. [34]

1.2 Types of Ramjet Engine Testing Facilities

Inadequate testing facilities and the potential size of the integrated vehicles have led to the use of a combination of ground testing, flight testing, and computer simulation for developmental test and evaluation of ramjets. [7] There are three main types of engine facilities that can be utilized for ground testing ramjet engines: direct connection test facilities, Free jet test facilities, and the Semi-free jet facilities. [26] These testing facilities are intended to make up for the fact that ramjets cannot produce static thrust and must be utilized in order to operate the engine. Other systems,

like the SABRE concept and other combined engine systems, utilize internal turbo machinery to operate in open test beds but still have special requirements to test aspects of the designs. This is internal turbo machinery can be used to accelerate the vehicle from rest, and can also minimize development costs by using existing testing areas during testing. [34]

Besides the ram pressure requirements, ramjets and scramjets are also highly integrated into the vehicles they power. When breaking the vehicle into a testable units so that the engine can be tested, many of the support systems are also taken away. Matching of flow conditions, cryogenic propellants that actively cool the airframe, electrical systems and more all need to be simulated for ground testing to occur. This makes adequate ground testing expensive and facilities hard to come by. Attempting to test the various pieces of the full system require separate facilities as well, increasing the costs. [7]

1.2.1 Direct Connection Testing

The direct connect test (connected-pipe) is not a full engine test in the pure sense. The ramjet relies heavily on the inlet, as it is its sole source of compression on a pure ramjet, but the Direct connection test bypasses the inlet. In a direct connection test, air is heated and pressurized to the same conditions that would be produced by the inlet, and is ducted into the combustion chamber of the ramjet. [26] This testing is used for performance determination of the ramjet combustor, no aerodynamic or inlet effects are considered. [12]

Direct connection testing is seen as a cost-effective method for evaluating a ramjet engine combustor during development. This testing is seen as a method for determining characteristics of the combustor prior to free jet testing and eventual flight testing. [12] It is not a method for testing the entire ramjet system, but there are multiple facilities capable of direct connection testing. These facilities can been found in France, the United Kingdom, Germany, Japan, Russia, and the United States. [7]

1.2.2 Free Jet Testing

Free jet testing is a full engine test, including the inlet, which is conducted by setting the whole engine into the air flow. Free jet testing requires much larger quantities of air than the direct connection test and is used to simulate steady flight conditions. [26] Large integrated vehicle design and extreme conditions required to simulate flight make free jet testing expensive for potential

designs and impractical for most with todays current facilities.

Several facilities for both the free-jet testing and direct connection testing are available around the world and are grouped based on the Mach ranges 0-4 and 4-8. Due to the extreme requirements for higher Mach numbers the facilities capable of 4-8 Mach are limited in number and greater Mach numbers are increasingly difficult to produce for any amount of time. Even if sufficient facilities existed to test some aspects of the engines, it would be likely to still require several facilities to completely test the vehicles. [7]

1.2.3 Semi-Free Jet Testing

Semi-free jet testing is a technique that combines aspects of both direct connection and free jet to simulate actual flight conditions for a specific piece of the vehicle. [26] As mentioned in the section 1.2.2, vehicle design greatly influences the choices of testing facilities. For some vehicles the free-jet test is not the entire system, and different conditions must be simulated to test each piece. Some large designs must be broken into various parts to complete free jet testing. When testing the engine, if the vehicle utilizes fore body compression, then the facility must be able to produce the temperatures of the flight altitude and the post shock pressures in order to test just the engine. Often times the nozzle is expanded by the aft body of the vehicle and so testing that must also be completed. Depending on the vehicle design, semi-free jet testing is required to accurately test each piece of the system [7]

1.3 Combustion Chamber Alternatives

Ramjet engines have been designed to use a vast array of combustion chamber designs. Early ramjets relied on kerosene as fuel, injected into the combustion chamber and ignited like an afterburner on a fighter jet. [18] It was seen as the most likely candidate for ramjet designs and was utilized successfully in the SR-71 reconnaissance aircraft. [18] [13] As performance requirements increased and the technology was pushed, more exotic designs were developed.

One method for adding, or removing, heat is the heat exchanger. Although not used as heating mechanisms, heat exchanges are utilized in the post nozzle environment of the SABRE engine to cool the air before it enters a turbo compressor. [34] Heat exchangers have also been proposed and tested for use with nuclear powered jet engines. [32]

Solid Rockets are common among space craft launch vehicles and toy rocket enthusiasts. Utilizing solid fuel for a ramjet is not a radical idea considering recent successes with hybrid rocket engines. [6] Similar to the hybrid rocket engine, the solid fuel ramjet offers and advantage over purely solid rockets by offering a level of control over the combustion rate of the solid fuel. By controlling airflow and specifically formulated fuel, solid fuel can be developed to operate a ram-pressure conditions. [28]

Another potential ramjet design that could be applied to direct space payload launches is an annular flow electro-thermal Ramjet. The electro-thermal ramjet utilizes hydrogen propellant which has been heated by electric current or electromagnetic radiation. The interesting aspect of this device is that its does not use air, and instead is accelerated through the hydrogen gas and adds energy to the hydrogen through the electric systems. [11]

A more conventional approach to the combustor is by using powdered metals as fuel instead of hydrocarbons like kerosene, to achieve higher performance ramjets. The powdered fuel ramjet is an attempt to combine the good characteristics of the solid fuel and liquid fuel ramjets. [35]

1.4 Thesis Objective

The goal of this thesis is to outline the design, methodology, and cold flow performance of the new ramjet attachment to the California Polytechnic State University(Cal Poly) Aerospace Engineering Department supersonic wind tunnel (SSWT). The modifications made to the SSWT to increase the capabilities to operate with the ramjet are also discussed. The ramjet is designed to match the air flow characteristics of the SSWT and therefore lends itself to a unique testing environment. Unlike typical engine test facilities, the ramjet attachment to the SSWT is designed only to operate in that environment and the SSWT will not have to create specific environments for the ramjet. It acts as an ideal free jet test setup where the test chamber is design for only the one engine, inlet included, but can be connected directly to the ramjet to decrease the airflow requirements like a connected pipe test. Although this design is not practical for testing a particular ramjet, it can be used to characterize the changes associated with specific design choices altering the new parameter but maintaining the other parameters. This design offers a unique environment for observing the combustion process in an engine.

The ramjet is designed with three main criteria in mind: repeatability of the data, modularity of the design, and visibility of the components during operation. The effects of these three guiding

principles can be found throughout the design process of the ramjet. Additionally, one other factor played a significant role in the design of the ramjet, its requirement for supersonic flow. For the ramjet to operate, the engine must be attached to the SSWT, and to avoid any unintentional flow distortion, the height and width of the ramjet needed to be the same size and shape as the current SSWT test section. The SSWT also has a frame for setting the test section on, so to utilize this frame the ramjet would be limited to the 10ft length of the frame. The ramjet length was set to 6ft early on in the interests of weight, cost, and portability, effectively beginning the ramjet design phase with a 6 ft long rectangular duct, 4.937 in. wide and 4.785 in. tall. Since the ramjet design was so heavily influenced by the SSWT, the ramjet cannot be easily adapted to other sources of supersonic flow, but this direct compatibility with the test apparatus makes it unique. So long as the SSWT is functioning properly, the ramjet should be capable of adapting to a wide variety of experiments.

The first principle, repeatability, is directly connected with the future use as a research tool. The ramjet's design and operation must yield consistent, repeatable results in order to be used to research modifications to the design. The base model of the ramjet will need to be operated for base data collection during each research study that intends to alter the ramjet. This way the alterations can compare against the base ramjets characteristics during the same time as their own data. By repeating the tests from this thesis for each future project, the researcher(s) can alter how the data is collected to make it more comparable to their own requirements, as opposed to just looking over the results from this thesis. The data will be available, but if the ramjet's results are repeatable, the researcher(s) can gather the necessary data, instead of trying to utilize the data presented in this thesis.

The second principle, modularity, allows for further development of the ramjet. The modularity designed into the ramjet is a way to ensure that the ramjet remains accessible for future research by allowing vast changes to the characteristics without requiring the rebuilding of the main components. The modularity of the ramjet is achieved by three distinct components: the inlet, the combustor, and the nozzle. Each of these components are comprised of an upper and lower plate which can be altered to achieve different characteristics. Alternative nozzle designs, including multiple ramp inlets, or exotic combustors, like the solid fuel ramjet or heat exchanger, could be swapped in and out in a manner of hours to replace the current component plates. The transition between modules will be seamless if the design requirements for the plates are met, and the SSWT requirements are adhered to. The base model will also make it so that any research being performed on one part of

the ramjet does not need to design the entire engine over.

The third principle to play a major role in the design of the ramjet is visibility, and would aid in the comprehension of the research. The clear walls will allow for visual confirmation of combustion and flow properties, such as oblique shocks in the inlet and turbulent mixing of fuel. It also poses considerable challenges for the structural design and for the safety of the experiment. After discussions with a safety committee during a design review, it was decided that the fused-silica walls should be replaced with stainless steel walls instead until the hot flow characteristics of the ramjet are better understood. The steel walls will be used for this thesis, and in the future to determine the the heat shock characteristics of the ramjet. If the heat shock characteristics are favorable, the fused silica will be purchased in order to complete the build. Since this upgrade is planned for the future, the ramjet designed to allow the fused silica plates was built.

1.5 Organization of Thesis

The following 6 chapters are used to discuss the work and results of this thesis. Beginning in Chapter 2, the basics of supersonic wind tunnels are discussed, with specific details pertaining to the SSWT. The specific requirements for the operation of the SSWT are followed by discussions of the modifications of the SSWT in order to meet the data and safety requirements. Chapter 3 delves into the specifics of ramjet operation, offering some of the basic equations for determining the performance of a ramjet as a lead in to the specific methods used for designing each component of the ramjet analytical model. The ramjet analytical model is discussed in three parts pertaining to each section of the ramjet and the tools used to model each individual section. After the analytical model, Chapter 4 describes the process of turning the results of the analytical model into the physical modular ramjet. Specifics on each part are indicated to allow for minimal confusion when assembling the ramjet. The specific components and desired results for each category of test are discussed in Chapter 5. The results of each of these tests are discussed in Chapter 6, including a discussion on potential sources of error. The conclusion, and a discussion on the potential future use of the ramjet, are presented in the final chapter of this document, chapter 7. Several modifications to both the SSWT facility and the ramjet are proposed to allow for greater utility of the ramjet in the future.

The Appendices of this work hold many important references for anyone who would wish to continue working with the ramjet and SSWT. Appendix A contains the MATLAB code for each of the basic flow equations used in this thesis, a script used to verify their functionality and accuracy,

and the results of this test which can be compared to a text book on gas flow. Appendix B contains the manufacturing drawing of the Basic Inner Plate used in the ramjet and is a necessary reference for anyone wishing to create a new plate for the ramjet. The standard operating procedures as used through the testing phase of this thesis can be found in Appendix C and include the procedures for building up and tearing down each ramjet configuration and the untested procedures for operating the ramjet in the "Hot Fire" setup. Even though the ramjet was never fired during testing, Jet-A was used during some of the testing and Appendix D contains the Material Safety Data Sheet of Jet-A to ensure that anyone attempting to further the work presented in this thesis has access to information on Jet-A. The final Appendix, Appendix E, contains the results of the structural studies completed on various pieces of the ramjet in order to determine the design would meet the desired 2:1 factor of safety used for the initial design.

Chapter 2

California Polytechnic State University Supersonic Wind Tunnel and Modifications

There are two major types of supersonic wind tunnels: an intermittent, also known as a blow-down supersonic wind tunnel and depicted in fig. 2.1, or a continuous closed circuit supersonic wind tunnel. Both types rely on pressure differentials but go about creating this differential in different ways. Another common trait is the necessity of a converging-diverging nozzle, visible in fig. 2.1, to create the supersonic flow in the test section. A converging-diverging diffuser is often used in supersonic wind tunnels to provide greater static pressure recovery. [19]

Intermittent tunnels can either be constructed by allowing air at atmospheric pressure to pass through a converging-diverging nozzle into a vacuum tank, or by allowing air from a high pressure tank to pass through a converging-diverging nozzle and into the atmosphere. With the first setup, constant conditions are maintained until the vacuum tank reaches too high a pressure, and the second setup will maintain constant conditions while the pressure tank maintains a high enough pressure. Intermittent tunnels get their name because they can only remain in operation for a short time. The static pressure recovery provided by a converging-diverging diffuser increases the run time in an intermittent supersonic wind tunnel over a tunnel that only relies on a normal shock diffuser. [19] A normal shock diffuser relies on the large total pressure loss associated with a normal shock, however by inducing weaker oblique shocks the total pressure loss would be less, requiring a lower total pressure ratio. [9]

Continuous closed-circuit tunnels can maintain conditions almost indefinitely by employing a compressor to increase the air pressure from after the wind tunnel to the inlet stagnation pressure required for the wind tunnel to operate. Since run time is not an issue in continuous closed-circuit tunnels, the converging-diverging diffuser allows for a smaller compressor. [19]

The SSWT is a lab currently operated by the AERO department at Cal Poly and is used in this thesis to produce the supersonic flow required for the ramjet to run. The ramjet was designed to

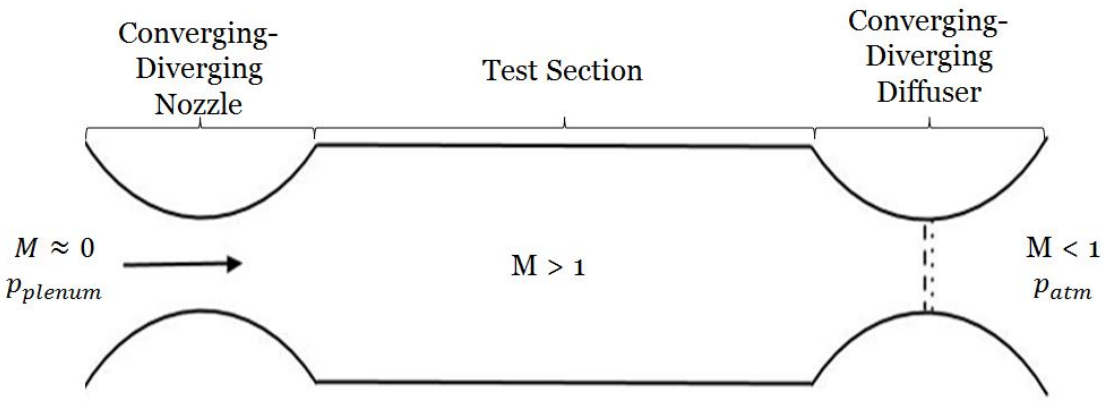

Figure 2.1: Pieces of a Supersonic Wind Tunnel

connect to the existing SSWT with as few modifications as possible, but a few modifications were still required. This chapter gives some background information on the SSWT and its characteristics and will also go into the modifications required for the ramjet's use. The modifications and characterization efforts of the SSWT increased the reliability and capabilities of the SSWT to allow for testing of the ramjet. This chapter focuses on the modifications to the SSWT that were necessary to achieve the acceptable conditions for testing the ramjet. The modifications made the SSWT more reliable in it's primary role, and will allow for future testing with the ramjet.

2.1 Background

The SSWT was donated to Cal Poly by the Boeing Company in 2000 and has been used to demonstrate supersonic flow to students as part of the senior level propulsion class for many years. [8] The SSWT is an example of an intermittent or blow down wind tunnel and relies on several different parts. The pressure tank is at 110 to 120 psi when the experiment starts, and is also at atmospheric temperature. This is dependent on the capabilities of the air compressor used to fill the tank. The SSWT can be run at lower tank pressures, but many of the follow characteristics are not guaranteed outside this range. There is a release valve outside the tank which is normally operated by a student during test runs. Down stream of the release valve, there is an electro-pneumatic valve that is actuated by an air line and electric switch located inside the SSWT control room, and is usually operated by a student as well. When both of these are open, air flows through the pipe to a pressure regulator, which is intended to keep the air in the plenum at a constant pressure.

The SSWT utilizes a Fisher 1098H-EGR pressure regulator with a type 6354L pilot valve, which

# of turns	Length of Adj. Bolt	Plenum Pressure	Expected Pressure
0	1.375 cm	48 psia	85 psia
1	1.275 cm	70 psia	93.4 psia
1.75	1.200 cm	82 psia	99.7 psia
2	1.175 cm	87 psia	101.8 psia
3	1.075 cm	99 psia	110.2 psia
7	0.975 cm	105 psia	143.8 psia

Table 2.1: Plenum Pressure related to Pilot Valve adjustment length

has an outlet pressure range of 85-200 psig. [15] [21]The pilot valve adjustment screw travels 13.75 complete turns of the screw from fully open to fully closed, which is equivalent to 8.4 psig and 1cm of adjustment bolt length per turn. The pressure regulator adjusts the pressure from the 110-120psig in the tank to the required pressure for supersonic flow. Although the pilot valve quotes an outlet pressure range of 85-200psig, these results are impossible from an inlet pressure of between 110-120. [20]After finding that the previous attempts to characterize the SSWT were unrepeatable, a new attempt was made to characterize the pressure values available at the plenum based on settings from the pilot valve. The pilot valve bolt was hand tightened to begin the testing at the fully closed position, which should equate to 85 psi at the plenum, according to the outlet pressure range. Results indicated a steady state plenum pressure reading of 33 psig, 47.7 psia, when the adjustment screw was unscrewed 1.375cm. This was measured from the top of the locknut, which differs from the convention found in the senior project by Curran. [15] After this initial result, several more pilot valve settings were attempted, all with an initial 110-120 psig in the tank.

The results of these tests that pertain to the SSWT characterization can be found in table 2.1. The plenum pressures recorded are peak pressures collected form inside the plenum if the pressure did not remain constant. The specific results of these tests will be further discussed in Section 6.5, and the procedures for the test are discussed in Section 5.3.1. The results displayed in table 2.1 and fig. 2.2 clearly indicate that the plenum does not see the pressure that is coming through the regulator, according to the pilot valve, and that the relationship is not linear. The relationship appears to curve, however it is more likely to plateau somewhere between three and seven turns, when the outlet pressure from the pilot-valve is supposed to equal the tank pressure, and stops regulating the flow. There is also a required 19 psig pressure differential for the pilot valve to operate. [20]However, if the initial tank pressure is set between 110-120 psig, then this data gives a reasonable estimate of

Figure 2.3: SSWT Converging Diverging Nozzle

how to set the pilot valve to achieve a certain plenum pressure.

Once through the pressure regulator the flow goes through a bend, which is a potential cause of the pressure loss, and enters the plenum. The plenum is designed to allow the flow to decelerate to a pseudo-stagnate state before entering the converging-diverging nozzle. Inside the plenum there are also flow straighteners to remove any turbulence in the flow caused by the turns and inconsistencies in the piping. However, the plenum flow not becoming completely stagnate could be one potential source for the discrepancies in table. 2.1

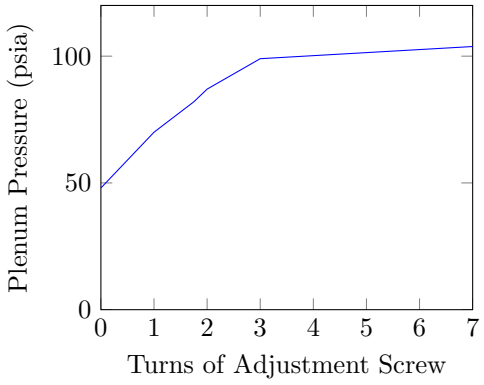

Figure 2.2: Plenum Pressure related to Pilot Valve adjustment length

Once in the plenum, the flow then enters the converging-diverging nozzle shown in 2.3. The throat of the converging-diverging nozzle was measured at 0.873in. wide by 4.785in. tall, but the previous literature states it is 0.9in by 4.8in. [8] [20]Once through the throat, the flow accelerates out into the test section which measures to 4.937in. wide by 4.785in. tall, giving the converging-diverging nozzle an area ratio of 5.655. Once again, Lovell and Gonzales give slightly different dimensions for the exit, 4.8in wide and 4.8in tall. [8]

$$\frac{A}{A*} = \frac{1}{M}\left[\left(\frac{2}{\gamma+1}\right)\left(1+\frac{\gamma-1}{2}M^2\right)\right]^{\frac{\gamma+1}{2(\gamma-1)}} \tag{2.1}$$

M	T/T_0	p/p_0	ρ/ρ_0	A/A*
3.28	0.3173	0.0180	0.0567	5.5234
3.30	0.3147	0.0175	0.0555	5.6286
3.32	0.3121	0.0170	0.0544	5.7358
3.34	0.3095	0.0165	0.0533	5.8448

Table 2.2: Isentropic Flow Table Excerpt

The relationship between Mach number at the exit of the SSWT converging-diverging nozzle and the SSWT nozzle expansion ratio is apparent in eq. (2.1). [19] The equation is non-linear and cannot be solved for M, the exit Mach number, but the SSWT nozzle area ratio can be looked up in a table of isentropic flow properties by assuming that the fluid is air with a γ, the ratio of specific heats, equal to 1.4. Interpolating from table 2.2 gives us a test section Mach number of 3.3050, assuming the converging-diverging nozzle is isentropic. Lovell and Gonzales assume a exit Mach number of 3.24. [8]

The current setup relies on three pressure transducers located in the pressure tank, the plenum and on a sting in the test section. The pressure tank transducer is for monitoring how close the tank is to the 19 psi differential. The test should be completed before this threshold is reached or the pressure will spike above the desired pressure potentially resulting in an over pressurization. The pressure transducer in the plenum measures the pressure of the pseudo-stagnant flow, allowing for measurement of the stagnation pressure of the flow in the isentropic converging-diverging nozzle. The pressure transducer in the test section measures the stagnation pressure off of the sting. By assuming isentropic flow in the converging-diverging nozzle, the Mach number in the test section can be determined by the ratio of stagnation pressures collected at these two points.

$$\frac{p_{0f}}{p_{0i}} = \left[\frac{\frac{\gamma+1}{2}M_i^2}{1+\frac{\gamma-1}{2}M_i^2}\right]^{\frac{\gamma}{\gamma-1}} \left[\frac{1}{\frac{2\gamma}{\gamma+1}M_i^2 - \frac{\gamma-1}{\gamma+1}}\right] \tag{2.2}$$

If the flow is supersonic in the test section, a normal shock will form on the sting and the ratio of stagnation pressures will follow the normal shock equation shown from John and Keith in eq.(2.2). [19]

Equation (2.2) cannot be solved for M_i, the test section Mach number, explicitly. The test section Mach number can be found by using either a look up table, similar to the area ratio, or with an iterative solver. In the lab, it is up to the students to use an iterative solver, like the FZERO function in MATLAB, to solve for the Mach number of the test section. The pressure transducers

gather data at 30hz, so looking it up in a table is unreasonable for finding the Mach number. The MATLAB code used to solve the eq. (2.2) in this thesis can be found in Appendix A. This same code will be used during a "Blank" run of the ramjet, described in Section 5.3.1, to determine the Mach number of the ramjet tests.

The results from solving eq. (2.1) and eq. (2.2) should be the same, any difference could mean problems with instrumentation or disturbances in the flow. A higher Mach number indication from the sting could occur if the sting was not mounted directly into the flow. If the sting is deflected by the flow, the stagnation pressure reading will have a static pressure component, lowering the pressure reading from the sting. This will make it appear as if a larger pressure drop occurred across the normal shock, leading to a higher predicted Mach number from eq. (2.2).

A lower Mach number could occur due to a normal shock forming inside the converging-diverging nozzle, effectively lowering the SSWT nozzle area ratio and limiting the amount of expansion. Whatever lower Mach number occurs is the Mach number at which the normal shock formed in the converging-diverging nozzle, and the effective SSWT nozzle ratio could be solved for using eq. (2.1). This normal shock occurs when the exit pressure of the converging-diverging nozzle is significantly lower than the ambient pressure, and the only way to remove it from the SSWT converging-diverging nozzle is to increase the plenum pressure. A high enough plenum pressure will move the normal shock further out the converging-diverging nozzle and into the test section and eventually to the sting, however for purposes of measuring the Mach number through the test section the shock wave need only move past the test section. The equation will work if the shock wave is on the sting or inches in front of it, the location of the shock makes little difference to the measurement. The moving normal shock wave must pass whatever apparatus is being tested, for the ramjet this means the normal shock must move into the inlet and past the throat. However due to the "Blank" ramjet being essentially a normal shock diffuser, the plenum pressure required is greater than the normal SSWT setup that has a converging-diverging diffuser to help with the pressure ratio.

The lower Mach number can occur when attempting to increase the run time of the SSWT by lowering the plenum pressure to decrease the mass flow rate. The pressure in the plenum can only be lowered so much to allow for a lower mass flow rate before the SSWT will unstart. To determine the minimum plenum pressure for the SSWT, the pressure ratio across the SSWT must be found. To determine the pressure ratio, the diffuser throat must be known so that an isentropic relationship through the converging-diverging nozzle can be used.

For full expansion and a useful test section, the shock wave needs to occur past the test section of the SSWT, and optimal operating conditions of a SSWT suggest the normal shock should occur at the diffuser throat. [19]

$$\frac{A_{ti}}{A_{td}} = \frac{p_{0f}}{p_{0i}} \tag{2.3}$$

To size the throat of the diffuser, eq. 2.3 gives the relationship of a tunnel's converging-diverging nozzle to the throat of the diffuser. For an approximate sizing, using the stagnation pressure ratio across a normal shock wave for the design Mach number of the wind tunnel can be used if the total pressure ratio across the tunnel is unknown. [9] This determines the ratio of the SSWT converging-diverging nozzle throat to the diffuser throat, which will be enough to determine the pressure ratio across the diffuser with isentropic relations. For the SSWT to operate at Mach 3.305, the normal shock would produce a stagnation pressure ratio of $\frac{p_{0f}}{p_{0i}} = 0.2526$, which means the diffuser throat area for the SSWT would be $16.57in^2$ based on eq. (2.3).

The stagnation pressure ratio across the tunnel is not enough to determine the pressure required in the plenum. As with converging diverging nozzle, the ratio of $\frac{p_0}{p}$ is what is important, so determining the $\frac{p_f}{p_i}$ for the converging-diverging nozzle, the diffuser inlet, the normal shock in the diffuser, and the diffuser exit will be necessary to determine the required plenum pressure. Although isentropic flow produces a stagnation pressure ratio of one, the pressure ratio is not one and must be determined. To determine the pressure ratio across the diffuser, eq.(2.1) can be used along with the areas of the SSWT test section and diffuser throat to determine the $\frac{p_f}{p_i}$ for the isentropic regions. The isentropic section for the inlet of the diffuser will be used to determine the Mach number at the diffuser throat.

$$\frac{p_f}{p_i} = \frac{\left[2\gamma M_i^2 - (\gamma - 1)\right]}{(\gamma + 1)} \tag{2.4}$$

$$M_f = \sqrt{\frac{[(\gamma - 1)M_i^2 + 2]}{[2\gamma M_i^2 - (\gamma - 1)]}} \tag{2.5}$$

The normal shock pressure ratio can be determined by eq. (2.4) and the Mach number behind the shock can be determined by eq. (2.5) if the Mach number at the throat is known.

The pressure change across the SSWT converging-diverging nozzle can be found in table 2.2, and the plenum pressure is represented as the stagnation pressure. Assuming the diffuser exit Area is the same as the diffuser inlet area, the final pressure ratio can be solved.

$$p_{plenum-min} = \left(\frac{p0}{p}\right)_{nozzle} * \left(\frac{p_i}{p_f}\right)_{diffuser_in} * \left(\frac{p_i}{p_f}\right)_{normalshock} * \left(\frac{p_i}{p_f}\right)_{diffuser_out} * p_{atm} \tag{2.6}$$

With eq. (2.6), and knowing $p_{atm} = 14.7psia$, the predicted $p_{plenum-min} = 45.02psia$. This equation does not take into account friction, and as mentioned above is only a good starting point without the actual pressure ratio across the wind tunnel. [9]

The Fanno Line Flow relations can be used to achieve greater fidelity in the pressure ratio across the SSWT, and determine a better approximation of A_{t2} and $p_{plenum-min}$.

$$\frac{fL_{max}}{D_h} = \left(\frac{\gamma+1}{2\gamma}\right)\ln\left(\frac{\frac{\gamma+1}{2}}{1+\frac{\gamma-1}{2}M^2}\right) - \frac{1}{\gamma}\left(1-\frac{1}{M^2}\right) - \left(\frac{\gamma+1}{2\gamma}\right)\ln\left(\frac{1}{M^2}\right) \tag{2.7}$$

The left side of eq. (2.7), known as the Fanno Parameter, contains the length, L, the Hydraulic diameter, D_h, and the Darcy friction factor, f. [19] The L in eq. (2.7) is the length of duct the flow being approximated travels. For the SSWT, under normal operation, L is the distance from the end of the converging-diverging nozzle to the beginning of the SSWT converging-diverging diffuser, approximately 3 ft.

The D_h refers to the hydraulic diameter of a duct with flow moving through it.

$$D_h = \frac{4wh}{2(w+h)} \tag{2.8}$$

Equation (2.8) is the equivalent hydraulic diameter of a rectangular duct. [19] Digging through the derivation of the Fanno Line flow equation, the $\frac{4}{D_h}$ term in the Fanno parameter is originally $\frac{C}{A}$, the circumference of the duct divided by the duct area. It is easier to see where eq. (2.8) comes from with this knowledge.

$$\frac{2(w+h)fL_{max}}{wh} = \left(\frac{\gamma+1}{2\gamma}\right)\ln\left(\frac{\frac{\gamma+1}{2}}{1+\frac{\gamma-1}{2}M^2}\right) - \frac{1}{\gamma}\left(1-\frac{1}{M^2}\right) - \left(\frac{\gamma+1}{2\gamma}\right)\ln\left(\frac{1}{M^2}\right) \tag{2.9}$$

Substituting eq. (2.8) into eq. (2.7) makes the Fanno Line flow equation look like eq. (2.9).

The final piece of eq. (2.9) is the Darcy friction factor, f. The first step to finding f is determining whether the flow is turbulent or laminar. The SSWT has a Reynolds number between 1.7 and 2.2 million, depending on plenum pressure, making it turbulent pipe flow.

$$\frac{1}{\sqrt{f}} = -2\log\left(\frac{2.51}{Re\sqrt{f}} + \frac{\left(\frac{k_r}{D_h}\right)}{3.72}\right) \tag{2.10}$$

The Darcy friction factor is dependent on the Reynolds number of the flow for both laminar and turbulent flow, however the turbulent flow equation is much more involved. From eq. (2.10) it is clear that the Colebrook equation is implicit in f, and and solving for f will require an iterative solution. [2] Equation (2.10) also relies on the Absolute Roughness Coefficient k_r, which is a material specification, and the hydraulic diameter which was solved using eq. (2.8). With all of the pieces

solved for, the Fanno line flow calculation can be used to predict the pressure loss due to friction inside the SSWT test section.

For full expansion of the converging-diverging nozzle, fig. 2.3, the normal shock must at least occur at the SSWT converging-diverging nozzle exit. The plenum pressure required for this case can be predicted by using a combination of isentropic relations for the converging-diverging nozzle, normal shock equations for the normal shock, and Fanno flow relations to determine the pressure loss through the SSWT. The pressure change across the normal shock can be solved with the initial Mach number and eq. (2.4) and the final Mach number can be solved with eq. (2.5). Using the post shock Mach number, eq. (2.9), length of the test section L, and eq. (2.10) the value M_f across the test section can be solved.

$$\frac{p_i}{p_f} = \frac{M_f}{M_i}\left[\frac{2+(\gamma-1)\,M_f^2}{2+(\gamma-1)\,M_i^2}\right]^{\frac{1}{2}} \tag{2.11}$$

Using the Mach numbers, pressure ratio from the subsonic flow through the 3 feet of the SSWT test section can be solved by applying eq. (2.11).

Like the inviscid approximation, the stagnation pressure ratio across the SSWT converging-diverging nozzle when using an isentropic approximation is 1, which means the area of the diffuser throat can be solved for using the stagnation pressure ratios across the normal shock and the Fanno flow section.

$$\frac{p_{0i}}{p_{0f}} = \frac{M_f}{M_i}\left[\frac{2+(\gamma-1)\,M_f^2}{2+(\gamma-1)\,M_i^2}\right]^{\frac{\gamma+1}{2+(\gamma-1)}} \tag{2.12}$$

Equation (2.12) solves the stagnation pressure ratio for the Fanno flow approximation of the test section. With the flow at Mach 3.305 at the exit of the converging-diverging, the normal shock produces a stagnation pressure ratio of $\frac{p_{0f}}{p_{oi}}_{shock} = 0.25$. The Mach number after the normal shock $M_f = 0.46$, which gives a stagnation pressure ratio of $\frac{p_{0f}}{p_{oi}}_{fanno} = 0.95$. The combination of these two stagnation pressure ratios gives a diffuser throat area of $17.45in^2$.

The isentropic approximations of the diffuser are done much the same as in the inviscid approximation, since the isentropic flow relations do not account for friction.

$$p_{plenum-min} = \left(\frac{p0}{p}\right)_{nozzle} * \left(\frac{p_i}{p_f}\right)_{normalshock} * \left(\frac{p_i}{p_f}\right)_{fanno} * \left(\frac{p_i}{p_f}\right)_{diffuser_{in}} * \left(\frac{p_i}{p_f}\right)_{diffuser_{out}} * p_{atm} \tag{2.13}$$

The atmospheric pressure, $p_{atm} = 14.7psia$, multiplied by each of the pressure ratios, as shown in eq. (2.13), will solve for the required plenum pressure to fully expand the SSWT converging-diverging nozzle and produce a normal shock at the exit of the converging-diverging nozzle in the SSWT. Any plenum pressure above this $p_{plenum-min}$ will result in Mach 3.305 flow out the SSWT converging-

diverging nozzle, any plenum pressure below this and the Mach number will decrease as the shock wave backs up the SSWT converging-diverging nozzle and decreases the expansion ratio. The Mach number from the SSWT converging-diverging nozzle is 3.305, based on the area ratio, and it will only occur in the SSWT if the plenum pressure is greater than $p_{plenum-min} = 72.3psia$.

To achieve supersonic flow throughout the test section the shock wave must move past the test section and into the diffuser, with the ideal case again being a normal shock at the throat of the diffuser. For this calculation the stagnation pressure ratio for determining the diffuser throat area can be determined by completing the Fanno flow calculation with Mach 3.305, and the final Mach number after the length, $L = 3$, can be used to determine the pressure ratio across the normal shock. Once there is a reasonable approximation for the diffuser throat area, the pressure ratios can be solved again like before but using the supersonic Fanno flow, and a supersonic isentropic approximation of the inlet to the diffuser. The pressure ratio across the normal shock is then solved with eq. (2.4) and the final pressure ratio is solved with a subsonic application of the diffuser exit.

$$p_{plenum-min} = \left(\frac{p0}{p}\right)_{nozzle} * \left(\frac{p_i}{p_f}\right)_{fanno} * \left(\frac{p_i}{p_f}\right)_{diffuser_{in}} * \left(\frac{p_i}{p_f}\right)_{normalshock} * \left(\frac{p_i}{p_f}\right)_{diffuser_{out}} * p_{atm} \tag{2.14}$$

The minimum plenum pressure, $p_{plenum-min}$, for supersonic flow through the super sonic wind tunnel is solved for by combining the ratios in eq. (2.14). From eq. (2.14) and the $p_{atm} = 14.7psia$, the test section will have supersonic flow through out if $p_{plenum-min} = 78psia$. Running the SSWT for research purposes should be done with a plenum pressure no less than 78 psia.

These equations work well for the SSWT with its supersonic diffuser, but they can also be applied to flow through a duct without a diffuser. Without the diffuser, the task of determining the area of the diffuser throat is no longer necessary and the L in eq. (2.9) becomes the location of the normal shock in the straight duct. The straight duct is a representation of the ramjet when in "Blank" setup. The L in the SSWT refers to the location of the normal shock, when measured from the end of the converging-diverging nozzle, and must be beyond the test section, however for the ramjet L must reach past the throat of the inlet. For the ramjet, L is over 2 ft., less than the SSWT test section length, but the ramjet does not have a diffuser to recover pressure, instead, the ramjet has 4 more feet of ducting and therefore requires a greater pressure than the SSWT.

Much like the SSWT, the ramjet's minimum for full expansion occurs when the normal shock occurs at the end of the converging-diverging nozzle, and the pressure ratio can be solved by applying the normal shock pressure ratio and the Fanno flow calculation for the 6 ft. length of the ramjet

duct. For full expansion and a normal shock that occurs past the inlet of the ramjet, allowing oblique shocks to form when the inlet is installed, a higher plenum pressure will be required. A similar approach can be used to find the required plenum pressure for a normal shock occurring any distance down stream. Instead of assuming the normal shock occurs directly at the exit of the converging-diverging nozzle, use the Fanno flow relations for a supersonic section, followed by the normal shock relations, and then repeat the Fanno flow relations for the subsonic section. With this process it was found that $p_{plenum-min}$ for a shock at the end of the converging-diverging nozzle is approximately 79 psia, and to reach the pitot-static system in the ramjet requires approximately 88 psia. All of these calculations are dependent on where the SSWT nozzle truly ends, and the approximate required plenum pressures vary depending on where the line is drawn.

2.2 Modifications

The ramjet was designed to attach to the SSWT test section and be mounted on the SSWT frame. Because of this attention during design, the majority of the modifications were drilling and tapping holes for mounting the ramjet and the associated fuel and ignition system hardware to the frame. However a few modifications require more explanation.

2.2.1 Data Acquisition

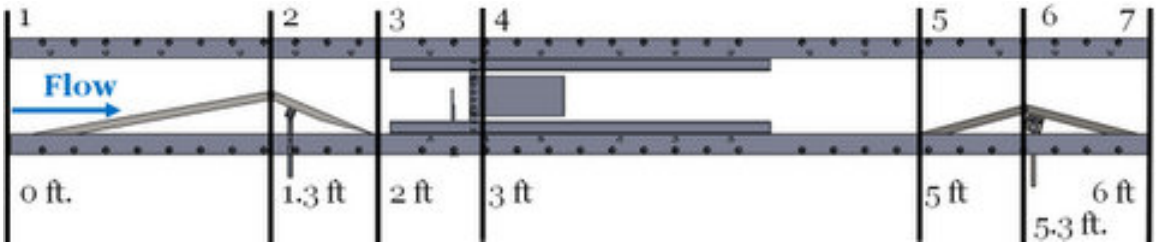

Figure 2.4: Diagram of the Ramjet sections

One of the minor modifications to the wind tunnel is the use of a different data acquisition system (DAQ) during the ramjet experiment than during normal SSWT operation. The National Instruments NI USB-6211 Data Acquisition Module used during SSWT was replaced by the National Instruments NI cDAQ-9174, with an NI 9211 thermocouple input module and an NI 9205 analog input module. The main reason for this modification was to use the NI 9211 module as data acquisition for the two thermocouples used in the experiment. So that a single DAQ could be used,

the pressure transducers will run through the NI 9205 module instead of the NI USB-6211 as was done during SSWT operation. Both of these DAQ setups can run on the SSWT lab computer, and require no software changes when switching. The only issue for switching back to running the SSWT would be to remove the tank and plenum pressure transducer leads from the NI 9205 mod and reinserting them to the NI USB-6211. The third transducer is for the sting pressure transducer which isn't needed during ramjet operation, and will remain attached to the NI USB-6211.

There are only two thermocouples used in the ramjet. These measure the average temperature of the flow at points before and after the combustion chamber to determine energy added to the flow. The two thermocouples attach to the NI 9211 in channel TC0 and TC1, depicted in the diagram in fig. 2.5. The thermocouple in front of the combustion chamber, measuring temperature T_{03} at station 3 in fig. 2.4, connects to channel TC0, and is distinguishable by its white wire sleeve. The red sleeved wires connect into channel TC1, and measure temperature T_{05} collected at station 5 in fig. 2.4, after the combustion chamber. Each thermocouple channel are connected yellow wires to the positive(+) pin, and red wires to the negative(-) pin.

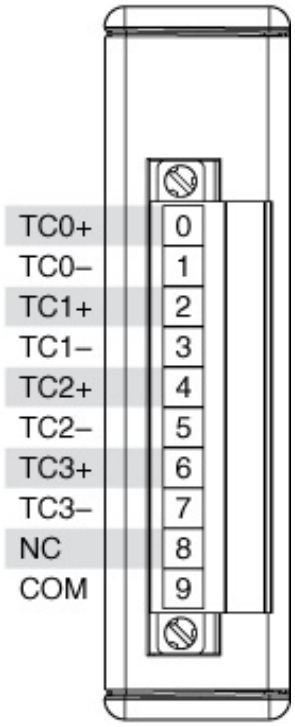

Figure 2.5: NI 9211 Thermocouple Module pin diagram

The two thermocouples purchased for the ramjet testing are Omega Engineering Part# TJ36-CAIN-14G-6-CC-XCIB. These are 1/4 in diameter, 6 in long, type K thermocouples that are clad in Inconel®600 and have an upper thermocouple junction temperature of 2100°F. [5] The thermocouple type is easily distinguished by its yellow and red wires, indicating the K-type in accordance with ANSI codes. K type thermocouples have an accuracy of within 4°F, for all temperature ranges, however this is equivalent to 0.75% above 32°F, and 2.0% below 32°F. [1] The two thermocouples are attached to the instrumentation plates by compression fittings, Omega Engineering Part #SSLK-14-14. The method and location of their attachment is described in subsection 4.1.

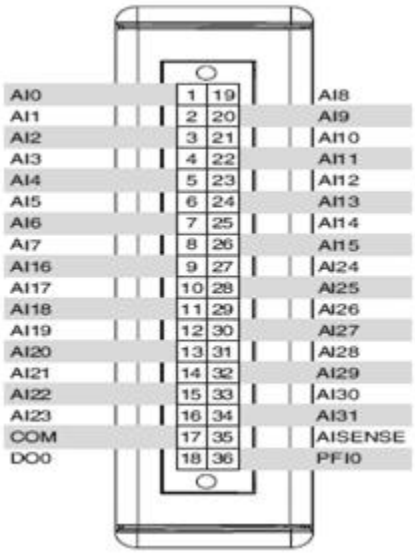

Figure 2.6: NI 9205 Analog Input Module pin diagram

Where only two thermocouples are needed for the ramjet testing, a total of eight pressure transducers are required for gathering the appropriate data. The first two were already connected to the SSWT tank and plenum, and have been re-purposed for the ramjet. The tank pressure transducer is an Omega Engineering PX613-300G5V, and is connected to the control room by an electrical connector strip behind the computer labled "Tank Press". The white lead in the shielded cable from that connector strip connects into channel AI0 of the NI 9205, the pin diagram of which can be found in fig. 2.6. The red lead from the shielded cable connects to a common positive 10 - 30Vdc power source, and the black lead to a common negative. A connecting wire from the common negative is then inserted into the AI8 channel in fig. 2.6. This setup allows for the PX613 pressure transducer to supply differential voltage to the NI 9205. The green lead is connected to an unused lead in the Omega Engineering PX613 and PX603 pressure transducers and can be tied out of the way.

As mentioned by Curran, the tank pressure transducer was not functioning when the lab modifications began. [15] This turned out to be poor connections inside the control room located at the connection shown in fig. 2.7. By removing and cleaning the connections in fig. 2.7, the tank pressure data came in correctly. The plenum pressure reading also contained significant noise in the data, but this was solved by re-soldering the connections between the pressure transducer and the cable that ran back into the control room.

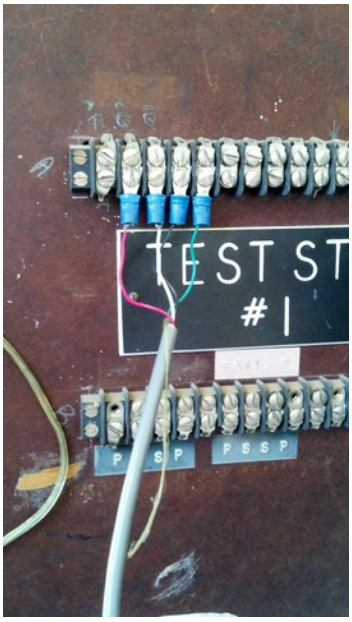

Figure 2.7: Wiring of the Tank Transducer connection

Figure 2.8 demonstrates what the data from the plenum and tank looked like during a normal run before these changes were made. The tank pressure reading simply stays in one place despite the pressure in the tank decreasing during the run, as noted by the external gage mounted on the tank. Before re-soldering the plenum pressure connections, the data is too noisy to use raw and required an exponentially weighted moving average to create meaningful data. This moving average was used to create the red line, and was used to make the Mach calculations in the lab. The main issue with the moving average is that it applies a delay to the data, and this causes some strange data effects that will be addressed in the results sections.

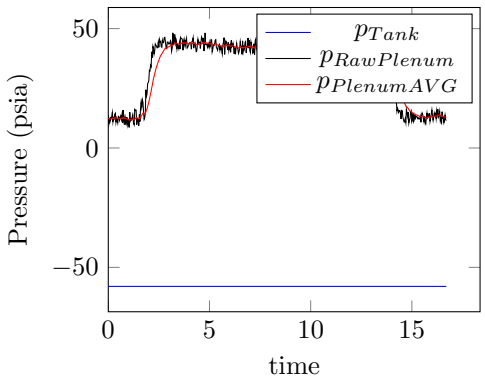

Figure 2.8: SSWT Data Irregularities

The plenum pressure transducer is an Omega Engineering PX603-300G5V as well and is connected to the control room by an eight-lead shielded cable that passes through the control room wall. When connecting the plenum pressure transducer, the white lead with a blue stripe is attached to channel AI1, while the solid blue lead that is intertwined with the white and blue striped lead is

attached to the common positive source. The white and brown striped lead is used to connect to the common negative source, and as with the tank pressure transducer a connector is run from the common negative source to the AI9 channel. For data with less noise, it is recommended to connect the shielded cables shielding wire to a common ground. All the other leads in the shielded cable are unnecessary and do not attach to anything. This concludes the modified connections of the current SSWT DAQ equipment, however there are six new pressure transducers that are connected to the NI 9205 for ramjet testing. The pressure transducers are split into three groups, ramjet stations 3, 5, and 7 from fig. 2.4, each with a transducer for static pressure and a transducer for stagnation pressure at each station.

Figure 2.9: Wiring of the Pressure transducers at Station 5

The new pressure transducers are all Omega Engineering PX613-100G5V, which means they have a 1-5Vdc output on a 3-wire system just like the plenum and tank pressure transducers. These transducers measure up to 100 psi with a 200psi burst pressure, and require the same 10-30Vdc excitation as the original transducers. A single eight lead shielded cable runs to the two transducers at station 3, and another to station 5, but station 7 has a four lead shielded cable for each transducer. The cable for station 3 is identified by the blue sleeve with two sets of four leads, and station 5 is the same but with a black sleeve. The wires from stations 3 and 5 are bundle by solids and stripes, solids refer to the static pressure transducer at that station and stripes refers to the stagnation pressure transducer. The wiring layout of station 5 can be seen in fig. 2.9, which shows both the black sheath and the solid and striped arrangements.

Stripes or solids, all of the wires in stations 3 and 5 in fig. 2.4 follow the connection scheme found in table 2.3. The output of the station 3 static pressure transducer connects to channel AI2, the stagnation pressure transducer in AI3. The outputs from station 5 follow the same order for

Green	Output
Orange	Common Positive
Brown	Common Negative
Blue	Unused

Table 2.3: Pressure Transducer Wiring stations 3 and 5

Green	Output
Red	Common Positive
White	Common Negative
Black	Unused

Table 2.4: Pressure Transducer Wiring station 7

channels AI4 and AI5.

The two pressure transducers at station 7 follow a different connection scheme. The static transducer cable has a blue sleeve, while the stagnation pressure cable has a black sleeve, but both sets of leads connect in accordance with table 2.4. The static transducer connects its output to channel AI6 and the stagnation transducer from station 7 connects to the channel AI7. To make all of the transducers operate differentially, connections from the common negative must be connected to channels AI10 to AI15.

2.2.2 Pressure Relief System

During a design review, the safety committee feared the ramjet could become sealed if one of the adjustable ramps broke. The decision made from this discussion was to modify the SSWT with some sort of pressure relief system so that if the pressure exceeds the design pressure, it will open and release the excess pressure. Some of the ideas discussed were pressure relief valves, burst disks, and spring loaded doors. The decision was made to design a burst disk to mount in the SSWT test section mounting plate, which is located directly upstream of the Ramjet.

The burst disk design was simple, it didn't have to break at an exact pressure, it just had to break before the ramjet. The most important design choice was the location of the burst disk, which had to protect the ramjet regardless of where the blockage occurred. Due to the both the inlet, stations 1 through 3 in fig.2.4, and the nozzle, stations 5 through 7 in fig. 2.4, of the ramjet utilizing

adjustable ramps, the potential for blockage occurs at both the beginning and end of the ramjet, so placing the burst disk inside the ramjet would not protect the system from an inlet failure.

To protect the ramjet from an inlet failure and blockage, the burst disk had to be installed in the SSWT itself. One of the possibilities was to install it into the plenum, but with the desired bursting pressure being the same as the operating plenum pressure, the burst disk would potentially burst if any fluctuation occurred in the plenum. The final location was to place the pressure relief system inside the test section of the SSWT, as part of the test section plate as shown in fig. 2.10. This location had its own disadvantages, like potentially creating oblique shocks in the flow, however a burst disk design that was flush to the test section plate would appear as a single plate and would not affect the flow.

Figure 2.10: Burst Disk installed before a run

The location being chosen as the test plate of the SSWT is what finalized the choice for a flush burst disk. The flush burst disk allowed for the smallest chance of any disruptions to the flow, and could still provide the required protection. Although some time was spend determining a size necessary for the burst disk, the safety committee decided that a required rate of depressurization was not required, and simply allowing for a high pressure state to bleed off would suffice. The goal was to ensure that once the burst disk broke, the SSWT could be turned off at the manual valve and allowed to bleed pressure until it reached safe levels again.

After searching on the Internet for suitable burst disks, it became apparent that a flush burst disk was not a very common request. It was then determined that a custom design would be necessary. To build the burst disk, a 0.497in hole was milled into the test plate. The 0.5in end mill was the largest available that also allowed the option of tapping it at a later date, if the need arose. The ability to tap the hole would allow for the use of some other mode of installing the relief system in the future.

Figure 2.11: Failed Burst Disk after a run

To create the membrane of the burst disk, several thicknesses of aluminum foil were tested for their burst pressures. A fixture was created to apply pressure to the aluminum foil when mounted on the test plate, and a pressure tank and pressure regulator were used to determine the burst pressures. The aluminum foil was placed over the hole and taped to the plate using strips of aluminum tape with the fixture placed over that to proved pressure. The tank was then opened and the pressure regulator was slowly increased until the foil burst. This process lead to an initial determination of the required aluminum foil thickness, but the test lacked one important factor, there was no flow.

After attaching the desired aluminum foil to the test section plate, the plate was installed and a ramjet run was performed with the SSWT. This caused the burst disk to rupture, despite no blockage of the flow, and no over pressurization. Increasing the thickness on the next run did not succeed in preserving the burst disk, even though both disks should have withstood the pressures based on the testing. After inspecting the ruptured disks, it became clear that the disks were not rupturing from pressure but from small inconsistencies in the how the foil was secured to the test plate. These inconsistencies allowed for the aluminum foil to be torn away at these higher stress points, when the flow was applied. This occurred even during early testing with subsonic runs.

The result was to use the aluminum tape as the burst disk to keep it from tearing. The aluminum tape used was Nashua 324A Cold Weather Premium Foil tape, which has a thickness of 4.8 mil, which is 3 times the thickness of the heavy duty aluminum foil used and can be expected to break around 85 psig. However 3 layers of aluminum foil was torn through by the SSWT which did not reach 85 psig during the test which led to the need for the aluminum tape. Although the aluminum tape was found to withstand higher pressures than the aluminum foils, the main reason it was chosen for the pressure relief system was because it could be applied as one continuous sheet. The lack of material changes meant that the flow could not tear through the disk as easily and would instead require the pressure of a blocked system to break. The 85 psig burst is higher than the planned burst rating, however due to the increased pressure reuirements with the SSWT, the 85psig is low enough to be effective.

Chapter 3

Analytical Model

A ramjet is composed of an inlet, a combustor, and a nozzle, its lack of compressors or turbines make it an incredibly simple engine conceptually. [17] The inlet makes up for the lack of a compressor with speed and the high rise in pressure associated with decelerating the high flight speed incoming air to the relatively low velocity in the combustion chamber. This makes it much more difficult for a ramjet to operate at lower speeds and it is impossible for a ramjet to develop static thrust. The low velocity flow from the inlet then mixes with fine droplets of fuel from fuel injectors, is ignited by an igniter, and passes by a "flameholder" which stabilizes the flame. Once combustion starts, the flow is expanded through a nozzle to a high velocity instead of passing through a turbine first. Since there is no compressor other than the nozzle, no turbine is required to turn it. [22]

For ideal analysis of the ramjet, it can be assumed that the compression from the inlet and the expansion from the nozzle are reversible and adiabatic, and that combustion occurs at constant pressure. These assumptions are not realistic, losses from heat exchange and friction occur in every section of a real ramjet, but the assumptions can be used to determine an upper limit to the performance of a ramjet.

$$\mathscr{T} = \dot{m}_a[(1+f)u_e - u] + (p_e - p_a)A_e \tag{3.1}$$

The standard thrust equation, eq. (3.1), can be applied to find the thrust of the ramjet, $\mathscr{T}$. It can be simplified when dealing with the ideal ramjet by assuming the nozzle is optimally expanded so that the static pressure at the nozzle exit, p_e, is equal to the ambient pressure, p_a.

$$\mathscr{T} = \dot{m}_a[(1+f)u_e - u] \tag{3.2}$$

If $p_e = p_a$, eq. (3.1) becomes eq. (3.2) and can be used to determine the thrust of the ideal ramjet. [22]

With isentropic compression and expansion of the inlet and nozzle, and assuming constant pressure heat and mass addition, $p_{0a} = p_{0e}$, which leads to the ambient Mach number, M_a is equal

to the exit Mach number M_e.

$$u_e = \sqrt{\frac{T_{04}}{T_{0a}}} u_a \tag{3.3}$$

From this assumption, the exit velocity, u_e, can be solved with eq. (3.3) which utilizes the stagnation temperature ratio $\frac{T_{04}}{T_{0a}}$. This stagnation temperature ratio is set by the material of the ramjet, and how high of a temperature the material can withstand. The stagnation temperature after combustion, T_{04}, is one of the most important aspects for increasing thrust, and is therefore highly protected by engine manufacturers. [22]

If the material chosen determines the T_{04}, then the final step is to solve for the fuel-air ratio, f.

$$f = \frac{\left(\frac{T_{04}}{T_{0a}}\right) - 1}{\left(\frac{Q_r}{c_p} T_{0a}\right) - \left(\frac{T_{04}}{T_{0a}}\right)} \tag{3.4}$$

The fuel-air ratio is dependent on the heating value of the fuel, Q_r, and the specific heat at constant pressure, c_p. Once these have been determined the thrust of an ideal ramjet can be determined. [22]

Some of these assumptions will be made in this thesis, others will be amended to try and better predict what is occurring in the ramjet. The modeling of the ramjet can be split into three major components: the inlet, the combustor, and the nozzle. This is the way the experimental model of the ramjet is split per its modular design and the way the theoretical model will be discussed. Each section of the ramjet is a potential thesis unto itself, and although the design may not be the"optimal" design for use with the SSWT it will be an adequate starting point for future work. This chapter will discuss the initial ramjet model which was designed based on inviscid relations and will discuss the attempt to rectify many of the early issues found in testing.

3.1 Assumptions

In order to develop a working model of the ramjet, a few assumptions had to be made about the design and the SSWT. The SSWT was tested and found that the Mach number associated with the converging-diverging nozzle area ratio was 3.24, however the experimental results concluded an average Mach number of 2.8. [8] The experiments done by Lovell and Gonzales resulted in an image of a 34° oblique shock formed by a 15° and test run lengths of nearly 20 seconds at an initial plenum pressure of 56 psia. From these results it was assumed that by using the newer compressor, similar test run lengths and results could be achieved using a higher plenum pressure. An initial assumption of the ramjet was that 15 seconds of runtime would be possible for plenum pressures of 60 psia.

The ramjet was theoretically designed to an inlet Mach number of 3.3. The SSWT can vary its Mach number, allowing for more options for future testing. This flow is delivered by the SSWT by expanding from a 2.19 in^2 throat to the test section area of 23.62 in^2 through a converging-diverging nozzle. This nozzle is attached to a plenum, which is fed air from the upstream pressure tank and can be considered stagnant flow. A pressure regulator is mounted between the plenum and main tank, and steps down the plenum pressure to 60 psia from the 100 psia main tank. The pressure regulator can be adjusted to various pressures, and is run at 30 psia for normal SSWT operations. To limit potentially un-starting the SSWT, 60 psia plenum pressure is required for the relationship between ambient pressure, combustion chamber pressure and plenum pressure during ramjet operation.

The relationship between ambient, combustion chamber, and plenum pressure is based on the requirement for choked flow at the throat of the SSWT. For choked flow to occur at a nozzles throat, the exit pressure of the nozzle must be less than $0.528 * p_0$ of the plenum. This back pressure requirement was a driving factor in the relationship between inlet design and ramjet nozzle design. The converging-diverging nozzle for the exit of the ramjet requires the $0.528 * p_0$ relationship between ambient air and the combustion chamber of the ramjet. With these relations in place, and knowing that standard pressure is 14.7 psia, we can setup the following equation to determine the required plenum pressure.

$$p_{cc} > 0.528 * p_{plenum}$$

$$p_{amb} > 0.528 * p_{cc}$$

$$p_{amb} > 0.528 * (0.528 * p_{plenum})$$

$$p_{plenum} > \frac{p_{amb}}{0.528^2}$$

$$p_{plenum} > \frac{14.7 \frac{lb}{in^2}}{0.528^2}$$

$$p_{plenum} > 52.8 \frac{lb}{in^2}$$

The relationship gives two design requirements, the ramjet must withstand 60 psia in the event of a blockage, and, the important one for the MATLAB modeling, that the pressure inside the ramjet must not exceed $p_{plenum} * 0.528$. Any higher and the back pressure could cause the SSWT to not reach supersonic flow. With the plenum set to 60 psia, the max internal pressure of the ramjet could be 31.7 psia. This limit had a large effect on the inlet design, and effectively limited the angle used

for the inlet.

Another requirement was the fuel choice of Jet-A. The Aerospace Department uses Jet-A in many of its labs, so using it on the ramjet is a reasonable choice. The final major hurdle for the MATLAB model was determining the size of the cross-section, and after some deliberation it was determined to use the entire SSWT test section area would be used for the Ramjet. To allow for the greatest amount of modularity and for ease in construction, the ramjet would attach directly to the SSWT without any changes in area or geometry to the main duct.

The early assumptions relied on inviscid analysis only, with the hopes of proving the differences experimentally. It was understood early on in testing that the results found in Lovell and Gonzales would not be possible with the "Blank" duct of the ramjet. It led to a review of all the initial design capabilities, and found that a 60 psia operating pressure nor the 70 psia operating pressure used for the 2:1 factor of safety for the physical design discussed in chapter 4 would not be enough to produce supersonic flow in the wind tunnel as desired. As discussed in section 2.1, the "Blank" configuration requires a minimum plenum pressure of 79 psia just to fully expand the nozzle. Bringing the shock past where the inlet is placed would require a plenum pressure of 88 psia, which not only decreased the factor of safety of the experiment but was also not sustainable. This led to experiments increasing the plenum pressure to the max it could reach 104 psia, which allowed for only 7 seconds of run time with the plenum pressure above 88 psia. One of the issues here was that the plenum pressure was constantly changing and would never allow the ramjet to stabilize.

The "Blank" duct of the ramjet was not originally modeled, but after initial issues with testing, a better understanding of the blank duct was required. Inviscid analysis would suggest that a constant area duct at the end of a converging-diverging nozzle would maintain constant Mach Flow, until a normal shock occurs at the exit to bring the pressures to balance. The ramjet in the blank setup is essentially a supersonic wind tunnel without a diffuser and the flow through the ramjet duct can be predicted using the method discussed in section 2.1.

Most of the "Blank" duct modeling of the ramjet was intended to match the Fanno flow equations with the data collected during testing. By validating the Fanno flow model in the blank duct, it could be used to further the understanding of the other models. With the current Fanno flow model, the blank duct is expected to have supersonic flow up through station 3 when the plenum pressure is at 88 psi in the plenum. At this point we would expect a shock to occur in front of the pitot probe, however it would not be a 3.305 flow due to the friction. Friction would have brought the

flow down from the 3.305 at the nozzle exit to 1.95 where the shock occurs in front of the pitot tube. The stagnation pressure pressure ratio after the 2.5 feet of supersonic flow is only 0.2880, and the stagnation pressure ratio across the normal shock would be 0.7425, resulting in a total pressure ratio of 0.2139. This is the pressure ratio that would be used in the solving for the Mach number in the ramjet and would result in a reported Mach number of 3.4950. This falsely high Mach reading will be even worse at station 5, where the friction results in another 18% loss in stagnation pressure, giving a mach number of 3.5886.

The static pressure ratios compound in a similar manner to the stagnation pressure ratios. At station 3, the effective static pressure ratio is 9.7290 where the ratio due to the Fanno flow sections accounts for 2.2698, and the oblique shock accounts for 4.2864. With the Fanno flow section before station 5 being assumed subsonic, the static pressure decreases, and the static pressure ratio is 0.8558. The effective static pressure ratio to station 5 is 8.3264. With the plenum pressure starting at 88psia, station 3 stagnation pressure based on the theoretical ratios would be 18.82 psia and the static pressure at station 3 would be 14.99 psia. The Mach number calculated from the isentropic pressure ratio would be 0.5855. Station 5 would have a static pressure of 12.77 psia, a stagnation pressure of 17.36 psia, with a resulting Mach number 0.6769. Th increase in Mach number from station 3 to station 5 is consistent with subsonic Fanno flow relations.

3.2 Inlet

The purpose of the ramjet inlet is to compress the incoming air, and makes up stations 1 through 3 in fig. 2.4. In a jet engine, normally the compressor stage is used to compress the air, but the ramjet does not have this luxury. The ramjet relies on geometry alone to compress the air. To build the theoretical model, oblique shock relations and geometry were applied to flow conditions from the Cal Poly Super Sonic Wind Tunnel (SSWT).

One of the most apparently simple inlet designs for getting subsonic flow in the combustion chamber would be to induce a normal shock in the inlet. The normal shock equation, eq. (2.5), states that the final Mach number decreases as the initial Mach number increases which, if a low Mach number in the combustion chamber was all that was required, would mean that the most effective inlet would simply cause a normal shock. However the static pressure plays a huge role in inlet design, and its relationship across the normal shock is defined by eq. (2.4) which increases as initial Mach number increases.

This relationship also holds for oblique shocks, however oblique shocks can increase the overall rise in pressure by reducing the Mach number gradually. Oblique shocks are created by deflections in the flow, so a ramp inlet would introduce the oblique shocks necessary to increase the pressure.

$$\tan\theta = 2\cot\beta\left[\frac{M_i^2\sin^2\beta - 1}{M_i^2(\gamma + \cos 2\beta + 2})\right] \tag{3.5}$$

The ramp inlet deflection angle can be solved for using the oblique shock equation, eq. (3.5), however an iterative method is required to solve for β from a given inlet angle θ. [9]

Once β is solved for, the normal shock equation, eq. (2.5), can be applied to the oblique shock by finding the Mach component of the flow normal to the oblique shock.

$$M_{n,i} = M_i \sin\beta \tag{3.6}$$

The normal component of the Mach number before the oblique shock can be found by eq. (3.6), and when applied to eq. (2.5) results in the normal Mach component of the flow after the oblique shock, $M_{n,f}$. Similarly, the static pressure ratio across the oblique shock can be determined using eq. (2.4), and the stagnation pressure ratio using eq. (2.2), if M_i is substituted with $M_{n,i}$. Because the normal Mach component to the oblique shock is smaller than the total Mach number, the static pressure ratio across the shock is smaller, but the stagnation pressure lost across the shock is also less. [9]

The static and stagnation pressures do not have normal components, but the Mach number of the flow does.

$$M_f = \frac{M_{n,f}}{\sin(\beta - \theta)} \tag{3.7}$$

The final Mach number behind the oblique shock can be solved from the normal component with eq. (3.7). This process can be completed for multiple oblique shocks in a row depending on the Mach number of the flow and angle change of the flow. [9]

A single ramp was chosen as the inlet geometry for the initial design. A single ramp will produce a single oblique shock from the ramp and a second oblique shock will reflect off opposite wall from the ramp when the flow is turned again. A final normal shock will occur at the throat of the inlet to make the supersonic flow subsonic before it expands back into the combustion chamber.

For a 2-D ramp inlet, the angle and length dictate the shape of the ramp. The angle of the ramp is what causes oblique shocks to form in the inlet and the angle is determined by the back pressure requirement from the SSWT. However the length of the ramp is determined by the oblique shocks. The end of the ramp occurs at the intersection of the second oblique shock and the ramp.

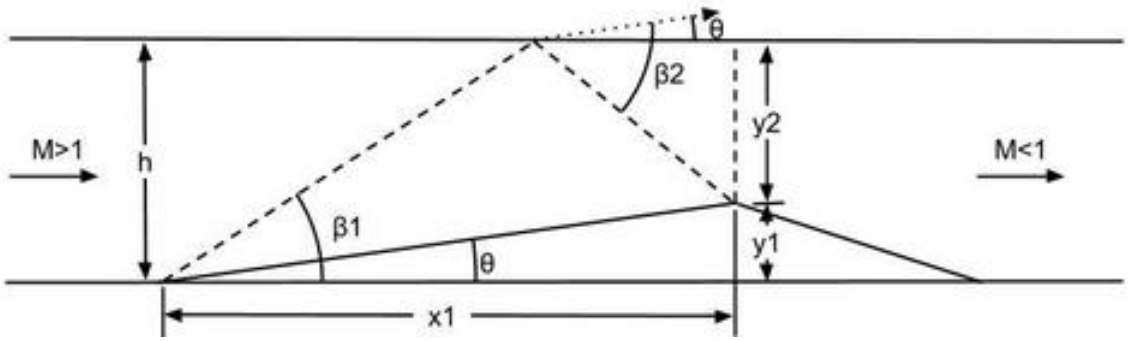

Figure 3.1: The Inlet Shocks and Reflections

The first oblique shock occurs at an angle β_1, due to the ramp angle θ. The flow in the post shock region will be at a lower Mach number, and a second oblique shock will occur at an angle β_2 from the deflection of the flow back to horizontal by the ceiling, also at angle θ to the deflected flow. This is visually represented in fig. 3.1. We can solve for the length and height of the ramp at certain deflection angles using the following relations between the angles in 3.1.

$$\begin{bmatrix} \frac{1}{\tan\theta} & \frac{1}{\tan(\beta_2-\theta)} \\ 1 & 1 \end{bmatrix} * \begin{bmatrix} y_1 \\ y_2 \end{bmatrix} = \begin{bmatrix} \frac{h}{\tan\beta_1} \\ h \end{bmatrix} \tag{3.8}$$

The relations in eq. (3.8) can be used to solve for the ramp height, y_1, and the height of the inlet throat, y_2, where h is the height of the tunnel.

$$x_1 = \frac{y_1}{\tan\theta} \tag{3.9}$$

With these heights solved for the x location of the throat is simple trigonometry, represented in eq. (3.9). In order to determine if the inlet angle will meet the back pressure requirement the normal shock that will occur at the top of the ramp, and decompression from the inlet exit must also be modeled.

The ideal location for the normal shock is at the top of the inlet ramp, much like the shock in the diffuser of the SSWT discussed in section 2.1. The throat is the ideal location for the normal shock so that the expansion that occurs on the backside of the inlet is slowing the flow even more. If the shock were to move down the exit of the inlet, the expansion would increase the Mach number instead and result in a more powerful normal shock.

The static and stagnation pressures are not the only pieces of information that need to be tracked through this series of shocks. Shocks are considered adiabatic processes when modeled, the

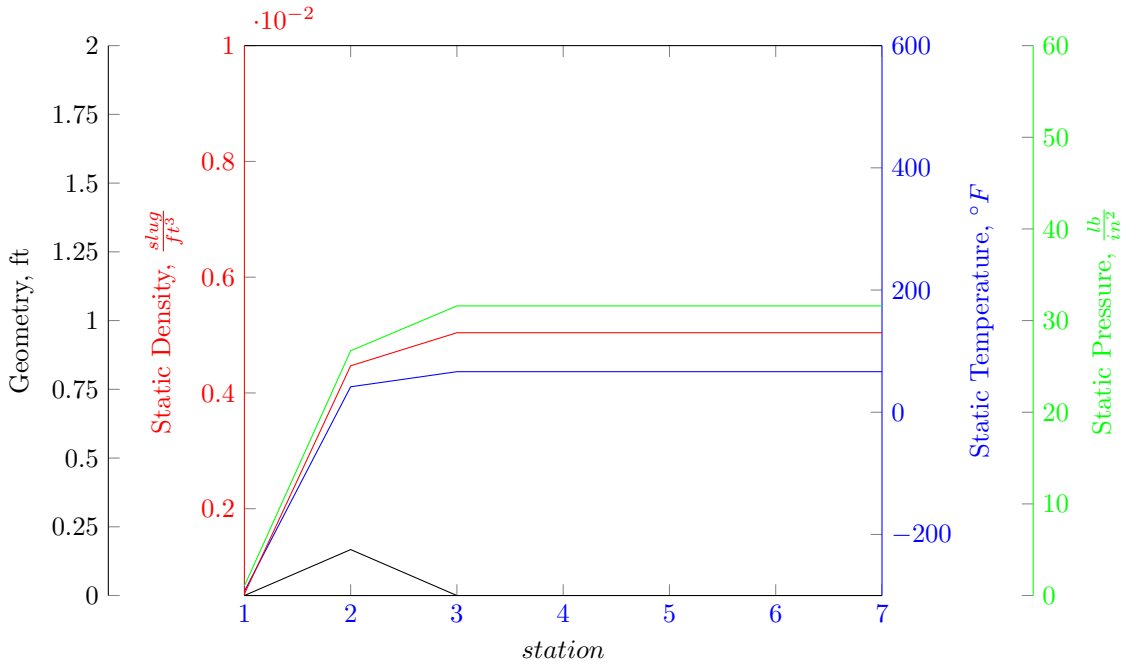

Figure 3.2: Ramjet Static Properties with the Inlet

assumption that air is a perfect gas means that stagnation temperature is constant across a normal or oblique shock.

$$\frac{\rho_{02}}{\rho_{01}} = \frac{p_{02}}{p_{01}} * \frac{T_{01}}{T_{02}} \tag{3.10}$$

Stagnation density can be determined from the ratios of stagnation temperature and pressure, as shown in eq. 3.10, however since the stagnation temperature is constant across a shock, stagnation density has the same ratio as stagnation pressure.

$$\frac{\rho_2}{\rho_1} = \frac{(\gamma+1)M_{n,i}^2}{2+(\gamma-1)M_{n,i}^2} \tag{3.11}$$

Static density can be solved with the initial normal component of Mach, $M_{n,i}$, by using eq. (3.11). [9]

Unlike stagnation temperature, static temperature is not constant, isentropic relations suggest that if the Mach number changes across a shock, and the stagnation temperature remains constant, then the static temperature must change. This means that each shock in the inlet produces a change in each static property. Static temperature can be solved by similar methods to stagnation density.

$$\frac{T_1}{T_2} = \frac{p_1}{p_2} * \frac{\rho_2}{\rho_1} \tag{3.12}$$

Using the relationship between pressure, density, and temperature in a perfect gas, eq. (3.12) can be used to solve for static temperature. [9]

Station	Geometry (ft)	$p\left(\frac{lb}{in^2}\right)$	$T\,(^\circ F)$	$\rho\left(\frac{slug}{ft^3}\right)$
1	0	1.0458	-293.0284	$5.2646 \cdot 10^{-4}$
2	0.17	26.7066	41.6531	$4.4691 \cdot 10^{-3}$
3	0	31.6054	66.366	$5.0404 \cdot 10^{-3}$
4	0	31.6054	66.366	$5.0404 \cdot 10^{-3}$
5	0	31.6054	66.366	$5.0404 \cdot 10^{-3}$
6	0	31.6054	66.366	$5.0404 \cdot 10^{-3}$
7	0	31.6054	66.366	$5.0404 \cdot 10^{-3}$

Table 3.1: Static Property Values with the Inlet

From these relationships, the inviscid analysis shows that after the inlet, the properties remain constant. With no change in the flow, due to mass influx, geometry change, or heat addition, there should be no change in the properties, as demonstrated in fig. 3.2. Because of the use of multiple shocks, the lines from station 1 to 2 in fig. 3.2 would more accurately have three steps, indicating each change accross a shock. Due to the use of stations instead of an actual distance scale, only the initial condition, station 1, and the final condition, station 2, are presented. The static properties in fig. 3.2 do not change after station 3, the end of the ramjet inlet. Without friction, there is nothing to change the properties.

The static pressure was key to the design of the inlet as mentioned above, and the green line for static pressure in fig. 3.2 does not exceed 31.7 psia. The exact data for fig. 3.2 is visible in table 3.1. This is accomplished by a 10° inlet ramp, and an isentropic expansion of subsonic flow on the inlet exit. The throat height would be equal to 2.78 in., and the location of station 2 would occur at 1 ft. and 3.78 in. (1.31 ft.) into the ramjet. Instead of optimizing for the exact desired inlet angle, the angles were chosen in degree increments to ensure that the design could be manufactured. These dimensions were used to design the inlet as discussed in section 4.1.

Much like the static properties, the stagnation properties in fig. 3.3 remain constant, but after station 2 instead of station 3. The stagnation properties are constant after the inlet throat at station 2 because the exit of the inlet is governed by isentropic relations, where stagnation properties remain constant. Stagnation temperature, the blue line, is constant across all of fig. 3.3 due to the adiabatic assumptions involved in the normal and oblique shock relations. The data associated with fig. 3.3 is visible in table 3.2, and shows the same trends. Early on in the design of the inlet code, the

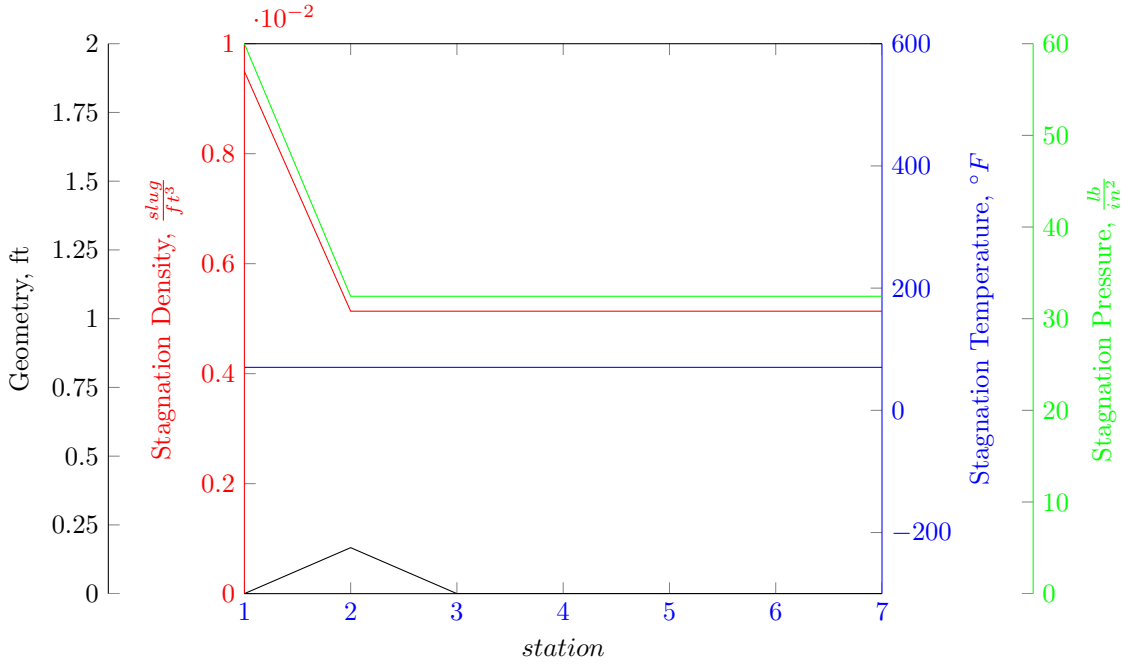

Figure 3.3: Ramjet Stagnation Properties with the Inlet

Station	Geometry (ft)	$p_0\left(\frac{lb}{in^2}\right)$	$T_0\,(^\circ F)$	$\rho_0\left(\frac{slug}{ft^3}\right)$
1	0	60	70.33	$9.4972 \cdot 10^{-3}$
2	0.17	32.4469	70.33	$5.1359 \cdot 10^{-3}$
3	0	32.4469	70.33	$5.1359 \cdot 10^{-3}$
4	0	32.4469	70.33	$5.1359 \cdot 10^{-3}$
5	0	32.4469	70.33	$5.1359 \cdot 10^{-3}$
6	0	32.4469	70.33	$5.1359 \cdot 10^{-3}$
7	0	32.4469	70.33	$5.1359 \cdot 10^{-3}$

Table 3.2: Stagnation Property Values with the Inlet

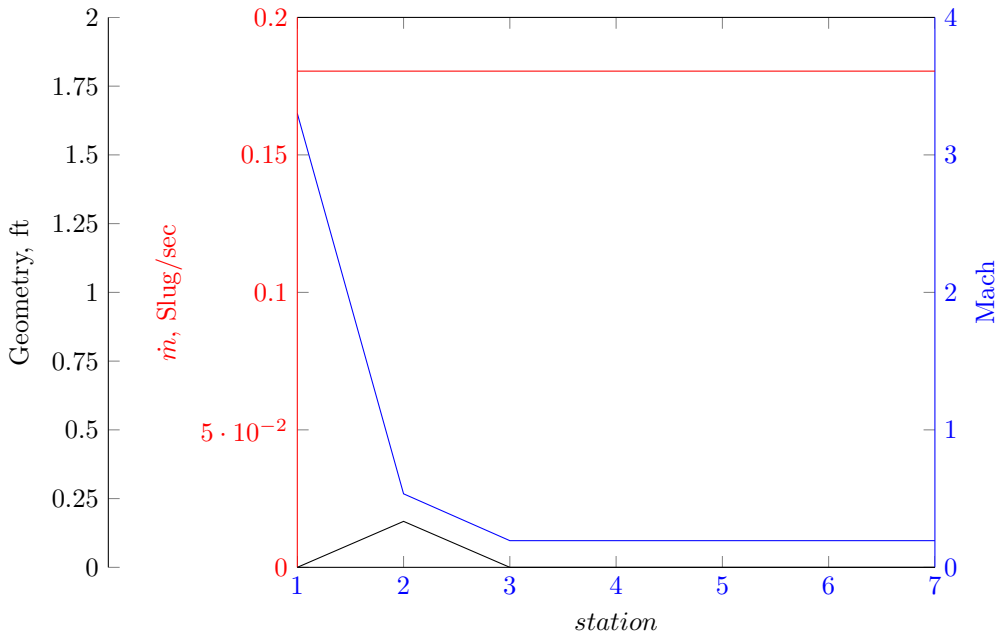

Figure 3.4: Ramjet Mass Flow and Mach with the Inlet

stagnation temperature was calculated in different ways to determine it was constant, to ensure that the equations were being used properly.

The other cue that the equations were not used correctly was the mass flow would not remain constant. Figure 3.4 shows the constant mass flow rate as well as the change in Mach number across the inlet. Similar to the static and stagnation properties, Mach number would also be more accurately stepped between stations 1 and 2 in fig. The mass flow is constant, visible in both fig. 3.4 and table 3.3, because no mass is added to the system and none is removed. The Mach number

Station	Geometry (ft)	Mach	$\dot{m}\left(\frac{slug}{sec}\right)$
1	0	3.3	0.1805
2	0.17	0.53	0.1805
3	0	0.19	0.1805
4	0	0.19	0.1805
5	0	0.19	0.1805
6	0	0.19	0.1805
7	0	0.19	0.1805

Table 3.3: Mass Flow and Mach Values with the Inlet

changes from the 3.3 of the SSWT to the 0.53 Mach after the normal shock of the inlet, and the 0.19 Mach after the expansion from the inlet. Table 3.3 is a collection of the data in fig. 3.4 at each station, as it would be collected during a "blank" run setup.

The ideal properties of the ramjet with the inlet installed are detailed in figs. 3.2, 3.3, and 3.4, but the potential for these properties to was quickly lost during actual testing. Due to many of the assumptions being changed, the ideal scenario for the inlet was quickly found to be lacking. One of the main issues was the increase in pressure causing the normal shock in the inlet throat to be swallowed by the inlet. The normal shock moving down the exit of the inlet means the flow can increase in speed, like with the diverging part of the converging-diverging nozzle, and resulting in a larger pressure loss begin the inlet than desired. When the shock occurs at the top of the ramp, the normal shock is a result of 2.30 flow, but if the normal shock moves all the way out of the inlet, the Mach number could increase up to 3.22 Mach before it shocks. The static pressure ratio across the ideal inlet is 25.5382 with a stagnation pressure ratio of 0.5408, but the pressure ratio across the swallowed normal shock inlet is only 12.4427 with a stagnation pressure ratio of only 0.2513. This unstable plenum pressure can cause significant issues with the operation of the ramjet. The best course of action to get a reasonable understanding of the ramjet's performance characteristics would be to increase the run time at the ideal pressure.

Factoring Fanno flow into the issue does alter the affects of the unstable plenum pressure. With the Fanno flow approximation, the inlet does not see 3.305 Mach, it actually sees closer to 2.61 Mach. With the ideal location of the normal shock in the inlet throat, the stagnation pressure ratio would be 0.7749, but the static pressure ratio would only be 12.15 across the inlet. The resulting static pressure ratio at station 3 would be 17.8442 which would be seen as a 2.76 Mach number, and the stagnation pressure ratio would be 0.4016. The isentropic pressure ratio would give a post inlet Mach number of 0.62 at station 3.

Station 5 would see similar changes from the "Inlet" setup as occurred in the "blank" setup. The Mach number at station 5 will appear higher, 2.87 based on the stagnation pressure ratio, and 0.71 Mach based on the isentropic pressure ratio.

3.3 Combustor

The combustor design was intended to ignite Jet-A to add energy to the flow. The modularity should allow for other options to be tested, like a heat exchanger or other novel ideas. For the base

design though, a simple igniter and fuel injector system was desired. Early designs of the combustor used the fuel flow rate that Selin predicted, but when Stone found the fuel injector did not work with the fuel system developed by Selin the new fuel system numbers were used. [30] [31] Testing of the new fuel system is covered in section 5.1, and the design is covered in section 4.1. Due to basing the ramjet design on the Selin fuel system, the predicted temperature rise was considerably higher than what could be achieved with the new system. [30] The material choices of the ramjet allowed for combustor temperatures of $1000°F$ for a factor of safety of 2, but the new fuel system cannot achieve the required flow to reach this temperature.

The modeling of the combustor began with attempting to model the fuel mixing with the incoming air. The ratios of each parameter were tracked through the inlet, and a similar approach is used in the combuster model to determine the station parameters. The isentropic relations were adapted to account for a change in the ratio of specific heats, γ, instead of a change in area or pressure. Similar to the other isentropic relations, this determined how the resulting gamma and increased mass flow changed the properties inside the combustor section. No significant flow effects occurred due to the subtle change of $\gamma = 1.4$ to $\gamma = 1.33$, and the changes were overshadowed by the increase in mass flow which resulted in an increase in density. The mass flow of the air and fuel mixture, $\dot{m}_{af}$, can be determined by the combining the incoming mass flow of air to the mass flow of fuel, which is determined by the fuel system limitations.

Like other mass flow, the relation between $\dot{m}_{af}$ and density ρ can be described in the following equation:

$$\dot{m}_{af} = \rho * V * A \tag{3.13}$$

Determining the velocity can be done by solving for Mach, using the pressure relations, and speed of sound, using the temperature. Then with the known cross-sectional area of the SSWT, the density of the air fuel mixture is now solved for.

With the required information related to the flow of the air fuel mixture known, Rayleigh line flow was used to determine the effect of burning fuel to heat up the flow. The basic equations for Rayleigh flow determine the ratio of static pressure at the current conditions to static pressure at the choked condition. Rayleigh flow equations also determine the the same ratios for stagnation

pressure, static and stagnation temperature and velocity.

$$\frac{p}{p^\star} = \frac{1+\gamma}{1+\gamma M^2} \tag{3.14}$$

$$\frac{T}{T^\star} = \frac{(1+\gamma)^2 M^2}{(1+\gamma M^2)^2} \tag{3.15}$$

$$\frac{V}{V^\star} = \frac{(1+\gamma) M^2}{1+\gamma M^2} \tag{3.16}$$

$$\frac{p_0}{p_0^\star} = \left(\frac{1+\gamma}{1+\gamma M^2}\right)\left[\frac{2+(\gamma-1)M^2}{\gamma+1}\right]^{\frac{\gamma}{\gamma-1}} \tag{3.17}$$

$$\frac{T_0}{T_0^\star} = \frac{\left((1+\gamma)M^2\left(2+(\gamma-1)M^2\right)\right)}{\left(1+\gamma M^2\right)^2} \tag{3.18}$$

Equations 3.14 to 3.18 can be used together to solve for the final conditions of a flow if one of the final conditions is known. [19] Once one parameter is known, the ratio of the final parameter to the initial parameter can be used with the ratio of the initial parameter to the choke parameter to find the final parameter to the choke parameter. The ratio of the final parameter to the choke parameter can then be used to solve for the final Mach number. This involves either a look up table or an iterative solution like what is used in the ramjet model, but once the Mach number is solved, the rest of the parameter final to initial ratios.

In the case of the ramjet, the final stagnation temperature can be solved based on the heat added to the flow.

$$q = C_p(T_{0f} - T_{0i}) \tag{3.19}$$

The q in equ. 3.19 is the heat transferred into the system. This quantity is found by using the energy density of the fuel used, Jet-A, and the fuel-to-air ratio. The fuel system produces 0.0033 gal/sec through the single injector, which results in a fuel mass flow of $6.27e^{-4}$ slug/sec. The air flow through the ramjet is 0.1805 slug/sec, and the combination of the energy density of the Jet A results in an overall heat addition of 64.24 BTU/lbm. The result of the Rayleigh flow relations are dimensionless ratios resulting from final mach number determined by the stagnation temperature ratio.

Rayleigh Line flow is used to determine all the conditions directly downstream from the combustion chamber. In the MATLAB code, a sanity check is done to determine the final Mass Flow rate to ensure that it is still equal to the incoming airflow and the fuel flow. The flow is also increased in Mach number, which increases from 0.19 to 0.22, and the speed of sound is predicted to increase from

1,090 $\frac{ft}{s}$ to 1,210 $\frac{ft}{s}$. This means the velocity also increases from 213 $\frac{ft}{s}$ to 264 $\frac{ft}{s}$ as it approaches the nozzle.

The main data to be collected from the ramjet is in pressure and temperature data at station 3 and station 5. The minor influx of fuel is good for safety, but not ideal for making a running engine. The heat addition will result in an increase of $115°F$, from the $67°F$ after the inlet to the $182°F$ of station 5. Although the $182°F$ wont be setting any records or pressing any limits, it will be enough to make the ramjet sustain itself.

Like the inlet, the combustor does not take into account friction when it is modeled with Rayleigh flow. However, unlike the inlet, there is not alternate mode of operation, either the fuel ignites and the Rayleigh flow relations take over, or the fuel does not ignite and the flow slows similar to what occurred with the post inlet section. The combustor does not have an equivalent to the inlets ideal position for the normal shock, the combustor is either on or off. The combustor is also not intended to be run without the nozzle, however it is possible. The important data to watch for in the combustor is the temperature, which should increase if combustion is present. The temperatures will be different from station 3 to station 5 during any run due to the friction effects, but station 5 should be less than station 3. When the temperature at station 5 begins to increase, combustion will have started in the combustor.

3.4 Nozzle

The ideal nozzle was relatively simple to implement in code. It relies on isentropic relations to determine throat area required to choke the flow and then isentropic relations to expand the flow to atmospheric pressure. No attempt was made to determine a method of characteristics solution, it will be left up to future students to try to optimize the nozzle to better suit the ramjet. In the event that the nozzle needed to be adjusted, it was built to allow for adjustment of the throat height and the exit height. The nozzles construction is detailed in section 4.1.

The throat area is determined by using the parameters from the end of the combustor, in particular the Mach number. From the post combustor Mach number, eq. (2.1) can be solved to determine the area change required to choke the flow. The higher the Mach number after the combustor, the less area change is required, which is fortunate because in the even that the combustor does not fire, and the mach number is lower than the design point, the nozzle will not restrict the mass flow. Higher mach numbers at the end of the combustor means a greater quantity of heat was

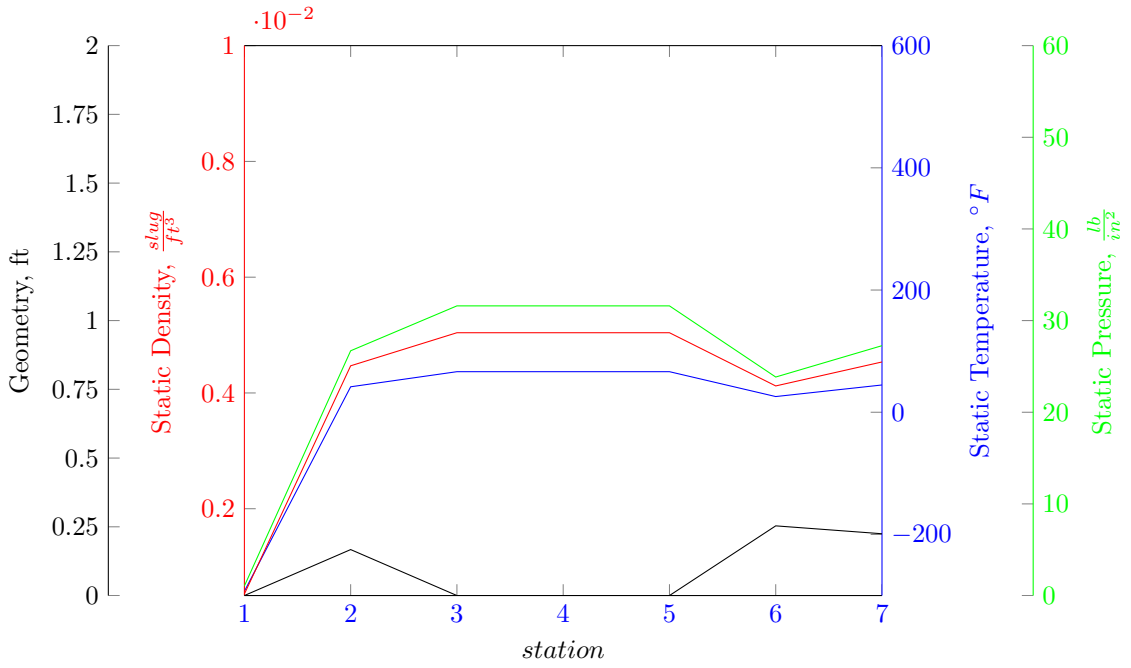

Figure 3.5: Ramjet Static Properties with the Inlet and Nozzle

added to the flow.

Once the flow is choked, the pressure inside the combustor takes over and a similar situation to the SSWT converging-diverging nozzle occurs. The flow chokes at the throat and supersonic flow expands out the end of the nozzle to the atmosphere. This expansion is also isentropic, and different approaches can be used to determine how far to expand the nozzle. In order to minimize the $(p_e - p_a)A_e$ in eq. (3.1), the exit area can be sized to make $p_e = p_a$ which will drive the term to zero. This would be the optimally expanded nozzle.

Another approach is to simply expand the nozzle out to the max area of the ramjet duct. This case would be over-expanded, and $p_e \neq p_a$, which could form separation in the nozzle. One way that we would see an improper matched nozzle to the flow would be if the nozzle were designed to match the combustor in operation, but the combustor fails to light.

The inviscid analysis of the nozzle shows that the properties remain constant between the inlet and nozzle but change once the flow reaches station 5. The improper nozzle shape is evident in fig. 3.5 by how the static properties decrease from station 5 to station 6, but increase again out to station 7. The static properties in fig. 3.5 make this dip at the nozzle throat because the flow is not choked, so the flow speeds up to the throat, but does not reach sonic flow. The subsonic flow is then expanded which slows it down and causes the properties to increase again.

Station	Geometry (ft)	$p\left(\frac{lb}{in^2}\right)$	$T\,(^\circ F)$	$\rho\left(\frac{slug}{ft^3}\right)$
1	0	1.0458	-293.0284	$5.2646 \cdot 10^{-4}$
2	0.17	26.7066	41.6531	$4.4691 \cdot 10^{-3}$
3	0	31.6054	66.366	$5.0404 \cdot 10^{-3}$
4	0	31.6054	66.366	$5.0404 \cdot 10^{-3}$
5	0	31.6054	66.366	$5.0404 \cdot 10^{-3}$
6	0.25	23.8423	25.6635	$4.1213 \cdot 10^{-3}$
7	0.22	27.2627	44.6133	$4.5354 \cdot 10^{-3}$

Table 3.4: Static Property Values with the Inlet and Nozzle

This nozzle is setup for a higher Mach number flow from the combustor so the nozzle throat is too large to choke the flow. The exact data for fig. 3.5 is visible in table 3.4. Unlike the inlet, the nozzle is not designed to the angle, and is instead design to the areas of the throat and the exit. The angles for the nozzle depend on the areas, but the physical nozzle was designed to have a 25° angle to the throat and a 15° angle to the exit when setup for the optimum nozzle during a hot fire test. These angles were chosen based on conic rocket nozzles, and the optimum design was constructed before it was discovered that the fuel system was inadequate to produce these results. [24] These dimensions are what helped finalize the design. The nozzle angle will no longer be as designed due to the lower heat addition of the combustor and the optimal nozzle having to change.

The stagnation properties in fig. 3.6 look exactly the same as in fig. 3.3 The stagnation properties are constant after the inlet throat at station 2 because all the other processes that are applied to the flow are isentropic and stagnation properties remain constant. Even though the nozzle is not the perfect design for the situation being modeled in fig. 3.6, the flow is always expected to be isentropic. The values in table 3.5 are all the same as table 3.2 with the exception of the geometry column. The nozzle throat height and exit height are visible in fig. 3.6, but the angles are not accurate because the x-axis is stations and not distance. This is why the inlet "Geometry" in both figs. 3.6 and 3.3 appears symmetrical when it is actually not.

Like earlier, the best indicator of poor use of functions is a non-constant mass flow line. Figure 3.7 shows the constant mass flow rate indicating that at least that aspect is correct. The Mach number line in fig. 3.7 gives another confirmation of the strange behavior of the static properties in fig. 3.5. Also visible in table 3.6, the Mach number increases up to station 6 and decreases to

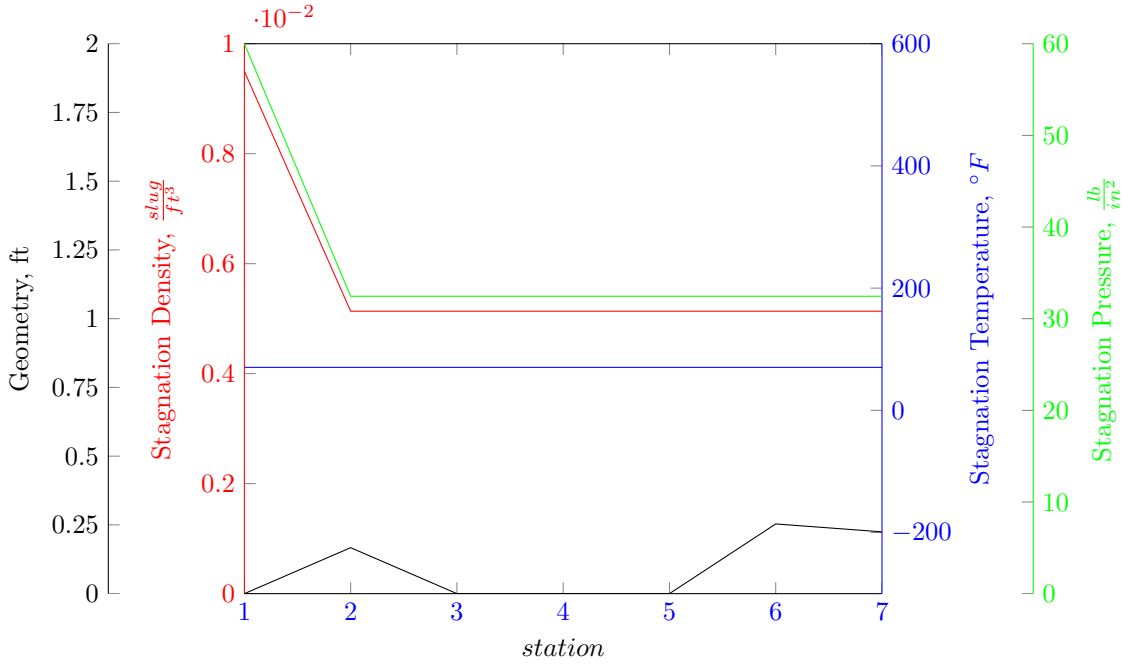

Figure 3.6: Ramjet Stagnation Properties with the Inlet and Nozzle

Station	Geometry (ft)	$p_0\left(\frac{lb}{in^2}\right)$	$T_0\,(^\circ F)$	$\rho_0\left(\frac{slug}{ft^3}\right)$
1	0	60	70.33	$9.4972 \cdot 10^{-3}$
2	0.17	32.4469	70.33	$5.1359 \cdot 10^{-3}$
3	0	32.4469	70.33	$5.1359 \cdot 10^{-3}$
4	0	32.4469	70.33	$5.1359 \cdot 10^{-3}$
5	0	32.4469	70.33	$5.1359 \cdot 10^{-3}$
6	0.25	32.4469	70.33	$5.1359 \cdot 10^{-3}$
7	0.22	32.4469	70.33	$5.1359 \cdot 10^{-3}$

Table 3.5: Stagnation Property Values with the Inlet and Nozzle

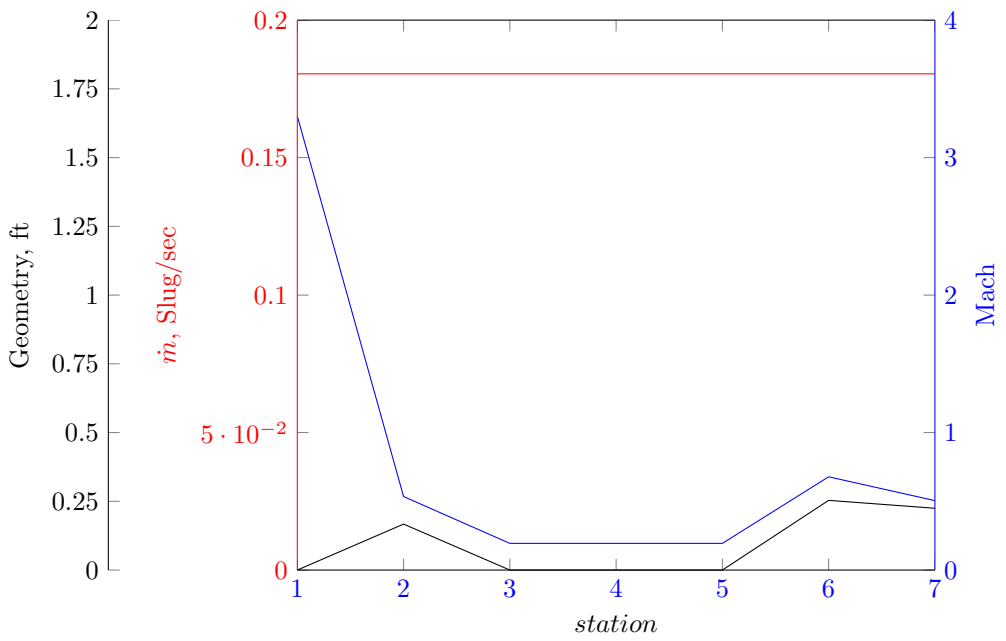

Figure 3.7: Ramjet Mass Flow and Mach with the Inlet and Nozzle
[Ramjet Mass Flow and Mach with the Inlet and Nozzle]The Mach and Mass Flow at each ramjet station when the inlet and nozzle are installed.

Station	Geometry (ft)	Mach	$\dot{m}\left(\frac{slug}{sec}\right)$
1	0	3.3	0.1805
2	0.17	0.53	0.1805
3	0	0.19	0.1805
4	0	0.19	0.1805
5	0	0.19	0.1805
6	0.25	0.68	0.1805
7	0.22	0.5	0.1805

Table 3.6: Mass Flow and Mach Values with the Inlet and Nozzle

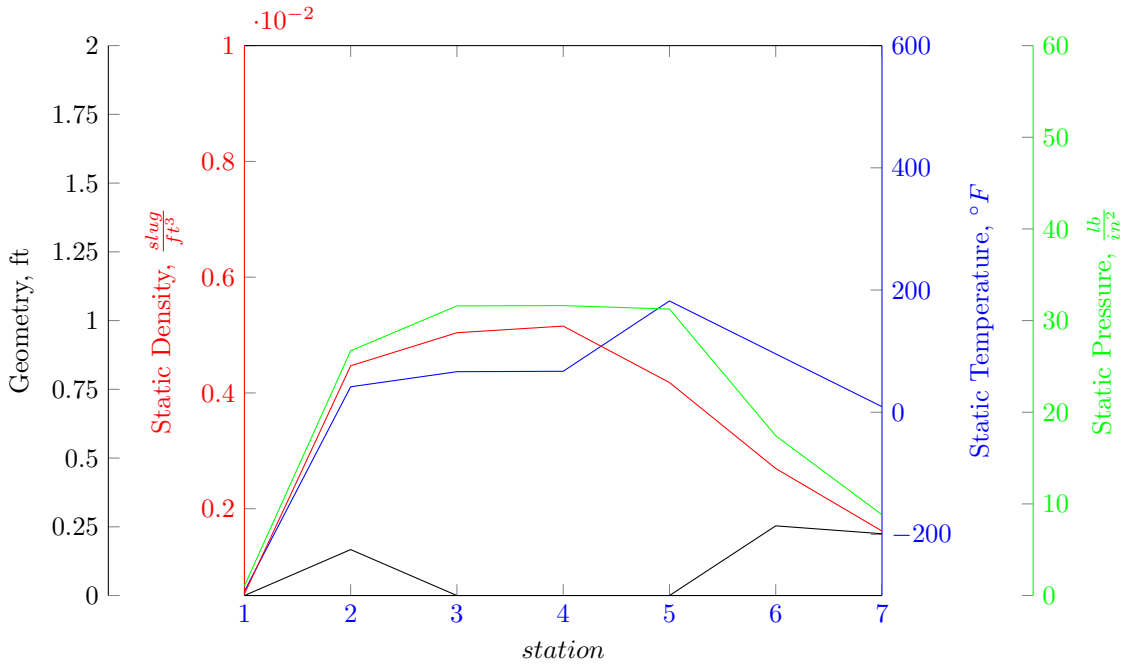

Figure 3.8: Ramjet Static Properties for a Hot fire

station 9, which is exactly what was predicted from the static parameters in fig. 3.5. This behavior is only present because the nozzle is designed for the hot flow case, and the cold flow case does not produce a high enough Mach number in the combustor to allow for choked flow in the nozzle in the inviscid analysis.

The inviscid analysis of the hot run shows that the properties no longer remain constant at any section of the flow. The proper nozzle shape is evident in fig. 3.8 by how the static properties continue to decrease from station 5 to station 7. The static properties in fig. 3.8 do have a slight bend above station 6, the nozzle throat, but this indicates that the flow is changing from subsonic flow to supersonic. The subsonic flow in the combustion chamber is choked at station 6 and then expands supersonically after the throat. This increase in mach number is represented by the decrease in static properties.

. Unlike the inlet and nozzle, the data for fig. 3.8, found in table 3.7, is constantly changing between each station. As with the nozzle, the static properties increase in the inlet, and then continue to increase as the inlet expands into the combustion chamber. What changes between fig. 3.8 and the others is the fuel inject that occurs between station 3 and 4, which is visible in the minor changes in the properties value between those stations. As was mentioned earlier, the density takes in most of the change in terms of the static properties.

Station	Geometry (ft)	$p\left(\frac{lb}{in^2}\right)$	$T\,(^\circ F)$	$\rho\left(\frac{slug}{ft^3}\right)$
1	0	1.0458	-293.0284	$5.2646 \cdot 10^{-4}$
2	0.17	26.7066	41.6531	$4.4691 \cdot 10^{-3}$
3	0	31.6054	66.366	$5.0404 \cdot 10^{-3}$
4	0	31.6345	67.0063	$5.1549 \cdot 10^{-3}$
5	0	31.2594	182.0725	$4.1804 \cdot 10^{-3}$
6	0.25	17.434	95.5201	$2.695 \cdot 10^{-3}$
7	0.22	8.82	9.1602	$1.6146 \cdot 10^{-3}$

Table 3.7: Static Property Values for a Hot fire

The actual combustion effects are visible between stations 4 and 5 in fig. 3.8 and table 3.7. The sharp rise in temperature between stations 3 and 5 is exactly what should be recorded by the thermocouples during a hot run. Due to the constant pressure heating assumption from eq. (3.19), the pressure remains the most constant between stations 4 and 5, and a drop in density makes up for the rise in temperature.

The stagnation properties in fig. 3.9 have changed now that the combustor is operational. The stagnation properties are the same as the Inlet and Nozzle configuration up to station 4 because the fuel mixing was modeled isentropically. The constant pressure heating from station 4 to 5 has similar effects on the stagnation properties as the static properties. The stagnation temperature will rise, which is understandable since eq. (3.19) acts directly on the stagnation temperature. Stagnation density takes a hit as it did with static density, and the stagnation pressure remains mostly constant. There are no changes from station 5 and on because the nozzle is still being modeled isentropically, even though now it is choked flow. The geometry values in table 3.8 are the same as table 3.5 but the other columns now vary with the hot run. The nozzles in figs. 3.9 and 3.6 are the same nozzle, which was designed for the hot flow in this model. The nozzle still produces no change in the stagnation values because of the isentropic models used to predict the nozzles characteristics. The real nozzle was originally designed for a much larger heat addition, but the adjustable height of the nozzle will allow the nozzle to match the design in this model.

Unlike the other mass flow figures, the mass flow in fig. 3.10 does in fact change during the addition of the fuel between stations 3 and 4. The model also predicts a slight increase in Mach number with the addition of the fuel, but the increase from stations 4 to 5 is easier to make out.

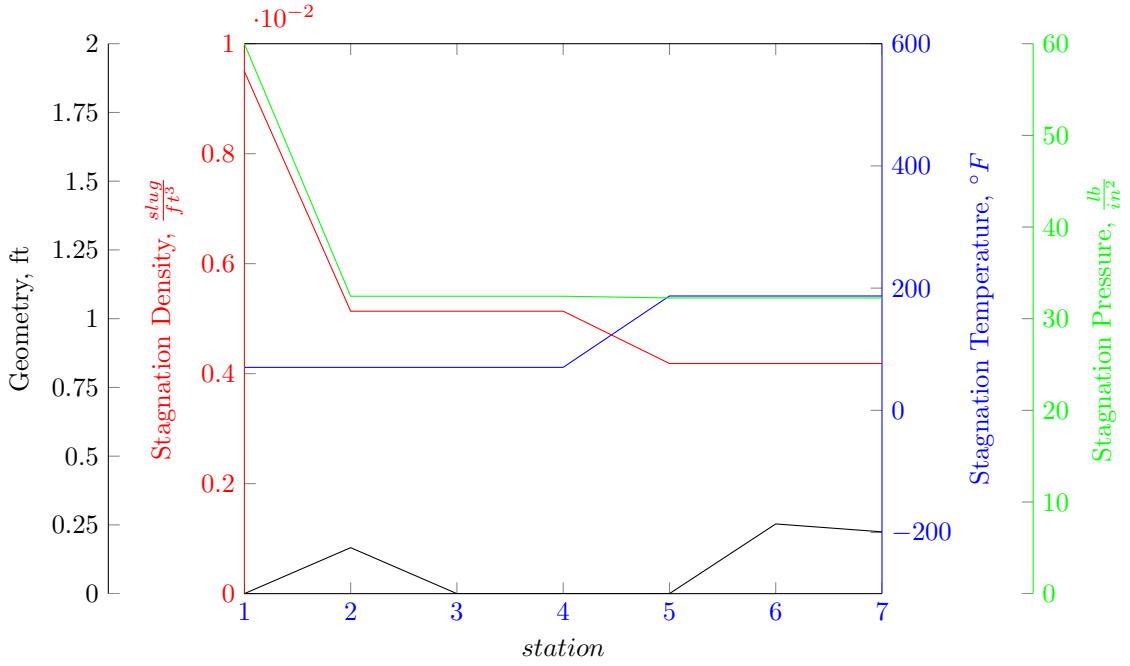

Figure 3.9: Ramjet Stagnation Properties for a Hot fire

Station	Geometry (ft)	$p_0\left(\frac{lb}{in^2}\right)$	$T_0\,(^\circ F)$	$\rho_0\left(\frac{slug}{ft^3}\right)$
1	0	60	70.33	$9.4972 \cdot 10^{-3}$
2	0.17	32.4469	70.33	$5.1359 \cdot 10^{-3}$
3	0	32.4469	70.33	$5.1359 \cdot 10^{-3}$
4	0	32.4469	70.33	$5.1359 \cdot 10^{-3}$
5	0	32.2635	187.1264	$4.1847 \cdot 10^{-3}$
6	0.25	32.2635	187.1264	$4.1847 \cdot 10^{-3}$
7	0.22	32.2635	187.1264	$4.1847 \cdot 10^{-3}$

Table 3.8: Stagnation Property Values for a Hot fire

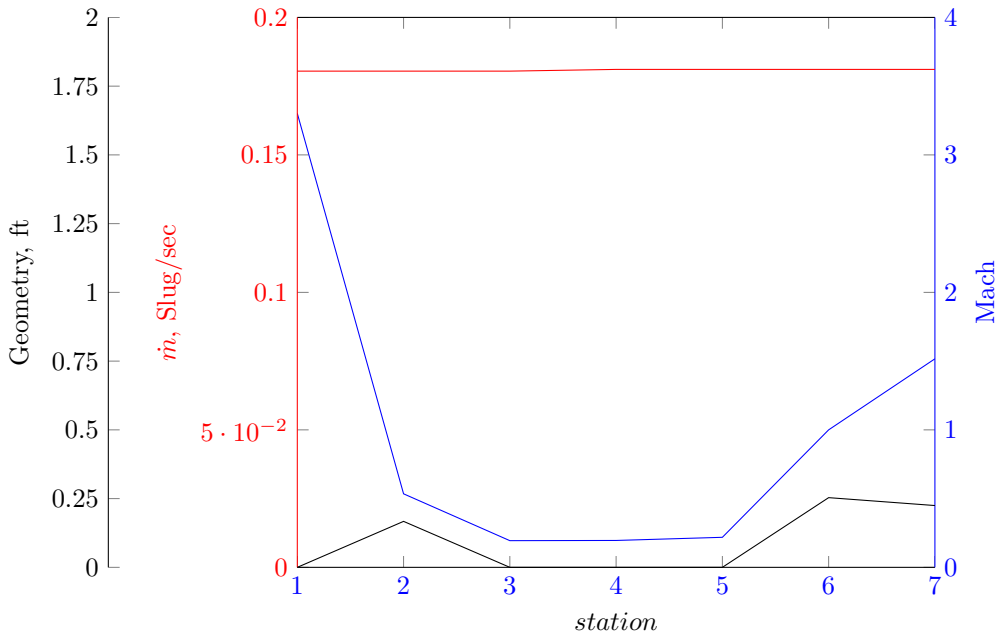

Figure 3.10: Ramjet Mass Flow and Mach for a Hot fire

This rise in Mach number from stations 4 to 5 is a result of the combustion occurring in the ramjet. Although minor, table 3.9 does indicate a change mass flow from stations 3 to 4. Table 3.9 also indicates a change in Mach number between each and every station, with very gradual changes from station 3 to 5, and with Mach 1 at the throat of the nozzle as designed.

The Fanno flow approximation can be completed for both the hot and cold run. Although the hot run has separate approximations for each area of ramjet, the Fanno flow can be applied to the 1 ft. of SSWT test section between the SSWT converging-diverging nozzle end and the inlet. For both

Station	Geometry (ft)	Mach	$\dot{m}\left(\frac{slug}{sec}\right)$
1	0	3.3	0.1805
2	0.17	0.53	0.1805
3	0	0.19	0.1805
4	0	0.2	0.1811
5	0	0.22	0.1811
6	0.25	1	0.1811
7	0.22	1.52	0.1811

Table 3.9: Mass Flow and Mach Values for a Hot fire

the hot and cold flow models, this results in an initial Mach number at the inlet of only 2.61. This lowered initial mach number makes the inlet's ramp not line up correctly with the oblique shocks, and makes the inlet less effective. This results in a higher station 3 Mach number of 2.66 for both hot or cold.

From here the two models diverge, the cold flow moves through the combustion chamber as a Fanno Flow calculation, but the hot flow uses its individual approaches. For the cold test, the Fanno Flow predicts that the Mach number will increase by station 5 to 0.27 Mach which is a greater Mach number than the inviscid hot flow approximation. What results is the flow over the nozzle chokes before the throat. This effect actually "breaks" the isentropic code used to analyze it because the there is no isentropic approximation of what occurs when you choke the flow with a smaller area than is necessary. What occurs is that the mass flow out of the nozzle decreases, and the essentially the Fanno Flow predicts that the combustor chamber pressure will start to build up as the run continues. What is interesting about this approximation is that the friction appears to have a greater affect on the flow than the minuscule amount of fuel that was intended for the hot flow test. At first glance this claim would appear correct until comparing the actual Mach number change from 3 to 5 for both approximations.

The friction approximation of the cold flow results in a 1.02 M_5 to M_3 ratio where the inviscid hot flow approximation accounts for a 1.17 M_5 to M_3 ratio. The issue then lies with the initial drop in Mach number before the inlet. Both the cold and hot Fanno Flow approximations result in an improperly choked flow at the nozzle. Redesigning the nozzle to handle the hot Fanno Flow approximation will fix the "broken" function, but will result in the inviscid hot analysis no longer reaching sonic flow a the nozzle throat. The results in fig. 3.8 would look more similar to the nozzle response that the inviscid cold flow nozzle approximation had in fig. 3.5.

Chapter 4

Solidworks Model and Construction

The SolidWorks models were completed in two phases, the shape phase and the strength phase. The shape phase took into account the physical design requirements developed in the math model from chapter 3, which includes the areas, temperatures and fuel requirements determined to produce the desired effects. The strength phase made the pieces capable of withstanding the maximum pressure of 70 psia with a factor of safety of 2:1 and wrapped them in a chassis that holds the interior in place and supports the ramjet itself. This effectively led to the majority of the structural burden being held by the chassis, and the majority of the heat burden to fall to the internal plates. It also determined the material requirements for the different pieces, based on the heat and strength requirements, and once the materials were purchased the construction of the individual parts began.

Of the three main ideas, modularity played the largest role in the modeling of the ramjet. Every step of the design process was guided by the idea that the ramjet should be easy to tear down and set up and it even factored into the construction of the ramjet. Some of the design choices, like using the same 1/4-20 socket cap bolts for the majority of the connections, make it easier to tear down by requiring less tools. Other choices, like holding the inner plates in with end plates instead of bolting them down, make it easier to change out the plates. Modularity was the leading goal, and making each step easier was a good way to increase the usefulness of the ramjet.

4.1 Modular Plates

The modularity of the ramjet is largely achieved through the six inner plates that make up the internal surface of the ramjet. The Inner plates are interchangeable and can be placed in any of the locations, although in certain configurations specific plates are required at each location. The final design utilizes 5 different types of these inner plates, all based on the standard plate which can be found in Appendix B. The inner plates, like many of the ramjet parts, have been designed to remove as much complex machining as possible.

The standard inner plates are made from either 6061 aluminum or 304 stainless steel. The standard inner plates are made from two plates held together by twelve 0.5 in long 14-20 socket cap bolts. The top plate is the face of the standard plate and it is the piece that forms the internal duct. The bottom plate is the inner plate base, and once connected to the face, it is used to secure the inner plate in the ramjet assembly with the walls.

There are four basic inner plates currently available to the ramjet, three aluminum and one stainless steel. In a cold run configuration, the location of the aluminum plates and stainless steel plates is not important, but when a hot configuration is required, the stainless steel plate is needed after the combustion chamber in order to withstand the temperature of combustion. Only one stainless steel plate is required for the ramjet and due to the difficulty in manufacturing, the weight, and the cost of stainless steel, only the one was made.

The second type of plates are the instrumentation plates. The instrumentation plates are very similar to the standard plates but have pitot-static assemblies, fig. 4.1, and thermocouples installed. There is one aluminum instrumentation plate and one stainless steel, however both pitot-static assemblies are made from stainless steel. The difference between each instrumentation plate, besides the plate materials, is the location of the pitot-static assembly. The aluminum plate is intended to mount on top of the inlet, and the pitot-static system is mounted towards the rear of the plate to be out of the way. The stainless steel plate sits opposite the nozzle and the pitot-static system is in front of the nozzle, which means it is mounted more central on the plate. The tubes are staggered to give an average of the flow characteristics from the center of the duct and closer to the edge. The thermocouple can move up and down in the flow, but not side to side, in an attempt to account for combustion instabilities. The bent tubes in fig. 4.1 are stagnation pressure ports and connect to a single pressure transducer, and the vertical tubes are static pressure ports and connect to a separate pressure transducer. The assemblies are mounted so that the stagnation pressure ports point upstream. The ports can be distinguished from the outside

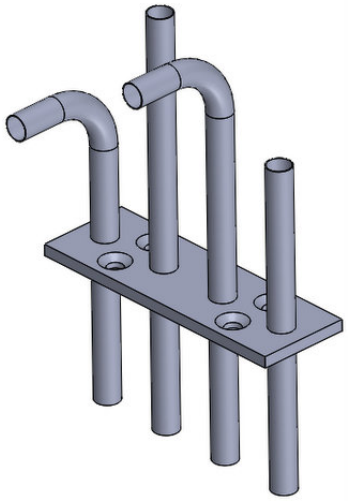

Figure 4.1: Pitot-Static assembly

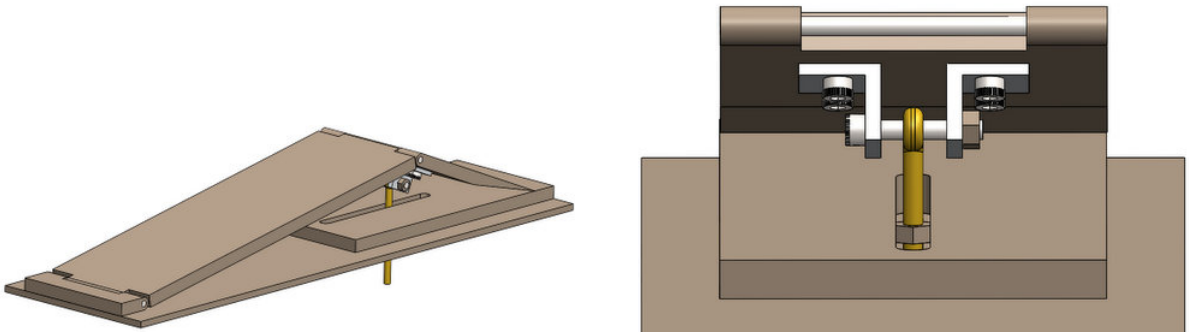

(a) The inlet could have been made from aluminum had there not been a 70 psi requirement.

(b) The inlet was designed to be at a 10° angle, but the adjustable support was added to dial in the perfect angle

Figure 4.2: Solid model design of the Inlet plate

when the ramjet is fully assembled by knowing that the longer tubes are for stagnation pressure and the shorter tubes are for static pressure.

The next two kinds of plates are the inlet plate and the nozzle plate of the ramjet. Designed by two senior projects, the inlet and nozzle are very similar in their final designs, utilizing three piece double hinges as shown on the inlet in fig. 4.2(a). [23] [14] To change the geometry of the nozzle and inlet, adjustment screws, fig. 4.2(b), are mounted to the third plate downstream. [23] [14] This mounting location allows the angle of the inlet and the area of the nozzle to be adjusted between runs. [14] One limitation to the design is that the adjustment screws do not allow the inlet or the nozzle to be changed without opening the ramjet assembly.

One major change occurred to the design after an early test with the inlet led to a failure of the adjustment bolt. The results of this test will be discussed in greater detail in chapter 5, but the design change resulting from this test increased the diameter of the adjustment rod from 0.25 in. to 0.5 in. It was found that the adjustment rod chosen did not meet the factor of safety of two, and when the pressure was increased during the test, the rod failed. To make amends for this, the new adjustment rod not only increased in diameter, but the material was changed from plain steel to alloy steel. As shown in fig. 4.3, the old rod failed when the pressure was increased to 85 $\left(\frac{Lb}{in^2}\right)$ in the plenum, however the new adjustment rod has almost a 3 times factor of safety at this same condition. The new adjustment rod would successfully complete several test runs, and the increased sized rod was also added to the ramjet nozzle

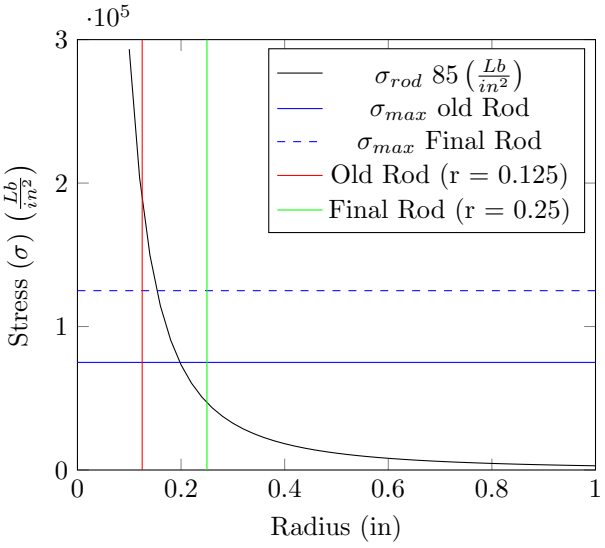

Figure 4.3: Strength of adjustment rod study

The last kind of plates are the combustor plates, which were initially design by a senior project, but during construction the plates changed considerably. [31] The combustor is made up of two plates that mounts one on top of the other with the baffle and igniter suspended between them. The track system is intended to give as many options for baffle location as possible. The location of the fuel injector was chosen so that the baffle could be moved to a point either far upstream or far downstream from the injector. By flipping the plate, the fuel injector can be either on the front half of the plate or the back half, and the baffle can be moved along either side of the injector. The baffle, tracks, and igniter design and position were finalized during construction.

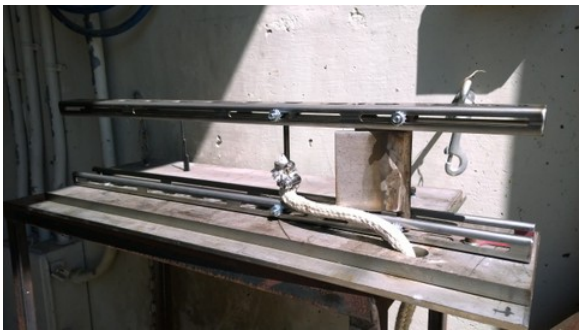

Figure 4.4: Full build of the Combustor plates

4.2 Complete Design

One benefit of the modular design is that the entire ramjet can be put together by hand, and the use of the same sized socket cap bolts means that for normal setups, only one tool is needed. Unlike the SSWT, the ramjet does not need an engine hoist to move, and only the walls and outer

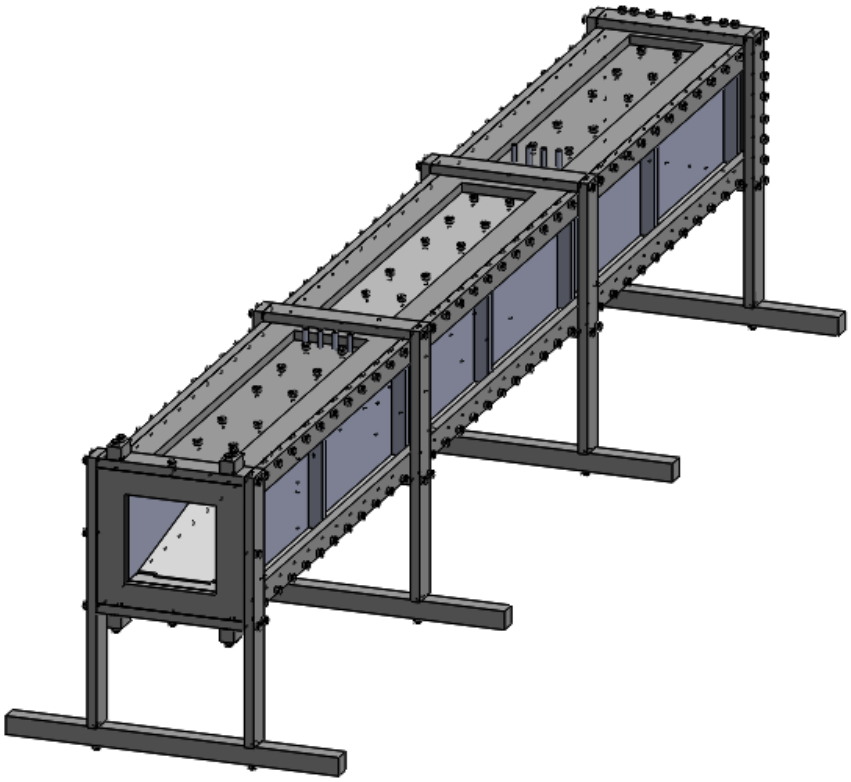

Figure 4.5: The complete buildup of the ramjet model

plates are heavy enough that some may require two people to lift. Despite many construction issues, the final ramjet design pictured in fig. 4.5 and one that was built are very similar. Although the ramjet in fig. 4.5 is pictured with the instrumentation plates on the top and the inlet ramp on the bottom, running the ramjet with the inlet and nozzle on the top is equally possible.

Even though there were many changes during the construction process, the ramjet is still assembled as designed. Figure 4.6 lists the steps involved in setting up the ramjet, which are common amongst all setups. The desired plates may change between each setup, but the basic steps remain constant. Place inner plates in an outer plate, insert walls, add the top inner plates, and cover with the other outer plate. This assembly is all placed in the four braces and the braces are tightened to secure the ramjet in place.

When designing the ramjet, it was important to prove that the ramjet would not fail at the pressures to which it would be subjected. The safety committee agreed that a 2:1 factor of safety for the design pressure would be a reasonable strength for the design. The 2:1 factor of safety was applied to the 70 psia pressure to determine the required structure of the ramjet.

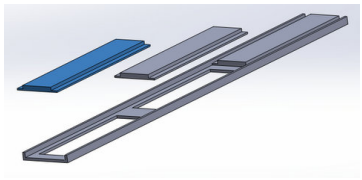

(a)

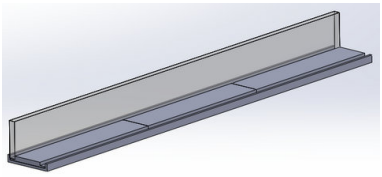

(b)

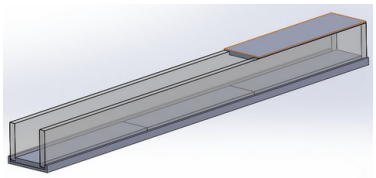

(c)

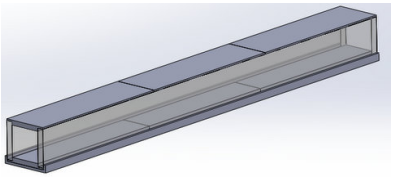

(d)

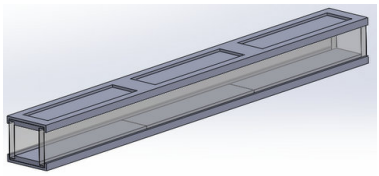

(e)

Figure 4.6: Assembling the ramjet

This was not a structural design thesis, so when a piece was deemed too weak, the size was increased in an attempt to deal with the pressures The structural testing led to the designs described in this chapter, however there was little effort put into optimizing the structural design. It was deemed unnecessary to determine techniques for limiting the weight of the ramjet when the ramjet was never intended to fly. The main considerations for changes in geometry were for manufacturing considerations.

To determine the structural requirements of the ramjet the first step was to build the SolidWorks model as a single part instead of an assembly. This was done so that the stress estimation program, SolidWorks SimulationXpress, could be used on the entire ramjet. SolidWorks SimulationXpress does not work with assemblies, at least in the student version, and so the single part version of the ramjet was analyzed in its place. Because of this limitation in the program, the single part version of the ramjet was only analyzed for the highest stress concentrations in the ramjet. The parts with the highest stress on the single part version of the ramjet were then analyzed in the program individually. The individual testings were seen as the worst case, and the single part version as the best case.

The test cases are located in Appendix E, however a brief discussion will be presented here. Although the main issue with SolidWorks SimulationXpress is that it cannot simulate assemblies, it also has some limitations to how it applies loads and fixtures that result in some potentially unrealistic simulations. This is the main reason for testing both the single part version and the high

stress individual parts. The load and fixture applications can create vastly different simulations because of the fixtures and forces being applied to whole faces and not point loads. Faces with a fixture attached to it are treated as rigid and do not flex in the simulation, so choosing the fixtures was very important for each piece.

The single part ramjet simulation requires the use of only one material, so to get a good spread of possible factors of safety, a simulation was completed with both an all aluminum and an all steel ramjet. The loads simulation from the single part version determined that a minimum factor of safety for the aluminum case was 20.44, and the steel case was 36.02. These were well over the 2:1 factor of safety, however the simulations were used to determine the highest stress points in the ramjet and not the overall factor of safety. These simulations indicated that the parts with the highest stress were the walls, inner plates, and horizontal cross bars on the braces.

Each of the high stress parts were subjected to individual simulations to determine the factor of safety of the ramjet. The first simulation was the wall, which appeared to have the highest levels of stress. The fixtures of the wall simulation were applied to the top of the wall and the bottom of each support, with a pressure of 70 psia applied to the inside of the wall. With the fixtures on the top of each support, the attempt was to mimic the way the wall was held in at the top and bottom by the outer plates but it is not a direct approximation because the tops of each support are not held vertically like in the simulation. Some other things not taken into account by this simulation are the welds which hold the supports on each walls, and also the two kinds of metals, steel for the supports and stainless steel for the wall, which were used in construction. This simulation came out with a factor of safety for the wall of 2.5:1, which is very different from the single part ramjet prediction.

The inner plates, both stainless steel and aluminum were then subjected to simulations as well. Fixtures for the simulation were applied on the steps of the inner plates, to simulate the wall holding it into place. This fixture position does not account for the support afforded by the outer plates, but it does not keep the inner plate from flexing. A 70 psia pressure was applied to the face of each inner plate and the factor of safety of the stainless steel plate was found to be 1724.00, and the aluminum plate was found to be 2821.14. Although this simulation did not account for the inner plates being made up of two plates, the results were very high and deemed acceptable.

The final simulation was done on the horizontal cross bars used in the braces. This bar proved the most difficult to simulate as the positioning of the fixtures made for very large changes in the

(a) The orange safety paint is visible in the partially assembled ramjet.

(b) Once correctly assembled, the orange paint is not visible.

Figure 4.7: The safety paint scheme

results The final location for the fixtures was placed on the ends of the rod, with the force applied to the top of the bar. This simulates the lower brace, however it would be equally applicable to the upper brace. The final factor of safety for the brace cross bar was 2.17, which was applied to the entire ramjet for its overall factor of safety. Initial designs for the braces had thinner cross bars but the results of earlier versions of this test resulted in an increase in thickness to the 0.5 in. thick bars of the current design. Each of the outputs from these simulations can be found in Appendix E

Many of the individual parts of the ramjet were painted to make the assembly of the ramjet easier, the braces that support the ramjet are letter coded so that they are easy to put back together and have a system of dots punched onto the metal in the event the paint is removed. Some paint schemes are applied to the ramjet as a whole as well. For safety reasons, it seemed prudent to make an improperly assembled ramjet easy to identify. To accomplish this task, the orange paint seen in fig. 4.7(a) was applied to each surface that would be covered up once the ramjet was fully assembled. This paint coats the inner surfaces of the outer plates and the inward facing surfaces of each brace. Each of these faces is covered once the ramjet is fully assembled, and if the ramjet is assembled correctly, there will be no orange showing on the ramjet. This is a very obvious sign that the ramjet is assembled properly.

Each brace is also given a specific location on the frame that also bears the letter designation. The braces also follow the orange safety paint approach, and each position has a strip of orange paint that is covered up by the foot. An example of the paint strip at station “D” is shown in fig. 4.8(a), and the paint strip is covered at station “C1” in fig. 4.8(b). The front brace location is marked with an “A” and the rear brace location is marked with a “D.” The mid braces are marked

(a) Each brace foot hides an orange safety paint strip.

(b) The same letter used to identify the braces mark their locations on the frame.

Figure 4.8: Brace feet paint schemes

with "B1" and "C1" on one side and "B2" and "C2" on the other, to signify the orientation of the mid braces. Station "C1" aligns with the same side of the "C" brace as shown in fig. 4.8(b), and the "B" brace follows the same setup.

The design of the ramjet model has made the ramjet easier to assemble and use. Design methods used in this design were well planned and offered many time saving and safety innovations that lend to the continued use of the ramjet in the future. The main issues with the design were caused by poor manufacturing techniques, and had the first pieces been made with the same precision as the last pieces, many of the issues would have been mitigated.

Chapter 5

Testing

This chapter on testing outlines all the testing completed in conjunction with the ramjet. The testing discussion of the pressure relief system is discussed in detail in section 2.2.2 and will not be repeated here. This chapter will discuss the original intentions of the testing portion of this thesis and what the actual testing looked like. The test procedures will be discussed in a general sense but for examples of the actual procedures used for each test see Appendix C.

Despite the original intentions, much of the testing was changed after early results indicated that the SSWT was not functioning properly. A large portion of the testing completed in this thesis was done to determine how to use the SSWT effectively and consistently. Some of the testing of the actual ramjet was conducted, but the final testing of the live fire portions of the test were canceled due to safety concerns.

5.1 Fuel System Testing

The fuel system has gone through three major testing phases. The first phase was completed by Selin, who designed the fuel delivery system based on the diesel fuel pump. [30] The second phase was completed by Stone, who tested the diesel fuel pump system with the J85 fuel injector. [31] The procedures for these tests can be found in the respective senior projects.

The phase 3 testing of the fuel system was conducted using the pressurized fuel system of the bi-propellant rocket and the j85 fuel injector in an attempt to meet the required pressures for atomization. [25] The fuel system uses a highly pressurized nitrogen bottle and a pressure regulator to step down the pressure to desired levels. The fuel system is actuated by a solenoid valve, which can be operated from inside the control room in the propulsion lab to limit safety concerns during testing of the fuel system. The first step to testing the fuel system was to perform an auditory check of both the fuel valve and the fuel lines for pressure leaks. The auditory fuel valve check is

completed by connecting the control box and the fuel valves. The bi-propellant rocket utilizes a fuel and oxygen solenoid, testing both will confirm what the actuator should sound like.

The leak check requires the entire fuel system to be connected, and a nitrogen bottle. Although leak testing was done during every run with the setup, this leak testing was done with just nitrogen and no fuel. To test the system for pressure leaks, each of the valves in the fuel system will be opened sequentially until it reaches the fuel valve. This is the same sequence that is used to pressurize fuel during a hot fire test. The valve used for filling the fuel tank will not be opened during this test and the valve for purging the fuel tank will be used at the end of the test to purge the nitrogen from the system. The test was completed by pressuring the fuel line to 85 psig and checking the first line for leaks. Next the valve in between the bottle and the fuel tank was opened which pressurizes the fuel tank. If the fuel tank fill valve or purge valve were open, nitrogen would vent during this step, so it is important to ensure that the valves are closed before this step. The final valve is opened after checking the connections to the fuel tank for leaks. This valve is located next to the fuel purge valve, but it is connected to the line to the fuel valve. With this valve open and no leaks being present, the test would be complete, and the nitrogen tank pressure regulator should be closed and the valve to purge the fuel tank should be opened.

The testing completed by Stone did not result in atomized fuel, so the third phase of testing began by trying to atomize fuel. The testing was completed by successive runs at successively higher fuel pressure levels until fuel atomization occurred. Starting with the 85 psig rated from the fuel pump, each successive run was approximately 10 psi higher than the previous run. [30] Once fuel atomization occurs, the gage pressure required to atomize fuel was known, once the pressure inside the combustion chamber is also known then the required fuel pressure could be determined.

After atomization was achieved, the volumetric fuel flow rate through the fuel injector was tested by filling a beaker and measuring the times to each level. The timing of test began when the fuel reached 200 ml (the lowest graduation on the beaker). Starting at 200 ml means that the fuel flow is steady and the time required for the fuel to pass through the tubes of the system does not need to be taken into account. Although a liter of fuel was put into the fuel tank, between 500ml and 600ml the fuel would start to bubble, indicative of nitrogen leaking out of the system in place of fuel. This is a common occurrence when testing the bi-propellant rocket, the flame starts to sputter when the fuel gets to low and instead of pushing out fuel, the Nitrogen passes through the system instead. This meant that once the sputtering of the fuel began, the test was continued until the nearest 100ml graduation which for the testing was the 600ml and then the final time was called.

Two of these runs were completed for greater confidence in the results The fuel flow rate had to be higher than the lower explosive limit, which in the ramjet would be a fuel flow rate of 12 gal/hour, or 0.0032 gal/sec. The testing of the fuel system is required before hot flow testing could occur. Without hot flow testing, completing the fuel system testing assures that the design meets the requirements of the ramjet, unlike the previous designs.

5.2 Ignition System Testing

The ignition system was borrowed from the bi-propellant rocket lab. The major differences between the labs ignition system was a new igniter for use with the ramjet and a new safer control box. The new igniter was designed to install right into the borrowed ignition system. The initial tests of the ignition system did not use the new igniter, and instead used the old igniter to ensure that the system was working.

The initial testing of the ignition system involved setting up the bi-propellant rocket ignition system and the initial control box in the same configuration as Mehrparvar. [27] This included using the propulsion lab's power supply grid and the igniter tested by Mehrparvar and used in the testing done by Johnson. [27] [25] This testing needed to be completed because the ignition system had been taken apart since its last use and ensuring that the system worked before making changes would lead to the best results. Once fully connected, the ignition is actuated by switching the "MAIN" switch to on and holding the "SPARK" switch down. These steps for firing the ignition system are used in each of the ignition system tests.

The next stage of testing involved moving the entire system from the propulsion lab to the SSWT building. The SSWT does not have the same power grid as the propulsion lab, although one was originally intended to be installed before testing occurred. This meant that a power supply was used for this testing, and ensuring the apparatus worked with the new power supply would mean that any changes that occurred when the new igniter was installed would be due to the igniter. Altering the systems location also meant that any unknown effects of the power grid would no longer take effect on the ignition system.

The control box was setup inside the control room of the SSWT, along with the 12V DC power supply. The 120v AC power is supplied by the wall outlet in the control room and runs through the control box as before. The remainder of the ignition system was setup in the same way described above. Mehrparvar's igniter was placed in a location easily visible from the control room instead of

in the ramjet, where a spark would not be visible.

The final set of testing was done on just the ramjet igniter. The ramjet igniter was first placed in the same position as Mehrparvar's igniter and not inside the ramjet. After a spark was documented, the igniter was moved to its position in the combustor plates, but no walls were added. This test allowed the final apparatus to be tested while still being visible to the test team.

The testing was designed to allow for a visual assessment of the spark in each setup. As discussed by Mehrparvar, the MSD box supplied with 12V DC produces a continuous 10000+V, meaning a constant arc should be visible when power is supplied. [27] As with Mehrparvar's testing of the ignition system, visualization of the continuous spark was all that was required for a successful test of each ignition system configuration. [27] The build-up approach was designed to ensure that the ignition system, in its normal operation worked before trying to modify it for the ramjet. The power grid used in the propulsion lab does not have visual current readings, but the 12V DC power supply used in the SSWT did. This allowed for a secondary confirmation of the correct power setup during tests at the SSWT, but could not be used to determine if a spark had occurred.

Some of the major things to be adjusted during the test of the ramjet igniter are the length and separation of the open leads of the igniter and the way the insulation is wrapped around the igniter. The length of the open leads and the separation of the two leads was tested independently at first, but wrapping the insulation around the leads led to more testing being undertaken to ensure a spark occurred during the operation of the igniter. Like the fuel system testing, the ignition system testing is required before hot flow testing, without hot flow testing, the ignition system tests can be used to verify the design of the igniter and ignition system are adequate for future testing.

5.3 Safety Buildup Approach

The ramjet testing was to be completed in a build up manner, so that any issues with individual components could be caught before there was fuel involved. The build-up in testing was meant to steadily add to the capabilities of the ramjet, without exposing any operators to excess risk. This safety build-up began with the testing of the ramjet in the "Blank" setup, where the duct had no geometry changes or heat addition except for the pitot-static tubes located at stations 3 and 5.

Each test has a configuration matrix and a test variable matrix associated with the test. The configuration Matrix, like the one in table 5.1, is a short list of all the possible plates and a description of the particular configurations of each plate. Configuration Matrices, like table 5.1, are used in each

		Run #	1					
Configuration	Plates	Location	1	2	3	4	5	6
		Blank Aluminum						
		Blank Stainless Steel						
		Inlet						
		Nozzle						
		Pitot-Static Aluminum						
		Pitot-Static Stainless Steel						
		Flame Holder Track + Igniter						
		Flame Holder Track + Fuel Injector						
	Particular Configuration	Inlet Angle	N/A					
		Nozzle Throat height	N/A					
		Nozzle Exit Height	N/A					
		Baffle	N/A					
		Fuel Injector Location	N/A					
		Igniter location	N/A					
		Fuel Pressure	N/A					

Table 5.1: Example of the Configuration Matrix

1	Lower plate in the forward section
2	Upper Plate in the forward section
3	Lower plate in the middle section
4	Upper Plate in the middle section
5	Lower plate in the aft section
6	Upper Plate in the aft section

Table 5.2: Reference numbers for plate locations

test to accurately convey what the ramjet must look like in order to operate during the test. For a particular configuration, the correct plates to use and in what location are displayed in the "Plates" section.

A numbered system for the location of each plate was made to describe the locations of the plates. Table 5.2 details the location numbering convention. Remember that the modularity of the design makes it possible for the ramjet to be put together incorrectly. Each plate can fit in any station, there is no exact fit for any one plate. Another interesting modularity effect is that the ramjet can be turned upside down and will have no effect on the testing, but reversing the ramjet order could have disastrous effects.

Most of the plates have a "Particular Configuration" that describe specific features of the plate. As visible in table 5.1, some of the particular configuration options include the inlet angle, and the Nozzle shape. Other things include the igniter and baffle location, and the fuel pressure for the test. The configuration matrix is designed to ensure the Ramjet is assembled accurately for the test.

The testing plan starts with the "Blank" setup, and it is followed by the "Inlet" test. After successful completion of the "Inlet" test, the "Inlet + Nozzle" configuration is tested. To add extra build-up to the "Hot Fire" run, tests of the "Hot Fire" configuration were to be tested without fuel, but with every piece in place, and again with water in place of the fuel to ensure the fuel system is acting correctly. The testing and setup procedures associated with each test can be found in Appendix C.

The results matrix outlines the desired results from each test. Although originally intended to check Mach numbers at each location, there was discussion about whether or not using stagnation pressures at each station could achieve faster understanding of the results of the test. For the stagnation pressures to be used as success criteria, the plenum pressure would have to remain

Results	M_3	TEST	
		Expected	
	M_5	TEST	
		Expected	

Table 5.3: Example of the Results Matrix

constant. Since the plenum pressure fluctuates, the stagnation pressures will also fluctuate making the desired criteria hard to determine, however by judging based on Mach number, so long as the ratio of plenum to stagnation pressure stays constant, the success criteria can be used. The results matrices, like the one in table 5.3, will look slightly different for some tests, and the desired results from each test are specific. For instance, the "Hot Flow" test requires a comparison of the temperatures at each location as well as the Mach numbers. The results matrix was intended to give quick and accurate understanding of the results of each test so that testing of the ramjet could continue without delay. It went through a few iterations during the early testing to try and find a single matrix that works for all tests, like the configuration matrix, but for each test the specific requirements were similar but not the same.

5.3.1 Blank Test

For the "Blank" tests, the configuration is all the blank inner plates and the two instrumentation plates. The configuration in table 5.4 was determined to be the best for the "Blank" tests. Having the instrumentation plates on the bottom allowed the inlet and nozzle to be added to the ramjet for subsequent tests without requiring the entire ramjet be torn down. Set up procedures for the "Blank" setup can be found in Appendix C.2.3, along with the testing procedures in Appendix C.3.4.

For successful completion of the "Blank" run, the flow through the duct must behave like a SSWT without a diffuser. Using the Fanno flow approximation results for the "Blank" ramjet in section 3.1, the test success criteria in table 5.5 can be set. The band around the values for the test criteria account for the 0.4% error associated with the pressure transducers. [4] Mach number was chosen for the success criteria because it allows for greater flexibility in the test. The plenum pressure constantly changing will make reach specific pressure difficult, but if the models are correct, the Mach numbers should remain constant for the test.

		Run #	1					
Configuration	Plates	Location	1	2	3	4	5	6
		Blank Aluminum		x	x	x		
		Blank Stainless Steel						x
		Inlet						
		Nozzle						
		Pitot-Static Aluminum	x					
		Pitot-Static Stainless Steel					x	
		Flame Holder Track + Igniter						
		Flame Holder Track + Fuel Injector						
	Particular Configuration	Inlet Angle	N/A					
		Nozzle Throat height	N/A					
		Nozzle Exit Height	N/A					
		Baffle	N/A					
		Fuel Injector Location	N/A					
		Igniter location	N/A					
		Fuel Pressure	N/A					

Table 5.4: "Blank" Test Configuration Matrix

Results	M_3	TEST	
		Expected	3.495 ± 0.009 psia
	M_5	TEST	
		Expected	3.589 ± 0.009 psia

Table 5.5: "Blank" Test Results Matrix

		Run #	1					
Configuration	Plates	Location	1	2	3	4	5	6
		Blank Aluminum			x	x		
		Blank Stainless Steel						x
		Inlet		x				
		Nozzle						
		Pitot-Static Aluminum	x					
		Pitot-Static Stainless Steel					x	
		Flame Holder Track + Igniter						
		Flame Holder Track + Fuel Injector						
	Particular Configuration	Inlet Angle	10°					
		Nozzle Throat height	N/A					
		Nozzle Exit Height	N/A					
		Baffle	N/A					
		Fuel Injector Location	N/A					
		Igniter location	N/A					
		Fuel Pressure	N/A					

Table 5.6: "Inlet" Test Configuration Matrix

5.3.2 Inlet Test

For the "Inlet" tests, the configuration is set up following the procedures in Appendix C.2.4. The configuration in table 5.6 follows the configuration choices made in section 5.3.1 which allow for easier addition and removal of the inlet plate. Testing of the "Inlet" follows the procedures laid out in Appendix C.3.5

The success criteria for the "Inlet" test are based on the Fanno Flow approximation for the "Inlet" configuration described in section 3.2. The success of this test is hard to judge based on pressure due to the issue with the unsteady plenum pressure. As the plenum pressure changes, normal shock that is supposed to be in the throat moves and because of the high initial pressure starts down stream of the inlet and slowly moves back towards the throat. This will result in a varying range of pressures seen after the inlet, and the actual desired condition would be hard to

Results	M_3	TEST	
		Expected	2.76 ± 0.01 psia
	M_5	TEST	
		Expected	2.78 ± 0.01 psia

Table 5.7: "Inlet" Test Results Matrix

isolate. In order to make the success criteria possible to meet, Mach number was used as shown in table 5.7. This assumes that while the stagnation pressure may fluctuate, its ratio to the plenum pressure will be more constant.

5.3.3 Inlet and Nozzle Test

For the "Inlet + Nozzle" tests, the configuration is set up following the procedures in Appendix C.2.5. The configuration in table 5.8 follows the configuration choices made to allow for easier addition and removal of the nozzle and inlet plates. Testing of the "Inlet + Nozzle" configuration follows the procedures laid out in Appendix C.3.6. Unlike the inlet, the nozzle is not tested on its own. Some discussion has occurred to determine whether a separate test of the nozzle was necessary, but it was determined that the steps required to adjust the converging-diverging nozzle on the SSWT make the nozzle only test unfeasible.

The success criteria for the "Inlet + Nozzle" test are based on the Fanno Flow approximation for the "Inlet + Nozzle" configuration described in section 3.4. As with the "Inlet" test in section 5.3.2, the success of this test would be hard to judge based on pressures because of the issue with the unsteady plenum pressure. The same issue with the normal shock moving causes various effects throughout the ramjet. This will result in a varying range of pressures seen after the inlet, and the actual desired condition will be hard to isolate.

It should be noted that the desired outcome of the "Inlet+Nozzle" test is identical to the "Inlet" test. The Nozzle should not restrict the flow when installed, however the Fanno Flow approximations suggest that operating the nozzle could cause a decrease in mass flow, resulting in increased pressure, and lower Mach Numbers, inside the ramjet and moving the normal shock upstream at greater speed. If this occurs, the nozzle will be adjusted to meet the Fanno Flow hot run design which increases the area of the nozzle throat.

The cold flow test of the complete ramjet, as described in Appendix C.3.7, has the same desired

		Run #	1					
Configuration	Plates	Location	1	2	3	4	5	6
		Blank Aluminum			x	x		
		Blank Stainless Steel						
		Inlet		x				
		Nozzle						x
		Pitot-Static Aluminum	x					
		Pitot-Static Stainless Steel					x	
		Flame Holder Track + Igniter						
		Flame Holder Track + Fuel Injector						
	Particular Configuration	Inlet Angle	10°					
		Nozzle Throat height	3 1/32 in					
		Nozzle Exit Height	2 11/16 in					
		Baffle	N/A					
		Fuel Injector Location	N/A					
		Igniter location	N/A					
		Fuel Pressure	N/A					

Table 5.8: "Inlet + Nozzle" Test Configuration Matrix

Results	M_3	TEST	
		Expected	2.76 ± 0.01 psia
	M_5	TEST	
		Expected	2.78 ± 0.01 psia

Table 5.9: "Inlet + Nozzle" Test Results Matrix

characteristics as the "Inlet + Nozzle" test. Any flow adjustments due to the baffle are not accounted for in any of the models, and its believed that any disturbances caused by the baffle will not be visible at station 5.

5.4 Hot Fire Testing

For the "Hot" tests, the configuration is set up following the procedures in Appendix C.2.7. As mentioned in Appendix C.2.7, a "Hot" test was never attempted due to safety concerns. The configuration in table 5.10 details the intended first hot fire test configuration. Since the hot fire tests were never completed, the actual best configuration is unknown and if the hot fire tests were to be completed, the final configuration could be very different. Testing of the "Hot" configuration was intended to follow the procedures laid out in Appendix C.4.4, however these procedures are untested and should be used as a starting point and not as the final test procedures.

The success criteria for the "Hot" test are based on the Fanno Flow approximation described in section 3.4. The main point for success of this test will be whether or not the Ramjet actually ignites. The same issue with the normal shock moving will cause issues with the pressure readings as with the earlier tests, but the increase in temperature should be unmistakable. The thermo couples do not measure stagnation or static pressure, but the average of the two. This total temperature will still show the correct trends of an increase at station 5 instead of a decrease as seen in the other tests.

		Run #	1					
Configuration	Plates	Location	1	2	3	4	5	6
		Blank Aluminum						
		Blank Stainless Steel						
		Inlet		x				
		Nozzle						x
		Pitot-Static Aluminum	x					
		Pitot-Static Stainless Steel					x	
		Flame Holder Track + Igniter				x		
		Flame Holder Track + Fuel Injector			x			
	Particular Configuration	Inlet Angle	10°					
		Nozzle Throat height	3 1/32 in					
		Nozzle Exit Height	2 11/16 in					
		Baffle	1 in ahead of injector					
		Fuel Injector Location	Forward					
		Igniter location	2 inch behind injector					
		Fuel Pressure	215 psia					

Table 5.10: "Hot" Test Configuration Matrix

Results	M_3	TEST	
		Expected	3.495 ± 0.009 psia
	M_5	TEST	
		Expected	3.589 ± 0.009 psia
	$T_{@3}$	TEST	
		Expected	$68.4 \pm 0.5°F$
	$T_{@5}$	TEST	
		Expected	$185 \pm 1°F$

Table 5.11: "Hot" Test Results Matrix

5.5 The Wedge Test

The wedge test was completed after a technical review of the ramjet design determined that secondary confirmation of supersonic flow in the ramjet was required. The testing was completed against the ramjet instead of the standard SSWT test section, with the desired outcome of photographing an oblique shock forming off a wedge in the SSWT test section. The ramjet configuration was the same as shown in table 5.4, because the wedge was inside the SSWT test section.

The desired outcome of this test was an oblique shock to form off of the 15° wedge. The oblique shock was expected to form at $30.7° \pm 0.4°$ from inviscid analysis. The shock angle brackets account for the location of the wedge with respect to full expansion of the converging-diverging nozzle on the SSWT. If the wedge was placed too far forward it could produce an oblique shock before the nozzle is fully expanded. Viscous analysis shows that this shock wave could fall between to 31.5° and 32.9°. The unknown location of full expansion the SSWT converging-diverging nozzle accounts for the uncertainty.

Chapter 6

Results and Discussion

This chapter discusses the results of the ramjet testing that occurred over the course of several months. Early on testing of the fuel system and ignition systems individually, led to testing of the ramjet components attached to the SSWT. Comparisons of the SSWT data acquired from before the ramjet test runs is discussed in this chapter to showcase the differences of what the ramjet testing has achieved.

Testing of the pressure relief system was discussed in the section 2.2.2 along with the results of that testing It will not be discussed in this section as it was part of fixing the SSWT for ramjet operation. The ramjet was tested in three of the proposed configurations, the "Blank" setup, the "Inlet" setup, and the "Inlet+Nozzle" setup. These are all cold flow tests, without any fuel or ignition source, and the combustion chamber hardware was never tested in the ramjet either. The hot flow tests and combustion chamber hardware testing was canceled due to safety concerns.

6.1 Fuel System Testing Results

Selin's fuel system testing resulted in a fuel flow rate between 22.7 and 41.55 gallons per hour depending on the fuel pressure regulator settings. [30] Stoichiometric air to fuel mass ratio for Jet-A fuel is 14:1, which means that a fuel flow rate of 0.06 gal/sec would be required for optimal performance. Selin's design produced a fuel flow rate of 0.012 gal/sec, which would significantly lower the temperature increase during combustion. The results of Selin's design are positive because the fuel flow rate is between the lower explosive limit of 0.7% and upper explosive limit of 5% based on volumetric fuel ratio. [3] Selin's design results in a volumetric fuel ratio of 2.14%, which is within the limits. Selin's results were used to determine the max temperature for use in the ramjet design.

The testing conducted by Stone resulted in the scrapping of the diesel fuel pump system. Conducted during the construction phase of the ramjet, Stone determined that the fuel system, with

Vol.(ml)	T. (sec)	ΔT	Flow rate (Gal/s)
100	-	-	-
200	0	-	-
300	8.41	8.41	0.0031
400	17.29	8.88	0.0030
500	26.30	9.01	0.0030
600	36.95	10.65	0.0025

Table 6.1: Results of Fuel Flow test 1

the J85 fuel injector installed, could only produce 0.0005 gal/sec. [31] The fuel injector also did not atomize the flow, resulting in the need for phase 3 testing of the fuel system

The phase 3 testing, with the pressurized fuel system borrowed from the bi-propellant rocket attached to the ramjet's fuel injector, yielded better results than the previous two phases. The first step of the fuel system testing was determining if the fuel valve would open and close and if the fuel system was pressure tight. The audible noise of the fuel valve opening was used to determine if it actuated or not, and the valve used for oxygen in the bi-propellant rocket was also used to determine if the noise was similar to the fuel valve. One problem that was discovered during this testing was that the fuel valve must be operated in a vertical position, with the fuel flowing horizontally. During the setup, the fuel valve was tightened down too far and was tilted off vertical, which led to it not actuating when power was applied. The angles of operation were not determined during this testing, but it should be noted that the range is not very great. For best results ensure the fuel pump is set up vertically. Once the actuation of the valve was tested, the setup had to be tested for pressure leaks. After applying pressure to the fuel system, the fuel valves were open as described in section 5.1 and no leaks were found.

As described in section 5.1, the second step was to determine when the fuel would atomize from the injector. Starting with 85 psig, the results were the same as what Stone found with the fuel pump and no atomization occurred. [31] The fuel began to atomize at 175 psig, over double the pressure of what the fuel pump rating. The pressure required for fuel atomization was 175 psig when injecting at atmospheric pressure. To achieve 175 psig in relation to the combustion chamber which was predicted to be near 32 psi, the fuel pressure would need to be set at 215 psig to the atmosphere during a ramjet run.

Vol.(ml)	T. (sec)	ΔT	Flow rate (Gal/s)
100	-	-	-
200	0	-	-
300	7.04	7.04	0.0037
400	14.91	7.87	0.0034
500	21.89	6.98	0.0038
600	30.89	8.21	0.0032

Table 6.2: Results of Fuel Flow test 2

The third step of the fuel testing was completed at the 175 psig fuel pressure. The first test resulted in the data in table 6.1. Post analysis of the data concluded that the fuel flow rates were below the lower explosive limit for Jet A. The average of the first test fuel flow rates is 0.0029 gal/sec.

One of the issues noted during the test was that during the last 100 ml, the fuel would start to sputter as nitrogen leaked through the fuel system. This means that less fuel was passing through the fuel injector during the last 100ml and results in a lower volumetric fuel flow rate for the last data point. The time was stopped once the fuel reached the nearest 100ml graduation after sputtering occurred, meaning only the last line is questionable. Even when removing the last line of data from the calculation, the fuel system still appears to fail as it only produces an average fuel flow rate of 0.0029 gal/sec.

The second test was completed with greater fidelity involving the lessons learned from the first test. The testers were more comfortable with the data collection method and the apparatus. Results from the second test are grouped in table 6.2. The average fuel flow rate of the second test is 0.0035 gal/sec, with all the fuel flow rates being at or above the lower explosive limit. If the last line of data is removed from the average, like in test 1, the average fuel flow rate increases to 0.0036 gal/sec which would suggest that the fuel system succeeds at meeting the lower explosive limit.

Averaging all eight flow rates from both tests gives a fuel flow rate from the fuel system equal to 0.0032 gal/sec. Removing the last data set of each test increases the avg fuel flow rate to 0.0033, meaning the system succeeds in meeting the 0.0032 gal/sec requirement.

After reaching this conclusion, it was decided that a single fuel injector would be reasonable for the remainder of the testing in this thesis, even though it was so close to the lower explosive limit. The single injector effectively limits how much fuel could be injected into the ramjet, meaning that

the temperature in the ramjet would not exceed the design parameters. With the limited fuel, the ramjet would also be safer if a blockage occurred and fuel was allowed to burn in the blocked ramjet. The low fuel flow rate meant that any delay in shutting down the fuel system during a hot fire run would be less dangerous, and the system would burn out faster. The modularity of the design means that a future student could easily come in and design a new combustion chamber plate to allow for multiple fuel injectors, once this version is deemed safe.

6.2 Ignition System Testing Results

Despite following the setup employed by Mehrparvar and Johnson, initial results of the ignition system were poor. [27] [25] The continuous spark described by Mehrparvar could not be seen despite checking the connections. [27] In order to get the MSD box to work a relay was installed in between the MSD box and the control box. With the relay installed, the continuous arc was seen and the test was a success, so the system was moved up to the SSWT. With the new location the setup performed successfully and the visual spark was seen.

The final tests performed with the ramjet igniter worked initially. Setting the open leads so that only the base level of insulation was between it allowed for a continuous spark to form. However the spark was no longer occurring once the outer layer of insulation was wrapped around the igniter. Since the inner layer of insulation could not survive the temperature of the combustion chamber, the igniter was designed with an outer layer of insulation which was braided and the bare leads were supposed to stick through the insulation. The insulation blocked the spark, so reworking the insulation and the length of the leads was conducted until the test was successful.

Once the test of the igniter was completed, the insulation was secured in place with a hose clamp and the igniter was secured to the combustor plate. The final test of the igniter was completed with success, but due to the difficulties getting the igniter to work on the previous test, it is suggested that before any testing is completed, the igniter should be tested. Even though the final test was completed without the walls, the test was again completed with the ramjet set up in its hot fire test configuration. The light from the igniter spark is visible from the end of the ramjet, but this should be completed with extreme caution and a total avoidance of metal connected to the ramjet.

6.3 Previous SSWT Testing

In order to understand the testing results of the ramjet, the testing of the SSWT completed by students at Cal Poly needs to be discussed. The data collected from the SSWT were located on the SSWT computer and pertain to the the labs completed from 2012 and 2013. Some data is also presented from 2011 which illustrates the problem with a poorly aligned pitot probe. The purpose of this data is to establish the state of the SSWT before the ramjet was installed and before the changes to the SSWT were made.

Figure 6.1 is a combination of pressure data from 10 different runs conducted by the Cal Poly Aerospace Engineering Propulsion class in fall 2012 and fall 2013. The data is very consistent, with each set of data falling right on top of the others, with differences only in the length of run time. There are three different colored lines visible in fig. 6.1 but there are actually four different color lines, one is hidden below the axis. The black line is the raw plenum measurement, which was very poor due to a bad connection. The red line is the plenum pressure after an exponentially weighted moving average based on the last 10 data points was applied. The green line is the test section pressure which should occur after a normal shock appears in front of the pitot tube when supersonic flow is achieved. The invisible blue line is the tank pressure and it is hidden below the graph around -87 psi due to faulty wiring between the tank pressure transducer and the DAQ. Several fixes to the data acquisition system are described in section 2.2.1.

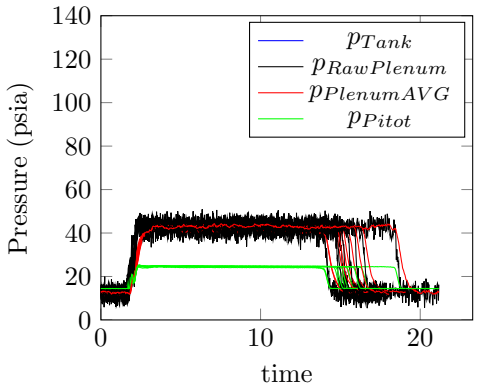

Figure 6.1: SSWT Lab runs pressure data

As mentioned in section 2 the SSWT operates with a converging-diverging nozzle with an area ratio equivalent to Mach 3.3 flow. The pressure data in fig. 6.1 however suggests a supersonic flow of 2.4 Mach, as shown if fig. 6.2. The Mach numbers are calculated using the stagnation pressures and eq. (2.2) as described in section 2.1. The Mach numbers are consistent like the pressure data because the pressure regulator was never touched and the tank pressure was filled to the max capabilities of the AERO department's compressor. The pressure in the plenum is around 42 psia, which is high enough for choked flow at the throat of the converging diverging nozzle, but, according to the Fanno

flow approximation in section 2.1, to reach Mach 3.3 flow in the SSWT a minimum plenum pressure of 74 psia is required.

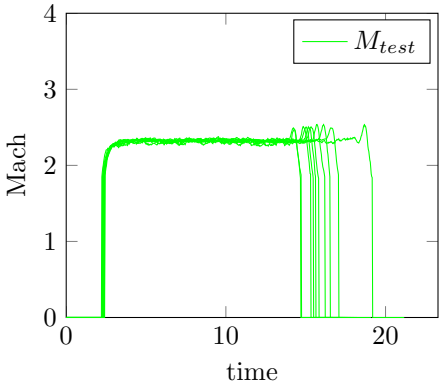

Figure 6.2: SSWT Lab runs Mach data

Apart from the incorrect Mach numbers calculated there is another peculiarity to the data in fig. 6.2. There are little bumps at the trailing end of the lines of Mach number in each data set. These bumps are visible in several of the following figures as well, but are not representative of any physical phenomenon. The bump is a result of a moving average applied to the raw plenum pressure to decrease the noise in the data. The moving average causes a lag in the apparent pressure changes. The Mach calculation in these tests relied on the moving average data, so when a change in pressure occurred the numbers in the plenum pressure lagged behind the pitot tube pressure readings. The result is a plenum pressure that appears to remain at the higher psi for longer than the pitot tube pressure which decreases the stagnation pressure ratio and tricks the function into thinking it is seeing a higher Mach number. The function works on the ratio of the stagnation pressures and any fluctuation results in a corresponding change in the Mach number. The modification of the plenum pressure transducer connections corrected the noisy data issue and the moving average was no longer required. The data presented later does not have these bumps.

One other data peculiarity of note is the straight lines that occur at around Mach 1.8 in the leading and trailing edges of the Mach figures. This is a direct result of clipping the data above a pressure ratio of 0.8 to give cleaner insight into when the test starts. Anything above a pressure ratio of 0.80 is considered a no flow state, because the Mach number calculation will only give a Mach number of zero when a stagnation pressure ratio of 1.0 occurs. The static in the pressure transducers resulted in very jagged Mach number figures before this clipping was added to the data. This was even worse during these early runs when a bad connection to the plenum pressure transducer cause very poor data. The clipping will continue through all the testing done on the SSWT and ramjet, but the peaks due to the moving average were taken care of when some of the upgrades described in section 2.2 were completed

The pressure data in fig. 6.3 was collected from a Propulsion class in 2010. Figure 6.3 has vastly

different characteristics than that of fig. 6.1. The plenum pressure is much higher, on the order of 105 psia, than the plenum pressure of fig. 6.1. Figure 6.3 does not require any averaging either on the plenum pressure, making the figure more legible, indicating that the pressure transducers were effectively connected at this time. The test section stagnation pressure, p_{03}, is also at a significantly smaller ratio to the plenum pressure and is a lower number all together than the pressures in fig. 6.1. It sits at around 20 psia when the test section pressure was closer to 25 psia in fig. 6.1.

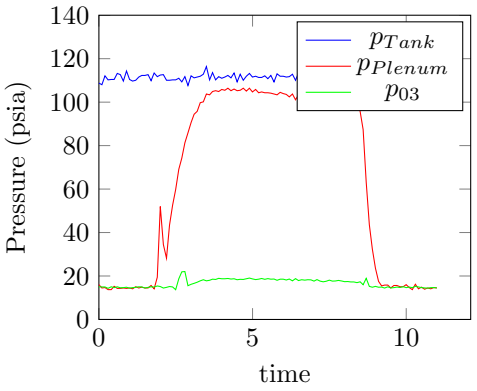

Figure 6.3: 2010 class SSWT Pressure data

Some important details form fig. 6.3 are also 2 interesting pressure spikes that occur at the leading and trailing edge of the elevated test section pressure that are not present in fig. 6.1. The reason these spikes is important will be discussed in section 6.5. Another important detail is the fact that the plenum pressure does not remain constant, it fluctuates considerably from the start to the end of the 8 second run. The pressure in fig. 6.1 remains constant for nearly 15 seconds in some cases, suggesting that the plenum pressure never reached the 18 psi differential of the pressure regulator. The tank pressure is also visible in this figure however it is not reliable.

Figure 6.4 is one of the most interesting figures available from the previous testing of the SSWT because it's Mach number is considerably higher than not only fig. 6.2, but it is also higher than the area ratio would suggest it should be. This is due to an issue with the pitot probe in the SSWT, but despite this issue, some good information can be gleaned from fig. 6.4. The most important distinction between fig. 6.4 and fig. 6.2 is the 2 large Mach spikes in the data that occur between 2 and 3 seconds into the run. These spikes correspond to the pressure spikes in the pressure data, the first spike aligning with the plenum pressure spike similar to that seen in fig. 6.2, and the second aligning with

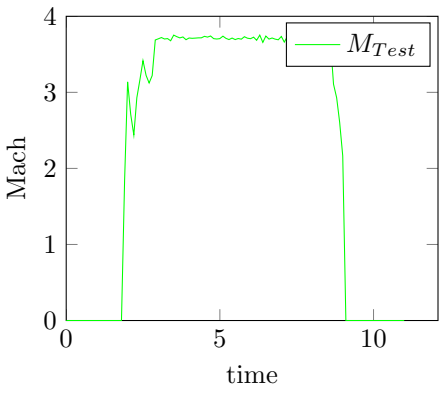

Figure 6.4: 2010 class SSWT Mach data

the spike in the test section pressure data. The second spike does not occur in fig. 6.2, and will be used in later testing to determine the location of the normal shock in the ramjet.

The pressure data for the final standard SSWT test discussed in this thesis is shown in fig. 6.5. This test appears to be a test in which the tank was filled up and was then run dry through the SSWT, with all the data captured for the whole run. The pressure lines in fig 6.5 all follow a very predictable pattern, the pressure readings from the plenum and the pitot probe remain constant and then slope downward to ambient, presumably as the pressure regulator can no longer maintain the 19psi differential at that pressure. Because of the required differential of the pressure regulator, a harder "corner" should have occurred when the pressure started dropping off but it appears to be more gradual. This observation will be visible in later figures as well and can be seen in fig. 6.3

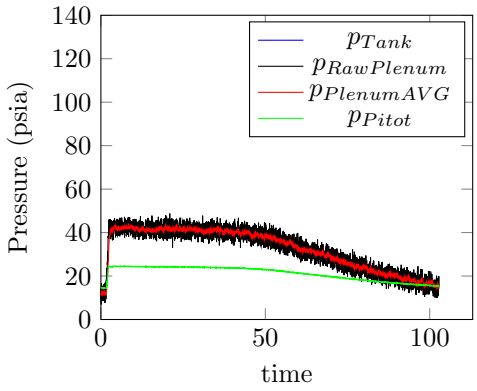

Figure 6.5: SSWT Lab run to empty pressure data

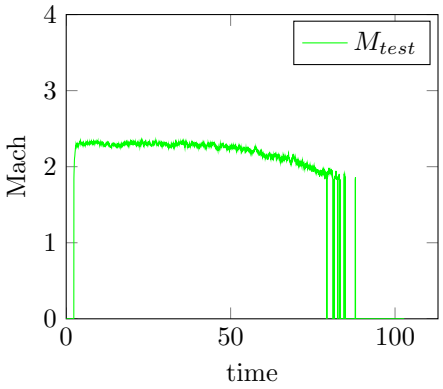

Figure 6.6: SSWT Lab run to empty Mach data

The Mach numbers in fig. 6.6 also display unique qualities found in this test. Figure 6.6 has the strange jagged trailing edge that begins around 1.8 Mach, but is simply a result of the data clipping mentioned along with fig. 6.2. The more important observation is the way the Mach number gradually falls off of the 2.4 line. This means that the shock wave is moving deeper into the nozzle and not expanding to the same location as before. The back pressure is not enough to maintain the 2.4 Mach expansion.

One of the most interesting and misleading aspects of this figure is the perceived "long" run time of the sswt at 40 psi in the plenum. It runs for nearly 50 seconds without loosing pressure significantly and it would appear that Mach 2.4 flow is sustainable for the duration. However, as predicted by the Fanno flow approximation and as discussed below, the Mach 2.4 flow isn't really

Mach 2.4 flow at the test section.

Figure. 6.6 is probably the best evidence of the normal shock occurring in the SSWT converging-diverging nozzle. If the normal shock were happening past the SSWT converging-diverging nozzle, firstly the Mach number should be around 3.3, but secondly, the Mach will not drop off as the pressure drops, or at least not right away. There would be some lag between the pressure reaching its lower limit and the Mach numbers dropping off if the normal shock occurred past the nozzle. However the drop off in Mach occurs exactly with the pressure drop, suggesting that the normal shock is being held in the SSWT converging-diverging nozzle where any change of pressure would result in a change in Mach number.

6.4 Ramjet Preliminary Test Results

The following data sets were all collected using the ramjet chassis in the "Blank" or "Inlet" Ramjet set up. This testing was completed before the Fanno flow approximations had been attempted. The results of this testing was to attempt to validate the inviscid approximations.

Where later testing was attempting to determine if the Ramjet operated like a supersonic wind tunnel without a diffuser, the early testing of the "Blank" ramjet was to determine if it operated the previous SSWT testing. Figure 6.7 is the pressure data from the first and second runs completed in the ramjet "Blank" configuration. Due to an error when ordering the pressure transducers, these initial runs relied on the same pressure transducers as the SSWT, and the error in the plenum pressure data had not been corrected. The first test was also completed with the safety committee present to help determine any issues with the procedures for running the "Blank" ramjet. The pressure results from these tests in fig. 6.7 matched all the data from the previous year's runs. The initial results discussed after this test were that the test was a success because the SSWT and Ramjet produced very similar results under the same conditions, meaning the ramjet was not introducing anything into the flow that was undesired.

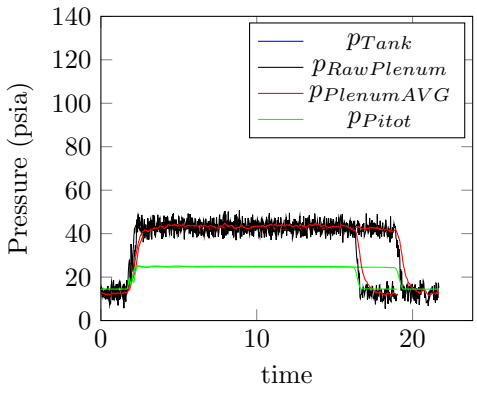

Figure 6.7: Ramjet initial pressure data

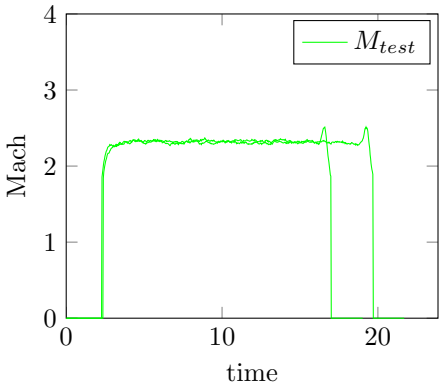

Figure 6.8: Ramjet initial Mach data

The Mach numbers in fig 6.8 also match the data from fig. 6.2. Although there was still the Mach disparity between the pressure data and the area ratio, these tests were considered "successful" because the disparity appeared to have nothing to do with the ramjet. It had been the responsibility of others to determine what was causing the issue in the SSWT but nothing had been determined at this point. It was determined that moving on to the inlet testing would be reasonable, despite the unknown cause of the Mach disparity.

The pressure data from the first test with the inlet installed is shown in fig. 6.9. The data presented in fig. 6.9 is what determined that there was a greater issue with the SSWT. The issue with fig. 6.9 is that it looks exactly the same as the data in fig. 6.7 and fig. 6.1. The inlet, a 10° ramp, in supersonic flow should cause some distinct changes in the pressure data. Even with the inviscid analysis, the angle of the inlet should have caused a pressure increased to 35 psia at station 3 where the stagnation pressure was collected.

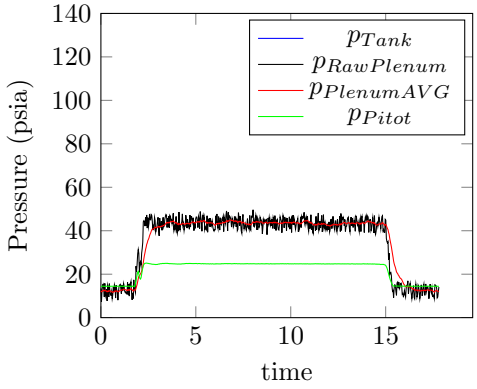

Figure 6.9: Ramjet "Inlet" run 1 pressure data

Plotting the Mach data, fig. 6.10, confirmed that no change had occurred in the flow at all. The data looks exactly the same as the other tests with a blank duct and the SSWT. The only reasonable takeaway from this test was that the SSWT was not producing supersonic flow at all. Supersonic flow disturbed by a ramp will have changes occur in the flow, the only possible explanation for the lack of change was a lack of supersonic flow. This led to the determination that the flow had not been supersonic for any of the previous tests, except the run which resulted in fig. 6.3 and 6.4, which meant that the ramjet had not been tested for supersonic disturbances in the first two runs. Figures 6.3 and 6.4 are also not available to demonstrate if the ramjet causes any supersonic disturbances due to there being a ramp in the test section during this test.

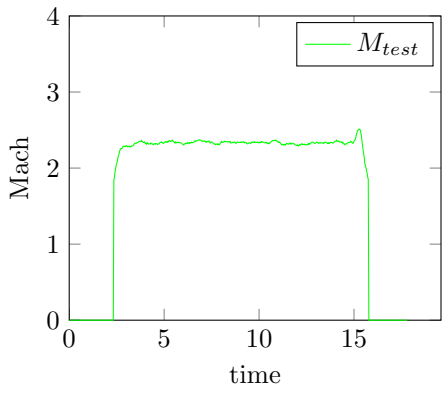

Figure 6.10: Ramjet "Inlet" run 1 Mach data

This test had been completed with the lower pressure of the previous testing to try to act as build up for the full pressure runs. It was determined that the low pressure could be the cause of the SSWT issues, as previous students had adjusted the pressure regulator to attempt longer runs. The decision was made to open the pressure regulator to increase the pressure in the plenum. The decision was made to attempt a full pressure run of the Inlet instead of returning to the blank run configuration. One of the issues that was uncovered was that there was no way to tell what the plenum pressure would be when adjusting the pressure regulator. Although previous projects had approached the subject, the pressure required for the ramjet was not part of the testing completed during the testing. [15]

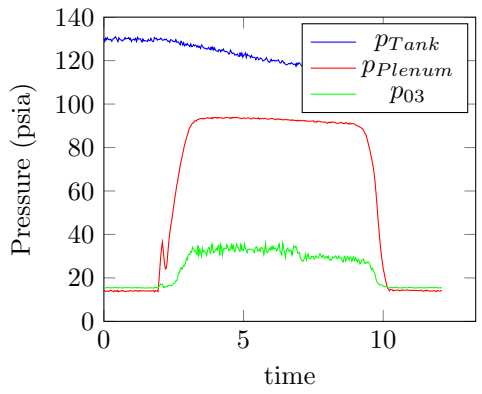

Figure 6.11: Ramjet "Inlet" run 2 pressure data

Between the first and second inlet tests however the issues with the tank pressure reading were solved, and the noisy plenum data was corrected as detailed in section 2.2. This is why there is no longer a black line in fig. 6.11 and why the blue tank pressure line is now visible.

The first issue that resulted form increasing the pressure in the plenum is that the pressure in the plenum far exceeded the 70 psi max pressure that was intended for the ramjet. This is visible in the plenum pressure of fig. 6.11, and it resulted in the bursting of the pressure relief disk in the test section. With the knowledge that the pressure relief disk burst, the decrease in the p_{03} in fig.6.11 appears to be the pressure relief disk bursting, however, it was actually the inlet breaking due to the pressure. The broken inlet was discovered when attempting to change the burst disk in the test section. It is evident from fig. 6.11 that the inlet was doing something to the flow, indicating supersonic flow occured in the SSWT up to the inlet's location.

The Mach number data also shows the break of the inlet quite well. Figure 6.12 shows a higher

Mach number than the tests before and it shows a dip when the inlet was still intact. This test determined that the low pressure was the cause of the subsonic flow in the SSWT. From here it was determined that the pressure requirements for supersonic flow in the SSWT and the "Blank" ramjet would need to be determined. The Fanno flow approximations were then developed to approximate these pressure requirements, which resulted in the success criteria in chapter 3.

6.5 Ramjet "Blank" Test Results

This section details the results of attempting to characterize the plenum pressure with relation to the pressure regulator. The data presented in this section was also used to validate aspects of the Fanno Flow approximation.

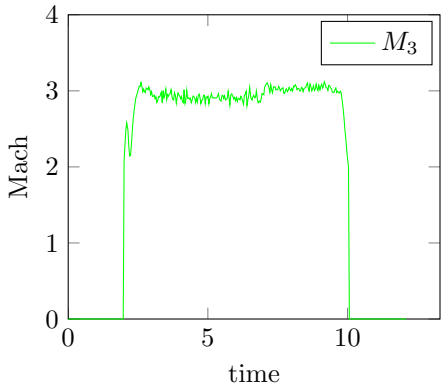

Figure 6.12: Ramjet "Inlet" run 2 Mach data

The data in fig. 6.13 was collected from the first run attempting to characterize the SSWT. Figure 6.13 was completed with the pressure regulator pilot valve set to 0.4 cm which resulted in approximately 105 psia initially in the plenum. As detailed in section 2.1, the pressure regulator allows greater pressure through as the pilot valve bolt is shortened. This is not only above the structural limit for a factor of safety of 2, but it also does not maintain this pressure. Part of the characterization approach was to determine where the SSWT achieved supersonic flow, but the other part was determining how long it could maintain supersonic flow. The result from fig. 6.13 were that the flow was supersonic but it was unsustainable.

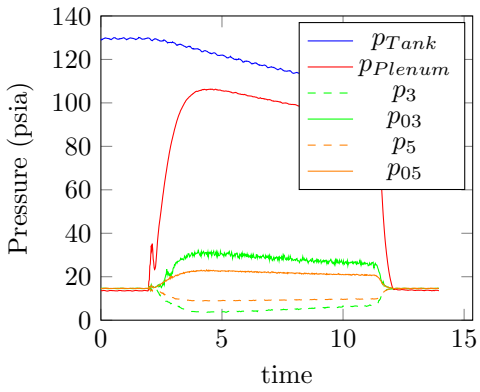

Figure 6.13: Ramjet "Blank" run 1 - Pressure data

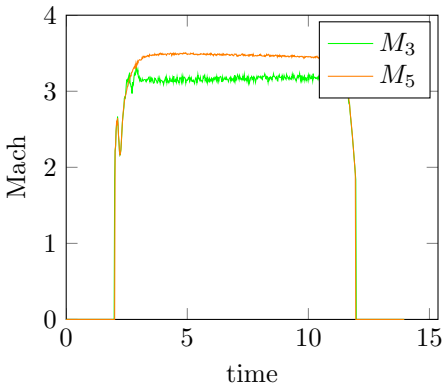

Figure 6.14: Ramjet "Blank" run 1 - Mach data

Despite the decreasing plenum pressure, the Mach number in fig. 6.14 is relatively constant for the entire 10 second run. This result is different than the data in fig. 6.6, where the Mach decreases at the same time as the pressure begins to drop. This suggests that despite the pressure dropping, the converging-diverging nozzle was still fully expanded even though the pressure was dropping. The average Mach number from fig. 6.14 is 3.167 with a peak of 3.33 Mach. The 3.167 Mach is a 4.2 % error form the expected 3.305 Mach number suggested from area ratio. However the error from the Fanno flow approximation, which predicted an apparent Mach number of 3.495 is 9.4%.

This test was the fist test completed with the full pressure transducer assemblies at station 3 and station 5. Although not exactly the same Mach numbers as predicted, the trend of having higher apparent Mach numbers at station 5 is visible in fig. 6.14. The higher Mach number is a result of stagnation pressure loss as discussed in section 3.1. The error between the 3.589 predicted by the Fanno flow and the average station 5 Mach number of 3.461 was 3.6%.

Increasing the length of the pilot valve to 0.8 cm, for the second run, only decreased the plenum pressure to 99 psia as displayed in fig. 6.15. This figure is difficult to read due to interference in the tank pressure, however the results are very similar to the first run. The pressure does not remain constant for any length of time and it drops at a a rate similar to the tank. The connections on the

tank pressure transducer were cleaned to fix the issue in this test, but even with the shaky data, the trend of the tank pressure is visible.

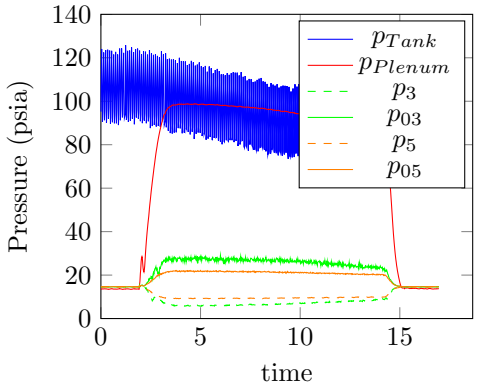

Figure 6.15: Ramjet "Blank" run 2 - Pressure data

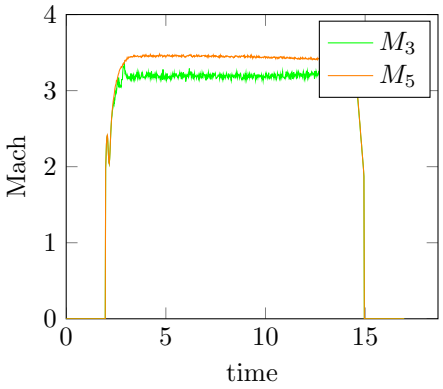

Figure 6.16: Ramjet "Blank" run 2 - Mach data

The average Mach number at station 3 in fig. 6.16 is 3.199 which is an 8.5% error from the Fanno flow predictions and a 3.22 % error from the area ratio prediction. The important gains from this test are recognition of pressure spikes on the leading edge of the p_{03} that aren't present in p_{05}. There is a similar pressure spike that occurs on all of the plenum pressures, but apart from the 2010 lab data in fig. 6.3, the bump never occurs on the test section pressure before these two runs. Due to it only appearing in these later tests, it was determined that the bumps indicate whether or not a normal shock hit the pitot tubes. This was determined due to its similarity to the bumps in the plenum pressure that occur exactly as the pressure in the plenum gets high enough to choke the flow in the converging diverging nozzle.

The pressure spike that occurs in p_{03} at station 3 does not occur at station 5. The M_5 data has a spike that correlates to the plenum pressure spike at 2 seconds in, but the bump that occurs in p_{03} has a response in M_3, but no correlation in M_5. Only M_3 has a clear effect from the p_{03} bump. This bump in p_{03} is what has been used to determine when the normal shock reaches the pitot-static system at station 3. If the spike does not occur then the normal shock never works its

way to station 3.

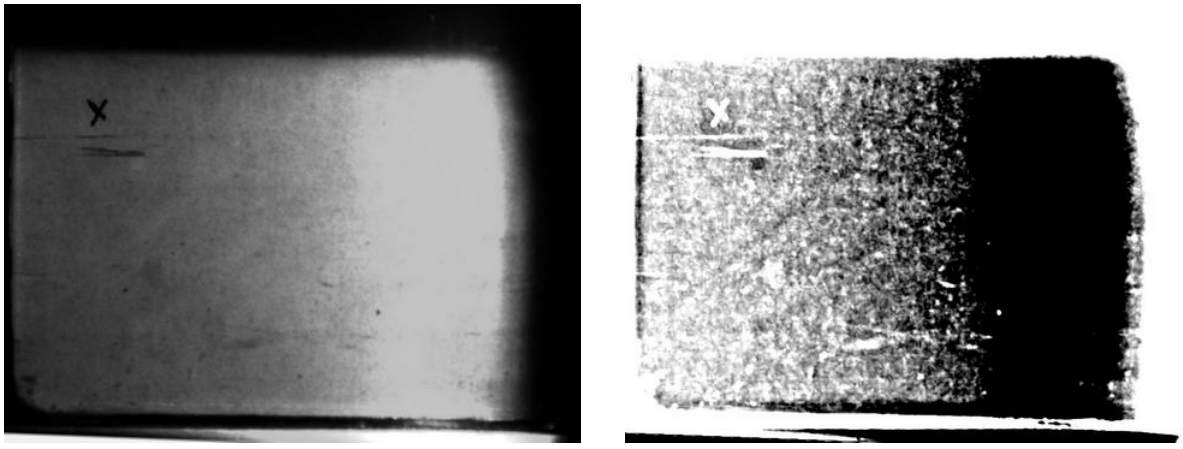

(a) The image of the oblique shock captured during the wedge test

(b) Some minor filters can be used to make the shock more visible.

Figure 6.17: The oblique shock during the "Wedge" test

Thirteen tests were performed in the blank setup to determine the characteristics of the pressure regulator and Fanno Flow approximations. However to prove finally whether or not the SSWT was producing supersonic flow in the "Blank" ramjet, the "Wedge" test, described in section 5.5, was performed to capture an image of an oblique shock in the viewing windows of the SSWT test section. Figure 6.17(a) is the result of the "Wedge" test, a picture of the shadow of an oblique shock projected onto a screen. Figure 6.17(b) is the same picture as fig. 6.17(a) with filters applied to it to bring out the shock wave that appears to cross the frame in middle and to the left. The original plan was to capture a shadow graph to attempt to use the picture to determine the Mach number of the flow in the SSWT with the "Blank" ramjet duct attached. This proved difficult due to how poor the viewing windows quality was after many years of operation. In order to capture the shock wave, the light and camera were mounted on the same side of the viewing windows and the camera was focused on a screen instead of the light shining through the viewing windows to the camera like a traditional shadow graph.

The setup of the picture means that the shadow may not represent the exact angle of the shock. The shock in fig. 6.17(a) is approximately 40°, which would mean a flow of only 2.48 Mach produce the shock. However because the light was mounted at an angle, to the shock, the image produced by the light is skewed. For the light and camera to be mounted on the same side of the SSWT, which was the only way any visualizations were possible, the light had to be at an angle to the flow. A light at a 14° angle from center could turn an oblique shock wave of 30.3°, which would suggest

the 3.305 Mach flow, into the 40° seen in fig. 6.17(a). This is a result of the shock wave being 3 dimensional across the width of the test section despite the flow being considered 2-dimensional.

What results is that the light shines through the shock wave instead of hitting it on end. The disturbance in the flow is still present so a shadow will still appear on the film but the angle will be skewed. The results of the "Wedge" test however are successful, the flow in the SSWT with the "Blank" ramjet was supersonic. All the effort and testing put into characterizing the SSWT resulted in a greater understanding of the properties of the SSWT.

6.6 Ramjet "Inlet" Test Results

Although the last test completed for this thesis was the "Wedge" test to determine if the effort placed on correcting the SSWT issues was effective, there were three full pressure tests of the inlet configuration and one of the Nozzle. As with any testing, the characteristics of the pressure regulator and plenum relationship continued to be documented to better understand the pressure regulators effects.

The first run of the inlet after determining the required pressure to operate the SSWT is shown in fig. 6.18. The plenum pressure was set approximately 82 psia max, but was done in error and was supposed to be a quarter turn more open to achieve the 88 psia required, however the data is still useful. As you can see over the 20 second run time the plenum pressure is not constant and slowly drops form the 82 psia it started at. The more important observation is that the pressure spike in the p_{03} is not present, indicating no super sonic flow reached the pitot tube. Meaning that as predicted by the Fanno flow approximations, 82 psia in the plenum is not enough to push the normal shock through the inlet. The data in fig. 6.18 is not noticeably different from the earlier blank runs where there was no inlet meaning the supersonic flow never interacted with the inlet.

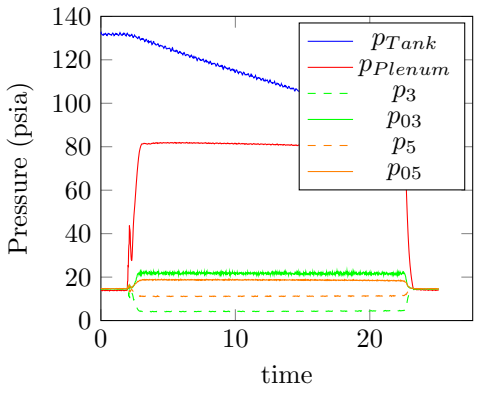

Figure 6.18: Ramjet "Inlet" upgrade run 1 - pressure data

Figure 6.19 is also showing the expected results of a nearly constant Mach number, indicating that, despite the dropping pressure, the normal shock was outside of the SSWT converging-diverging

nozzle. If the pressure was truly just enough to get the normal shock to the SSWT converging-diverging nozzle exit, then the Mach number at station 3 would begin to decrease as the pressure went down, but it does not. This was used as further proof that the 78 psia needed to fully expand the SSWT converging-diverging nozzle with the ramjet, as predicted by the Fanno Flow model, was accurate.

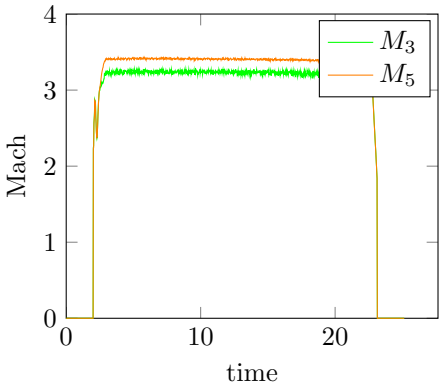

Figure 6.19: Ramjet "Inlet" upgrade run 1 - Mach data

The second inlet run resulted in the pressures in fig. 6.20, but the pressure in the plenum is only about 86psia. This was very close to the predicted 88 psia required for the normal shock to reach the pitot tube, however the data shows no shock in p_{03} so the shock never reached the pitot-static system. Again, the familiar drop off in plenum pressure is present, this run was slightly shorter but the pressure drops of faster at the higher pressure as expected.

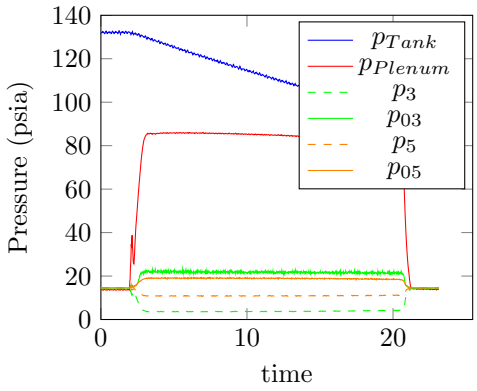

Figure 6.20: Ramjet "Inlet" upgrade run 2 - pressure data

The Mach values in fig. 6.21 are also very familiar, the Mach number remains mostly constant as the pressure drops. Neither figure shows any apparent effects by the inlet, meaning no supersonic flow made it through the inlet.

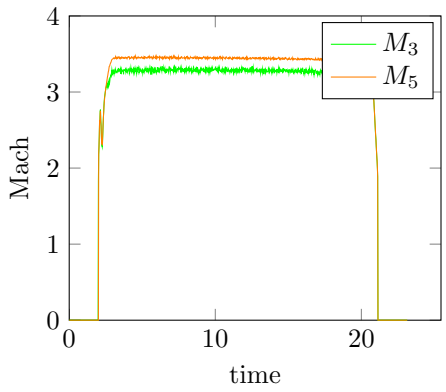

Figure 6.21: Ramjet "Inlet" upgrade run 2 - Mach data

The pressure data in fig. 6.22 shows significant differences to that of the other runs. Firstly the pressure in the plenum drops off extremely rapidly, due to its higher starting value. Although this run is longer, nearly 25 seconds total, the pressure decreases much faster than the other two inlet runs. That is partially to do with the much higher plenum pressure of around 103 psia. However what is remarkable about fig. 6.22 is the pitot pressure, p_{03}. There is clearly a bump in the pressure on the leading edge indicating the normal shock passed the pitot-tube system at station 3, which is also visible in fig. 6.23.

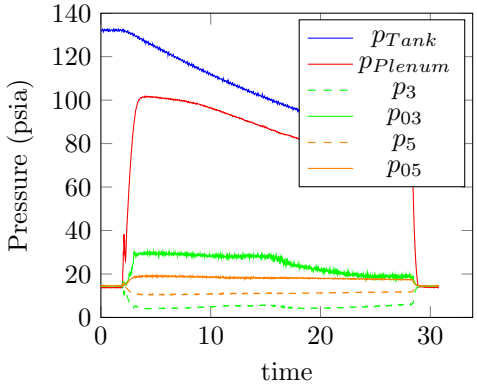

Figure 6.22: Ramjet "Inlet" upgrade run 3 - pressure data

The normal Shock interacting with the pitot tube indicates that the pressure is too high and is causing the inlet to swallow the normal shock which will cause poor inlet performance. However the location of the pitot tubes does not allow the normal shock to fully re-expand after the inlet. The pitot tubes induce a shock into the flow which keeps the shock from being swallowed by the inlet completely.

The p_{03} pressure in fig. 6.22 is also higher than the previous runs by nearly 10 psig. Some of this gain in p_{03} is due to the increased plenum pressure, but the increase in p_{03} pressure does not match the increase in plenum pressure. There is also clearly a dip in the pitot pressure at 15 seconds that corresponds with 88 psia in the plenum. This is clear proof that the wind tunnel must operate

above 88 psia to sustain supersonic flow through the inlet of the ramjet. The p_{03} then drops off to pressures more closely resembling that of the earlier tests, indicating the flow is no longer interacting with the flow.

The elevated p_{03} is not constant, and it drops with the plenum pressure maintaining an almost equal ratio to the plenum pressure meaning Mach is mostly constant, as is shown in fig. 6.23. The semi constant ratio between p_{03} and the plenum is only held for around 7 seconds before the Mach number in fig. 6.23 begins to drop. The station 3 pressure jumps and the Mach number falls, this can only be explained by the degradation of the oblique and normal shocks in the inlet.

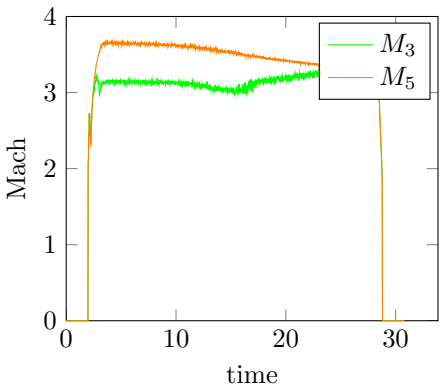

Figure 6.23: Ramjet "Inlet" upgrade run 3 - Mach data

The 7 seconds of run time with the inlet full involved results in an average apparent M_3 of 3.12 Mach, which is about 13.0% error with respect to the Fanno Flow predicted 2.76 Mach. Part of this is due most likely to the swallowing of the normal shock and the re-expansion on the back of the inlet. Other errors could be present in the alignment of the inlet. Although properly aligned before the test, the force of super sonic flow on the inlet is not trivial, so any slack in the supports could result in a slightly off angle.

Despite all the changes that occur with the station 3 pressure, p_{03}, the station 5 pressure remains steady through out the entire run. During the 7 second run with the inlet full involved the M_5 averages 3.62 Mach, which is a considerable error of 30.2% to the Fanno Flow predicted 2.78 Mach. The errors in station 5 are most likely due to unknown flow interactions at the nozzle most likely dealing with the pitot tube at station 3.

This test was done intentionally long to make fig. 6.24. Figure 6.24 is the difference between the plenum pressure and the tank pressure plotted over the length of the run. It was desired to run a long test to see if the plenum pressure and tank pressure difference ever stabilized at 19psi as was quoted. The results of this test however suggest that the pressure regulator stabilizes at a pressure difference of 14 psi

6.7 Ramjet "Inlet + Nozzle" Test Results

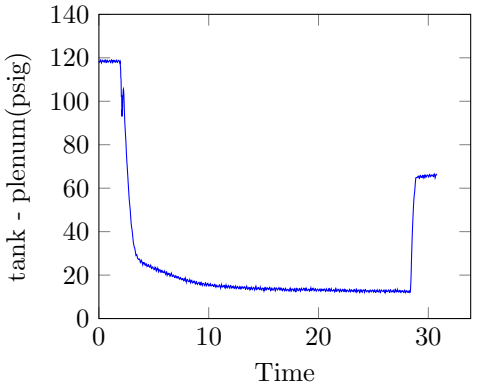

Figure 6.24: Tank-Plenum pressure difference

The farthest into the testing of the ramjet that occurred was a single run completed with the nozzle installed along with the inlet. Although the "Wedge" tests were completed after this test was completed, the wedge test did not further the testing schedule of the ramjet. The "Wedge" test was just completed to confirm supersonic flow in the "Blank" configuration and was not intended to further the ramjets capabilities but to put a cap on the testing already completed.

Figure 6.25 is the pressure data obtained from the ramjet when run in the nozzle and inlet setup. What is interesting about this figure is the fact that the inlet effects on p_03 from fig. 6.22 are not present, despite similar starting plenum pressures. The plenum pressure is not as high as the plenum in fig. 6.22 due to a lower starting pressure for the tank pressure. Although the pressure was above the 87 psi normally needed to reach the pitot static system, the characteristic bump is not present in p_{03}, indicating that the nozzle increases the pressure required to meet the pitot-static system. However we can also see that the inlet is still working because the pressure at p_{03} increases to a similar level as the inlet test, which is greater than the pressure in the blank tests.

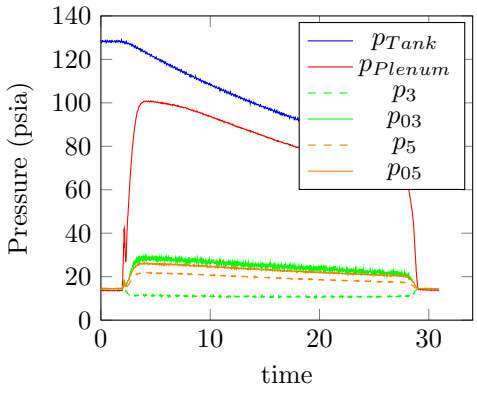

Figure 6.25: Ramjet "Inlet + Nozzle" run - Pressure data

What is different in fig. 6.25, that is not present in any other test is the results at station 5. Unlike fig. 6.22, where p_{05} does not appear to be affected by the inlet, p_{05} in fig. 6.25 is showing a large increase at the start. Also different is the results of p_5. The data produced by the static ports at both stations has not been discussed because it has not matched any predictions or models. In general the data has not made any sense, which could be indicative of poor alignment of the static

ports or adverse flow effects. Despite the poor characteristics during the other tests, p_5 in fig. 6.25 looks very different than any other run previous. Discussed in section 5.3.3, one of the concerns during the "Inlet + Nozzle" test is that the Fanno flow predicts that the nozzle will restrict the mass through the ramjet and results in a pressure rise during the run. The strange results of p_{05} and p_5 indicate that something of this nature is occurring, however without any other tests it is hard to draw conclusions from this one test.

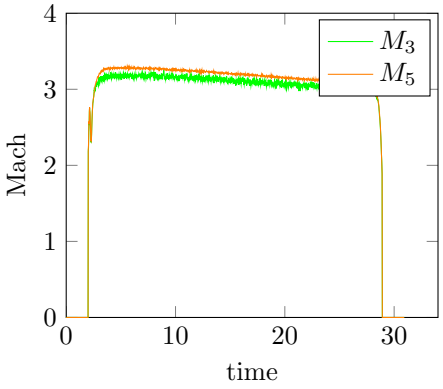

Figure 6.26: Ramjet "Inlet + Nozzle" run - Mach data

The Mach traces in fig. 6.26 are also distinct from previous tests. The line for M_3 looks similar to that in fig. 6.23 when the normal shock began to move back down the inlet, but M_5 also appears to follow the same track which did not occur in fig. 6.23. Although M_5 still appears higher as predicted by the Fanno flow approximations, it is not as high above M_3 as previously seen, which is a result of the higher p_{05}. As mentioned above, this is most likely due to the nozzle restricting the flow through the ramjet and building the pressure inside the ramjet. This is not a good thing to have occur, and is the cause of the "Inlet+Nozzle" test failing. The higher than expected pressures indicates that the nozzle needs to be setup closer to the Fanno flow predictions for the nozzle areas than the nozzle areas designed from the inviscid analysis. If testing on the ramjet is restarted, the nozzle setup needs to be amended before another nozzle test can occur.

Chapter 7

Conclusions and Future Work

The design and construction of the Ramjet attachment to the Cal Poly Supersonic Wind Tunnel was completed, but the testing was cut short due to changes in the safety requirements at Cal Poly. A greater understanding of the SSWT and it's requirements for operation were discovered and cataloged to increase the capabilities of the SSWT. Several known issues with the SSWT were corrected, and the procedures for operation were throughly reviewed to provide a safer lab environment.

The design of a modular ramjet was completed using verified custom MATLAB functions and SOLIDWORKS modeling and evaluation tools. The resulting design consisted of a 6 ft. long duct, with 6 interchangeable plates that could be replaced with various other plates allowing for a wide variety of potential experiments. The construction of the ramjet's modular design resulted in a simple piece of equipment that could be broken down into individual components small enough for one or two people to lift without mechanical aid. The use of common sized hardware made the ramjet easy to disassemble and reassemble with minimal tools. The design made it possible to completely alter the ramjet's internal geometry in less than 2 hours, meaning multiple different tests could be completed in single day. The modularity of the ramjet design was a complete success.

Many of the assumptions made during design of the ramjet were found to be incorrect during the early phases of testing. The fuel system initially designed for the ramjet was found to be incompatible with the fuel injector, resulting in a complete redesign of the fuel system, and a much leaner mixture than originally intended. The SSWT was found to be incapable of steady operation at supersonic speeds for any length of time, meaning the Ramjet would never be able to reach a steady state during operation. The initial max pressure that gave the Ramjet its factor of safety of 2 was found to not even produce supersonic flow in the ramjet. The unknown moisture level in the SSWT remained a constant potential source of error and the dry air desired for the ramjet was unable to be produced.

Despite the challenges during the design and early testing, twenty-five test runs were completed

with the Ramjet attached to the SSWT. The data of another seventeen lab tests of the SSWT were analyzed to help characterize the operation of the SSWT. Although initial design of the ramjet was completed using inviscid analysis techniques, a function to predict the friction effects in the SSWT was completed after early testing failed to produce supersonic flow. The Fanno Flow function was verified with data from the Ramjet tests, resulting in a minimum plenum pressure of 88 psia to make supersonic flow reach the pitot tubes in the Ramjet. The Fanno Flow can accurately predict the pressure requirements to place a normal shock at a particular location in the Ramjet duct. The verified Fanno Flow approximation was applied to the SSWT and the plenum pressure for normal operation of the SSWT should not be less than 78 psia. A working relation between the pressure regulator pilot valve and the plenum pressure was also developed to give the operator greater control over the SSWT parameters. To ensure that supersonic flow was occurring in the ramjet, a test involving a 15° wedge produced video proof of oblique shocks caused by the wedge, proving supersonic flow was present in the ramjet.

Most of the cold flow build-up testing was completed alongside attempting to characterize the SSWT. Testing of the redesigned fuel system and fuel injector resulted in a fuel flow capable of meeting the lower explosive limit of the Jet-A fuel that was intended to be used in this thesis. The ignition system borrowed from the bi-propellant rocket was adapted for use with the Ramjet as well. The "Blank" testing of the ramjet was completed resulting in an error of less than 10% from predicted values. The "Inlet" testing was also completed, but the varying plenum pressure made it hard to determine success due to flow interactions on the inlet. The resulting data was found to have between13-30% error based on the predicted results. A single"Inlet and Nozzle" test was completed resulting in a failed test due to the inviscid sizing of the nozzle restricting the flow in the ramjet. The follow up "Inlet and Nozzle" testing was canceled along with the remaining test points including the "Hot" fire testing of the ramjet due to safety concerns and new guidelines for operating experimental propulsion projects.

Despite not testing the full "Hot" setup, the cold ramjet testing was still successful. The ground work of successful cold flow testing and the analysis completed on the SSWT gives the ramjet and SSWT combination a number of options for future work. The multi-station pitot tube set up allows for a very effective tool in demonstrating the friction effects in flow. The ramjet also gave insights into the pitfall of trusting the equation over the concept. The modularity of the ramjet chassis will allow many other kinds of projects to occur that were not possible with the SSWT alone.

Some of the future work for this project should be directed at the SSWT. Although the aluminum

foil tape pressure relief system has worked successfully during testing, replacing the tape after it breaks requires removal of the entire ramjet. Some time and effort should be spent on redesigning a system that is both safe and easy to use. The benefit of the modular construction's lighter weight is seen in removing the ramjet to replace the relief system, however this is not the intended use of the modular design.

One of the constant potential error sources was the moisture in the air of the SSWT. An air drying method should be implemented for better operation of the SSWT and the ramjet. Dry air is an approximation made by most theoretical discussions on supersonic flow. The moisture in the air not only effects the supersonic characteristics of the flow, but also changes the constants used in calculating the pressure ratio in the SSWT and ramjet. Without understanding the moisture content of the air, the fuel to air ratios required for combustion are also relatively unknown resulting in potentially poor combustion performance during hot fire tests. Condensation also increased the difficulty of visualizing the oblique shock, and would pose similar problems for any future flow visualization attempts with the SSWT or the ramjet.

More effort should be taken to characterize the SSWT, including changing the nozzle dimensions and adjusting the diffuser to determine the requirements to use the SSWT to produce multiple different Mach numbers. Continue to develop and critique the Fanno Flow approximations during this testing so that a sound theoretical model is present alongside the actual data.

To increase the capabilities of the ramjet, the main goal should be to complete the testing. Determine if the ramjet meets the new safety requirements and whether or not it is capable of continuing on with the remaining testing. The fused-silica walls should be reconsidered to complete the ramjet's original desired function of allowing for flow and combustion visualization during testing. The issues with the static ports at stations 3 and 5 could be solved with a redesign of the pitot-static tube arrays, allowing for an alternate method for determining Mach number in the ramjet. Once these issues are resolved, the remaining future work would be to design new plates to be used in the ramjet. The standard blank inner plate design is located in Appendix B, and should be used as a starting point for any future designs. Many experiments are possible in the Ramjet duct, not just ones relating to supersonic flow.

BIBLIOGRAPHY

[1] ANSI and IEC Color Codes for thermocouples, wire and connectors. http://www.omega.com/toc_asp/frameset.html?book=Temperature&file=tc_colorcodes.

[2] Engineering Toolbox colebrook equation. http://www.engineeringtoolbox.com/colebrook-equation-d_1031.html.

[3] Engineering Toolbox gases - explosive and flammability concentration limits. http://www.engineeringtoolbox.com/explosive-concentration-limits-d_423.htm.

[4] Omega Engineering px603 and px613. http://www.omega.com/pptst/PX603.html.

[5] Omega Engineering tj36-xcib series. http://www.omega.com/pptst/TJ36-XCIB_CHB.html.

[6] Scaled Composites spaceshipone & white knight. http://www.scaled.com/projects/tierone/.

[7] V. S. A. Boudreau and D. Daniel. Developmental testing of ramjet/scramjet propulsion systems. *AIAA*, November 1993.

[8] G. A.Lovell and H. A. Gonzalez. Alterations of the cal poly supersonic wind tunnel to increase accuracy and prove the absence of shockwaves. Technical report, Aerospace Engineering Department, California Polytechnic State University, San Luis Obispo, California, June 2010.

[9] J. D. Anderson, Jr. *Fundamentals of Aerodynamics*. Anderson Series. McGraw-Hill, New York, fifth edition edition, 2011.

[10] W. H. Avery. Twenty-five years of ramjet development. *Journal of Jet Propulsion*, 25(11), 1955.

[11] C. E. M. B. D. Shaw and P. J. Wilbur. The annular flow electrothermal ramjet. *AIAA*, June 1984.

[12] J. A. Blevins and H. W. Coleman. An assessment of connected-pipe ramjet testing. *AIAA*, July 1995.

[13] D. H. Campbell. F- 12 series aircraft propulsion system performance and development. Technical report, Lockheed California Company, 1973.

[14] A. M. Carter. Nozzle design for the supersonic wind tunnel ramjet attachment. Technical report, Aerospace Engineering Department, California Polytechnic State University, San Luis Obispo, California, June 2013.

[15] N. Curran. Alterations and testing of the cal poly supersonic wind tunnel. Technical report, Aerospace Engineering Department, California Polytechnic State University, San Luis Obispo, California, June 2012.

[16] H. T. Daming Zhu, Zhili Zhu and J. Zhang. Overall performance design of ramjet for combine engine. *AIAA*, 2009.

[17] J. D.Mattingly. *Elements of Gas Turbine Propulsion.* McGraw-Hill, New York, 1996.

[18] G. L. Dugger. Recent advances in ramjet combustion. *ARS Journal*, 29(11), 1959.

[19] J. E.John and T. G. Keith. *Gas Dynamics.* Pearson Prentice Halll, Upper Saddle River, New Jersey, third edition edition, 2006.

[20] Emerson Process Management, McKinney, Texas. *6350 Series Pilots*, October 2009.

[21] Emerson Process Management, McKinney, Texas. *Types 1098-EGR and 1098H-EGR*, July 2011.

[22] P. G. Hill and C. R. Peterson. *Mechanics and Thermodynamics of Propulsion.* Addison-Wesley, Reading, Massachusetts, second edition edition, 1992.

[23] C. C. Humphrey. Design and fabrication of a ramjet inlet. Technical report, Aerospace Engineering Department, California Polytechnic State University, San Luis Obispo, California, June 2013.

[24] D. K. Huzel and D. H. Huang. *Modern Engineering for Design of Liquid-Propellant Rocket Engines.* AIAA, 1992.

[25] K. J. Johnson. Axisymmetric air augmented methanol/gox rocket mixing duct experimental thrust study. Master's thesis, California Polytechnic State University, San Luis Obispo, California, March 2013.

[26] T. K. M. Mitsuno and I. Nakagawa. Measuring method of ramjet test facility. *AIAA*, January 1995.

[27] A. Mehrparvar. Smore revision: Ignition and user interface. Technical report, Aerospace Engineering Department, California Polytechnic State University, San Luis Obispo, California, February 2013.

[28] I. Nakagawa and T. Kuwahara. Combustion of solid fueled ramjet. *AIAA*, July 1992.

[29] G. B. Northam and G. Y. Anderson. Survey of supersonic combustion ramjet research at langley. Technical report, NASA Langley Research Center, 1986.

[30] K. Selin. Ramjet fuel system. Technical report, Aerospace Engineering Department, California Polytechnic State University, San Luis Obispo, California, June 2012.

[31] P. C. Stone. Ramjet combustion chamber. Technical report, Aerospace Engineering Department, California Polytechnic State University, San Luis Obispo, California, June 2013.

[32] G. Thornton. Introduction to nuclear propulsion. Technical report, Flight Propulsion Laboratory Department, Deneral Electric, 1986.

[33] V. P. G. Valeriy I. Timoshenkoand, Vjacheslav P. Gusinin and I. S. Belotserkovets. The conception of a launch vehicles with ramjet and rocket-ramjet engines for a small payload injection into low earth orbit. *International Astronautical Congress*, 2006.

[34] R. Varvill and A. Bond. A comparison of propulsion concepts for ssto reusible launchers. Technical report, Reaction Engines Ltd, 2003.

[35] J. H. Zhixun Xia, Huijun Shen and B. Liu. Experimental investigation of powdered metals fuel ramjet. *AIAA*, 2008.

Appendix A

MatLab Code Verification

Listing A.1: This is the matlab script used to verify the results of my basic functions

```
% Harrison Sykes
% Proof of functions
%
clear all; close all; clc;

mypath = ['C:\Users\Harrison\Documents\college forms\MASTERS\',...
    'Thesis Paper\working template\FuncProof\'];


gamma = [1.4,1.3,5/3];
R = 1716.49;

Mach = [0:0.4:2,3,4:2:10];

for l = 1:length(gamma)
    %% Isentropic Flow - IsentropicPerfGas.m
    Isentropic = zeros(length(Mach),5);
    Isentropic(:,1) = Mach;

    %% Fanno Flow - FannoFlow.m
    Fanno = zeros(length(Mach),6);
    Fanno(:,1) = Mach;

    %% Rayleigh Line Flow - RayleighPerfGas.m
    Rayleigh = zeros(length(Mach),6);
    Rayleigh(:,1) = Mach;

    % PMfunc = zeros(length(Mach),3);
```

```
29
30      k = 1;
31      for i = 1:length(Mach)
32          %%% Isentropic Flow - IsentropicPerfGas.m
33          [Isentropic(i,2), Isentropic(i,3), Isentropic(i,4),...
34              Isentropic(i,5)] = IsentropicPerfGas(Mach(i), gamma(l));
35
36          %%% Fanno Flow - FannoFlow.m
37          [Fanno(i,6), Fanno(i,2), Fanno(i,3), Fanno(i,4), v_vstar,...
38              Fanno(i,5)] = FannoFlow(Mach(i), gamma(l));
39
40          %%% Rayleigh Line Flow - RayleighPerfGas.m
41          [Rayleigh(i,2), Rayleigh(i,3), Rayleigh(i,4), Rayleigh(i,5),...
42              Rayleigh(i,6)] = RayleighPerfGas(Mach(i), gamma(l));
43
44          if Mach(i) >= 1
45              %%% Normal Shock - obliqueshockfunct.m  -- w/ theta = 0
46              [~,Normshock(k,2),Normshock(k,5),Normshock(k,3),...
47                  Normshock(k,4),Normshock(k,6)] = ...
48                  obliqueshockfunct(0,Mach(i),gamma(l),R);
49              Normshock(k,1)= Mach(i);
50
51              %%% Rayleigh Pitot Tube Formula - RayleighPitotM.m for final
52              %%% norm shock variable p02/p1
53              [Normshock(k,7)] = RayleighPitotM(Mach(i), gamma(l), R);
54
55              k=k+1;
56          end
57      end
58
59      %% Oblique shocks - obliqueshockfunct.m -- with varying theta
60
61      Beta = linspace(0,90,200).*pi/180;
62      MachO = linspace(0,20,210);
63      for i = 1:length(Beta)
64          for j = 1:length(MachO)
65              % equation used in obliqueshockfunct.m actual function makes
66              %   this figure difficult to make
67              theta(j,i) = ...
68                  atan(2*cot(Beta(i))*(MachO(j)^2*sin(Beta(i))^2-1)/...
69                  (MachO(j)^2*(gamma(l)+cos(2*Beta(i)))+2));
```

```
70
71              % convert to degrees
72              theta(j,i) = theta(j,i)*180/pi;
73              if theta(j,i) < 0
74                  theta(j,i) = NaN;
75              end
76          end
77      end
78
79      [Betaplot,Machplot] = meshgrid(Beta*180/pi, MachO);
80      figure('name',['theta-beta-M',num2str(gamma(l))])
81      MachCon = contour(theta, Betaplot, Machplot,...
82          [1.05:0.05:1.5,1.6:0.1:2,2.2:0.2:4,4.5,5,6,8,10,20]);
83      clabel(MachCon)
84
85      % To align with John and Keith Tables B.1-B.3
86      Isentropic(:,2) = 1./Isentropic(:,2);
87      Isentropic(:,3) = 1./Isentropic(:,3);
88      Isentropic(:,4) = 1./Isentropic(:,4);
89
90      %Write to Data File compatable with pgfplotstable
91      filename = ['IsentropicPerfGasProof',num2str(gamma(l))];
92      colnames = {'Mach','TempRat0','PressRat0','DensRat0','AreaRat*'};
93      LaTeXpgfTable(Isentropic,filename,colnames,mypath,'.dat')
94
95      filename = ['FannoFlowProof',num2str(gamma(l))];
96      colnames = {'Mach','TempRat*','PressRat*','StagPressRat*',...
97          'DensRat*','fLmaxD'};
98      LaTeXpgfTable(Fanno,filename,colnames,mypath,'.dat')
99
100     filename = ['RayleighPerfGasProof',num2str(gamma(l))];
101     colnames = {'Mach','StagTempRat*','TempRat*','PressRat*',...
102         'StagPressRat*','VelRat*'};
103     LaTeXpgfTable(Rayleigh,filename,colnames,mypath,'.dat')
104
105     filename = ['obliqueshockfunct_NormProof',num2str(gamma(l))];
106     colnames = {'Mach1','Mach2','PressRat','TempRat','DensRat',...
107         'StagPressRat','Stag2Press1Rat'};
108     LaTeXpgfTable(Normshock,filename,colnames,mypath,'.dat')
109 end
```

Listing A.2: This is the matlab script for Fanno Flow relations

```
% Harrison Sykes
% FannoFlow - Function
%   This function Calculates the f*L/D and property changes for a given
%   Mach number and gamma for a duct flow with friction.
%       f - darcy friction factor

% Equations are from John and Keith

function [fLstar_D, T_Tstar, p_pstar, p0_p0star, v_vstar, rho_rhostar]...
    = FannoFlow(M, gamma)

fLstar_D = ...
    ((gamma+1)/(2*gamma))*log(((gamma+1)/2)/(1+((gamma-1)/2)*M^2))...
    - 1/gamma*(1-1/M^2)-((gamma+1)/(2*gamma))*log(1/M^2);           %(9.16)

T_Tstar = (gamma+1)/(2+(gamma-1)*M^2);                              %(9.25)
p_pstar = 1/M*sqrt(T_Tstar);                                        %(9.26)
p0_p0star = 1/M*(1/T_Tstar)^((gamma+1)/(2*(gamma-1)));              %(9.28)
rho_rhostar = 1/M*sqrt(1/T_Tstar);                                  %(9.27)
v_vstar = 1/rho_rhostar;                                            %(9.27)
end
```

FannoFlow.m - $\gamma = 1.4$					
Mach	$\frac{T}{T*}$	$\frac{p}{p*}$	$\frac{p_0}{p_0*}$	$\frac{\rho}{\rho*}$	$\frac{f*L_{max}}{D_H}$
0	1.2	∞	∞	∞	NaN
0.4	1.1628	2.6958	1.5901	2.3184	2.3085
0.8	1.0638	1.2893	1.0382	1.2119	0.0723
1.2	0.9317	0.8044	1.0304	0.8633	0.0336
1.6	0.7937	0.5568	1.2502	0.7016	0.1724
2	0.6667	0.4082	1.6875	0.6124	0.305
3	0.4286	0.2182	4.2346	0.5092	0.5222
4	0.2857	0.1336	10.7188	0.4677	0.6331
6	0.1463	0.0638	53.1798	0.4357	0.7299
8	0.087	0.0369	190.1094	0.4239	0.7682
10	0.0571	0.0239	535.9375	0.4183	0.7868

Table A.1: Fanno Flow, $\gamma = 1.4$

FannoFlow.m - $\gamma = 1.3$					
Mach	$\frac{T}{T*}$	$\frac{p}{p*}$	$\frac{p_0}{p_0*}$	$\frac{\rho}{\rho*}$	$\frac{f*L_{max}}{D_H}$
0	1.15	∞	∞	∞	NaN
0.4	1.123	2.6493	1.6023	2.3591	2.52
0.8	1.0493	1.2804	1.0395	1.2203	0.0804
1.2	0.9457	0.8104	1.0321	0.8569	0.0382
1.6	0.8309	0.5697	1.2712	0.6856	0.199
2	0.7188	0.4239	1.7732	0.5898	0.3573
3	0.4894	0.2332	5.1598	0.4765	0.6277
4	0.3382	0.1454	15.9441	0.4299	0.7726
6	0.1797	0.0706	120.0965	0.3932	0.9037
8	0.1085	0.0412	623.1235	0.3795	0.957
10	0.0719	0.0268	2,416.118	0.373	0.9832

Table A.2: Fanno Flow, $\gamma = 1.3$

FannoFlow.m - $\gamma = \frac{5}{3}$					
Mach	$\frac{T}{T*}$	$\frac{p}{p*}$	$\frac{p_0}{p_0*}$	$\frac{\rho}{\rho*}$	$\frac{f*L_{max}}{D_H}$
0	1.3333	∞	∞	∞	NaN
0.4	1.2658	2.8127	1.5603	2.222	1.8725
0.8	1.0989	1.3104	1.0351	1.1924	0.0559
1.2	0.9009	0.791	1.0268	0.878	0.0249
1.6	0.7194	0.5301	1.2076	0.7369	0.1229
2	0.5714	0.378	1.5313	0.6614	0.2113
3	0.3333	0.1925	3	0.5774	0.3456
4	0.2105	0.1147	5.6406	0.5449	0.4091
6	0.1026	0.0534	15.8438	0.5204	0.4617
8	0.0597	0.0305	35.0703	0.5116	0.4818
10	0.0388	0.0197	66.3063	0.5074	0.4914

Table A.3: Fanno Flow, $\gamma = \frac{5}{3}$

Listing A.3: This is the matlab script for Isentropic relations of a perfect gas

```
% Harrison Sykes
% IsentropicPerfGas function -
%   This function calculates the isentropic relations for flow at a given
%   mach number and gamma

function [T0_T, P0_P, Rho0_Rho, A_Astar] = IsentropicPerfGas(M, gamma)

T0_T = 1 + (gamma - 1)/2*M^2;
P0_P = (1 + (gamma - 1)/2*M^2)^(gamma/(gamma - 1));
Rho0_Rho = (1 + (gamma - 1)/2*M^2)^(1/(gamma -1));
A_Astar = 1/M*((2/(gamma + 1))*(1 + (gamma - 1)/2*M^2))^...
    ((gamma + 1)/(2*(gamma-1)));
end
```

IsentropicPerfGas.m - $\gamma = 1.4$				
Mach	$\frac{T}{T_0}$	$\frac{p}{p_0}$	$\frac{\rho}{\rho_0}$	$\frac{A}{A*}$
0	1	1	1	∞
0.4	0.969	0.8956	0.9243	1.5901
0.8	0.8865	0.656	0.74	1.0382
1.2	0.7764	0.4124	0.5311	1.0304
1.6	0.6614	0.2353	0.3557	1.2502
2	0.5556	0.1278	0.23	1.6875
3	0.3571	0.0272	0.0762	4.2346
4	0.2381	$6.5861 \cdot 10^{-3}$	0.0277	10.7188
6	0.122	$6.3336 \cdot 10^{-4}$	$5.1936 \cdot 10^{-3}$	53.1798
8	0.0725	$1.0243 \cdot 10^{-4}$	$1.4135 \cdot 10^{-3}$	190.1094
10	0.0476	$2.3563 \cdot 10^{-5}$	$4.9483 \cdot 10^{-4}$	535.9375

Table A.4: Isentropic Flow, $\gamma = 1.4$

IsentropicPerfGas.m - $\gamma = 1.3$				
Mach	$\frac{T}{T_0}$	$\frac{p}{p_0}$	$\frac{\rho}{\rho_0}$	$\frac{A}{A*}$
0	1	1	1	∞
0.4	0.9766	0.9023	0.924	1.6023
0.8	0.9124	0.6722	0.7367	1.0395
1.2	0.8224	0.4285	0.5211	1.0321
1.6	0.7225	0.2446	0.3385	1.2712
2	0.625	0.1305	0.2087	1.7732
3	0.4255	0.0247	0.058	5.1598
4	0.2941	$4.9765 \cdot 10^{-3}$	0.0169	15.9441
6	0.1563	$3.2104 \cdot 10^{-4}$	$2.0546 \cdot 10^{-3}$	120.0965
8	0.0943	$3.6059 \cdot 10^{-5}$	$3.8222 \cdot 10^{-4}$	623.1235
10	0.0625	$6.0555 \cdot 10^{-6}$	$9.6887 \cdot 10^{-5}$	2,416.118

Table A.5: Isentropic Flow, $\gamma = 1.3$

IsentropicPerfGas.m - $\gamma = \frac{5}{3}$				
Mach	$\frac{T}{T_0}$	$\frac{p}{p_0}$	$\frac{\rho}{\rho_0}$	$\frac{A}{A*}$
0	1	1	1	∞
0.4	0.9766	0.9023	0.924	1.6023
0.8	0.9124	0.6722	0.7367	1.0395
1.2	0.8224	0.4285	0.5211	1.0321
1.6	0.7225	0.2446	0.3385	1.2712
2	0.625	0.1305	0.2087	1.7732
3	0.4255	0.0247	0.058	5.1598
4	0.2941	$4.9765 \cdot 10^{-3}$	0.0169	15.9441
6	0.1563	$3.2104 \cdot 10^{-4}$	$2.0546 \cdot 10^{-3}$	120.0965
8	0.0943	$3.6059 \cdot 10^{-5}$	$3.8222 \cdot 10^{-4}$	623.1235
10	0.0625	$6.0555 \cdot 10^{-6}$	$9.6887 \cdot 10^{-5}$	2,416.118

Table A.6: Isentropic Flow, $\gamma = \frac{5}{3}$

Listing A.4: This is the matlab script for Rayleigh Line Flow relations of a perfect gas

```
% Harrison Sykes
% Rayleigh line flow - Flows With heat addition
% From the Equations in John and Keith
% Perfect gas assumed

function [T0_T0star,T_Tstar,P0_P0star,P_Pstar,V_Vstar] =...
    RayleighPerfGas(M, gamma)

% Static
P_Pstar = (1 + gamma)/ (1+gamma*M.^2);  %(10.11)
T_Tstar = ((1 + gamma).^2*M.^2)/((1+gamma*M.^2).^2);    %(10.12)
V_Vstar = ((1 + gamma)*M.^2)/(1 + gamma*M.^2);  %(10.13)

% Stagnation
T0_T0star = ((1 + gamma)*(M.^2)*(2 + (gamma - 1)*M.^2))/...
    ((1 + gamma*(M.^2)).^2);        %(10.14)
                    % v-- this is inverted in John and Keith
P0_P0star = ((1 + gamma)/(1 + gamma*M.^2))...
    *((2 + (gamma - 1)*M.^2)/(gamma + 1)).^(gamma/(gamma-1));
    %(10.15) - corrected using correct substitution for p/p*
```

```
21 end
```

RayleighPerfGas.m - $\gamma = 1.4$					
Mach	$\frac{T_0}{T_0*}$	$\frac{T}{T*}$	$\frac{p}{p*}$	$\frac{p_0}{p_0*}$	$\frac{V}{V*}$
0	0	0	1.2679	2.4	0
0.4	0.529	0.6151	1.1566	1.9608	0.3137
0.8	0.9639	1.0255	1.0193	1.2658	0.8101
1.2	0.9787	0.9118	1.0194	0.7958	1.1459
1.6	0.8842	0.7017	1.1756	0.5236	1.3403
2	0.7934	0.5289	1.5031	0.3636	1.4545
3	0.654	0.2803	3.4245	0.1765	1.5882
4	0.5891	0.1683	8.2268	0.1026	1.641
6	0.5363	0.0785	38.9459	0.0467	1.6809
8	0.5165	0.0449	136.6235	0.0265	1.6954
10	0.507	0.029	381.6149	0.017	1.7021

Table A.7: Rayleigh Flow, $\gamma = 1.4$

RayleighPerfGas.m - $\gamma = 1.3$					
Mach	$\frac{T_0}{T_0*}$	$\frac{T}{T*}$	$\frac{p}{p*}$	$\frac{p_0}{p_0*}$	$\frac{V}{V*}$
0	0	0	1.2552	2.3	0
0.4	0.5165	0.58	1.1515	1.904	0.3046
0.8	0.9614	1.0088	1.0193	1.2555	0.8035
1.2	0.9765	0.9235	1.0199	0.8008	1.1532
1.6	0.8701	0.723	1.1858	0.5314	1.3604
2	0.7659	0.5505	1.5518	0.371	1.4839
3	0.6032	0.2952	4.0074	0.1811	1.6299
4	0.5266	0.1781	11.5697	0.1055	1.6881
6	0.4639	0.0833	81.7942	0.0481	1.7322
8	0.4402	0.0478	413.4127	0.0273	1.7482
10	0.4289	0.0308	1,582.289	0.0176	1.7557

Table A.8: Rayleigh Flow, $\gamma = 1.3$

RayleighPerfGas.m - $\gamma = \frac{5}{3}$					
Mach	$\frac{T_0}{T_0*}$	$\frac{T}{T*}$	$\frac{p}{p*}$	$\frac{p_0}{p_0*}$	$\frac{V}{V*}$
0	0	0	1.2552	2.3	0
0.4	0.5165	0.58	1.1515	1.904	0.3046
0.8	0.9614	1.0088	1.0193	1.2555	0.8035
1.2	0.9765	0.9235	1.0199	0.8008	1.1532
1.6	0.8701	0.723	1.1858	0.5314	1.3604
2	0.7659	0.5505	1.5518	0.371	1.4839
3	0.6032	0.2952	4.0074	0.1811	1.6299
4	0.5266	0.1781	11.5697	0.1055	1.6881
6	0.4639	0.0833	81.7942	0.0481	1.7322
8	0.4402	0.0478	413.4127	0.0273	1.7482
10	0.4289	0.0308	1,582.289	0.0176	1.7557

Table A.9: Rayleigh Flow, $\gamma = \frac{5}{3}$

Listing A.5: This is the matlab script for Normal Shock relations of a perfect gas

```
% Harrison Sykes
% Oblique shock function
% 10/29/2012

function [Beta,Mf,rho2_rho1,p2_p1,T2_T1,p02_p01] = ...
    obliqueshockfunct(theta,Mi,gamma,R)
%%% INPUTS %%%%%%%%%%%%%%%%%%%%%%%%%%%%%%%%%%%%%%%%%%%%%%%%%%%%%%%%%%%%%%%%
% theta = deflection angle
% Mi = initial mach number before shock occurs
% gamma = ratio of specific heats
% R = gas constant

%%% Outputs %%%%%%%%%%%%%%%%%%%%%%%%%%%%%%%%%%%%%%%%%%%%%%%%%%%%%%%%%%%%%%%%
% Beta = Mach Angle
% Mf = final mach number after shock occurs
% rho2_rho1 = ratio of static densities, before shock / after shock
% p2_p1 = ratio of static pressures, before shock / after shock
% T2_T1 = ratio of static Temperature, before shock / after shock
% p02_p01 = ratio of stagnation pressure, before shock / after shock

```

```
cp = gamma*R/(gamma-1);

theta = pi/180*theta; % converts to radians

thetaequ = @(Beta)  thetasolve(theta, Beta, Mi, gamma);

if theta ==0;
    Beta = fzero(thetaequ,pi/2); % pi/2 start point gives the strong shock
else
    Beta = fzero(thetaequ,pi/4); % pi/4 start point gives the weak shock
end
Beta = 180/pi*Beta; % converts to degrees.
if Beta > 90 || Beta < 0
    Betaplot = linspace(0,90,200);
    Betaplot = Betaplot.*pi/180;
    M = linspace(1,20,length(Betaplot));
    thetaplot = zeros(length(Betaplot),length(M));

    for i = 1:length(M)
        for j = 1:length(Betaplot)

%             thetaplot(i,j) = atan(cot(Betaplot(j))*...
%               (M(i)^2*sin(Betaplot(j))^2-1)/...
%               ((gamma+1)/2*M(i)^2 - (M(i)^2*sin(Betaplot(j))^2-1)));
%                                 % john and keith (Eq. 6.18)

            thetaplot(i,j) = atan(2*cot(Betaplot(j))*...
                (M(i)^2*sin(Betaplot(j))^2-1)/...
                (M(i)^2*(gamma+cos(2*Betaplot(j)))+2));
                                % Anderson (Eq. 9.23)
            if thetaplot(i,j)<0
                thetaplot(i,j) = nan;
            end
        end
    end
    thetaplot = thetaplot.*180/pi;
    Betaplot = Betaplot.*180/pi;
    [Betaplot,M] = meshgrid(Betaplot,M);

    figure('name','Theta - Beta - M chart')
    hold on
```

```
62      C = contour(thetaplot,Betaplot,M,[Mi Mi]);
63      clabel(C);
64      plot([180/pi*theta, 180/pi*theta],[0,90])
65      hold off
66      xlabel('\theta - deflection angle')
67      ylabel('\beta - shockwave angle')
68
69      error(['Warning, theta is out of range for Mach number.',...
70          ' Fzero could not converge'])
71  end
72
73  %%% components of mach at oblique shock
74  % Parallel Component
75  Mpar = Mi*cosd(Beta);
76  % normal Component before shock
77  M1 = Mi*sind(Beta);
78  % normal component after shock #Anderson (9.14)
79  M2 = sqrt((1+((gamma-1)/2)*M1^2)/(gamma*M1^2-(gamma-1)/2));
80
81  %%% post shock values
82  % Mach
83  Mf = M2/(sind(Beta - 180/pi*theta));
84  % Density #Anderson (9.15)
85  rho2_rho1 = (gamma + 1)*M1^2/(2+(gamma-1)*M1^2);
86  % Pressure #Anderson (9.16)
87  p2_p1 = 1+2*gamma/(gamma+1)*(M1^2-1);
88  % Temperature
89  T2_T1 = (p2_p1)/(rho2_rho1);
90  % Entropy
91  s2_s1 = cp*log(T2_T1) - R*log(p2_p1);
92  % Stagnation Pressure
93  p02_p01 = exp(-(s2_s1)/R);
94
95  function zero = thetasolve(theta, Beta, M, gamma)
96
97  %             thetatest = atan(cot(Beta)*(M^2*sin(Beta)^2-1)/...
98  %                 ((gamma+1)/2*M^2 - (M^2*sin(Beta)^2-1))); % john and
99  %                 keith (Eq. 6.18)
100
101 thetatest = atan(2*cot(Beta)*(M^2*sin(Beta)^2-1)/...
102     (M^2*(gamma+cos(2*Beta))+2));               % Anderson (Eq. 9.23)
```

```
103
104  zero = theta - thetatest;
```

obliqueshockfunct.m - $\gamma = 1.4$						
M_1	M_2	$\frac{p_f}{p_i}$	$\frac{T_f}{T_i}$	DensRat	$\frac{p_0 f}{p_0 i}$	$\frac{p_0 f}{p_i}$
1.2	0.84	1.5133	1.128	1.34	0.9928	2.4075
1.6	0.67	2.82	1.388	2.03	0.8952	3.805
2	0.58	4.5	1.6875	2.67	0.7209	5.6404
3	0.48	10.3333	2.679	3.86	0.3283	12.061
4	0.43	18.5	4.0469	4.57	0.1388	21.0681
6	0.4	41.8333	7.9406	5.27	0.0297	46.8152
8	0.39	74.5	13.3867	5.57	$8.4878 \cdot 10^{-3}$	82.8655
10	0.39	116.5	20.3875	5.71	$3.0448 \cdot 10^{-3}$	129.217

Table A.10: Normal Shock, $\gamma = 1.4$

obliqueshockfunct.m - $\gamma = 1.3$						
M_1	M_2	$\frac{p_f}{p_i}$	$\frac{T_f}{T_i}$	DensRat	$\frac{p_0 f}{p_0 i}$	$\frac{p_0 f}{p_i}$
1.2	0.84	1.4974	1.0995	1.36	0.9926	2.3164
1.6	0.66	2.7635	1.2991	2.13	0.8891	3.6353
2	0.56	4.3913	1.5274	2.88	0.7006	5.37
3	0.45	10.0435	2.2804	4.4	0.2822	11.4409
4	0.41	17.9565	3.3181	5.41	0.0993	19.9589
6	0.37	40.5652	6.271	6.47	0.0142	44.3087
8	0.36	72.2174	10.4009	6.94	$2.8271 \cdot 10^{-3}$	78.4027
10	0.35	112.913	15.7096	7.19	$7.4021 \cdot 10^{-4}$	122.2391

Table A.11: Normal Shock, $\gamma = 1.3$

obliqueshockfunct.m - $\gamma = \frac{5}{3}$						
M_1	M_2	$\frac{p_f}{p_i}$	$\frac{T_f}{T_i}$	DensRat	$\frac{p_0 f}{p_0 i}$	$\frac{p_0 f}{p_i}$
1.2	0.84	1.4974	1.0995	1.36	0.9926	2.3164
1.6	0.66	2.7635	1.2991	2.13	0.8891	3.6353
2	0.56	4.3913	1.5274	2.88	0.7006	5.37
3	0.45	10.0435	2.2804	4.4	0.2822	11.4409
4	0.41	17.9565	3.3181	5.41	0.0993	19.9589
6	0.37	40.5652	6.271	6.47	0.0142	44.3087
8	0.36	72.2174	10.4009	6.94	$2.8271 \cdot 10^{-3}$	78.4027
10	0.35	112.913	15.7096	7.19	$7.4021 \cdot 10^{-4}$	122.2391

Table A.12: Normal Shock, $\gamma = \frac{5}{3}$

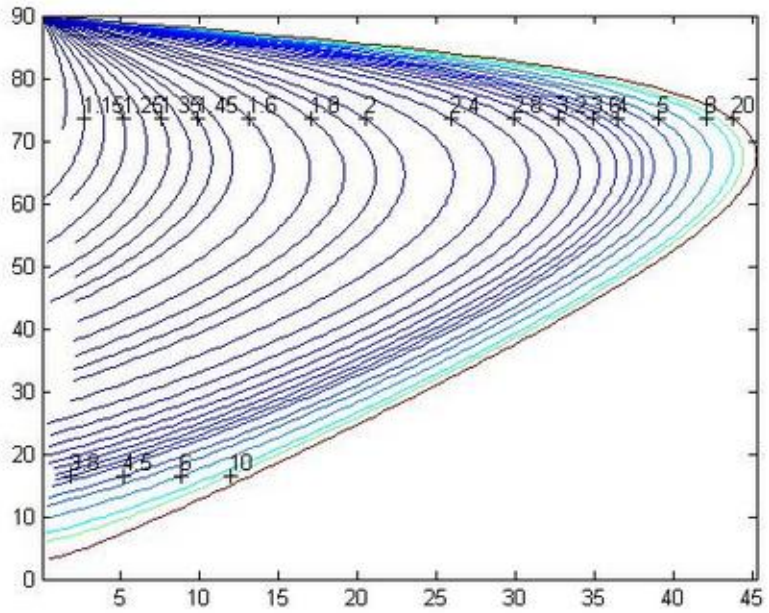

Figure A.1: Oblique Shock, $\gamma = 1.4$

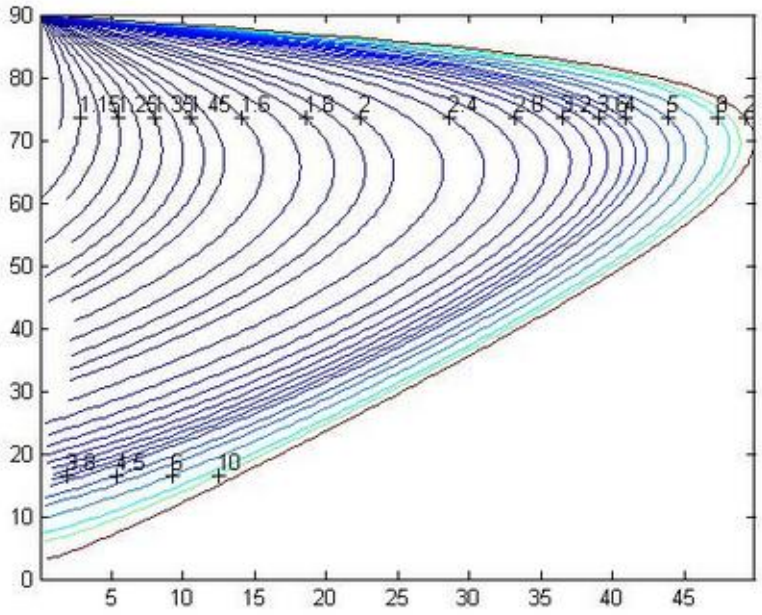

Figure A.2: Oblique Shock, $\gamma = 1.3$

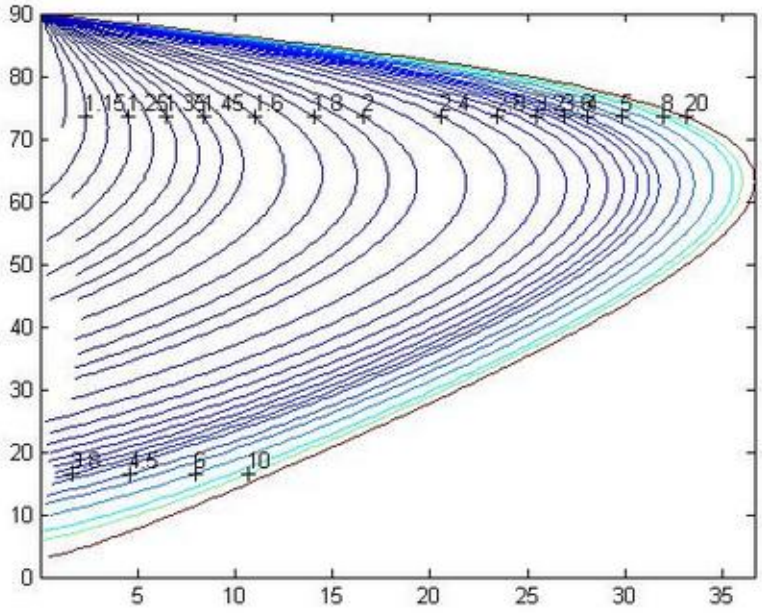

Figure A.3: Oblique Shock, $\gamma = \frac{5}{3}$

Appendix B

Basic Inner Plate

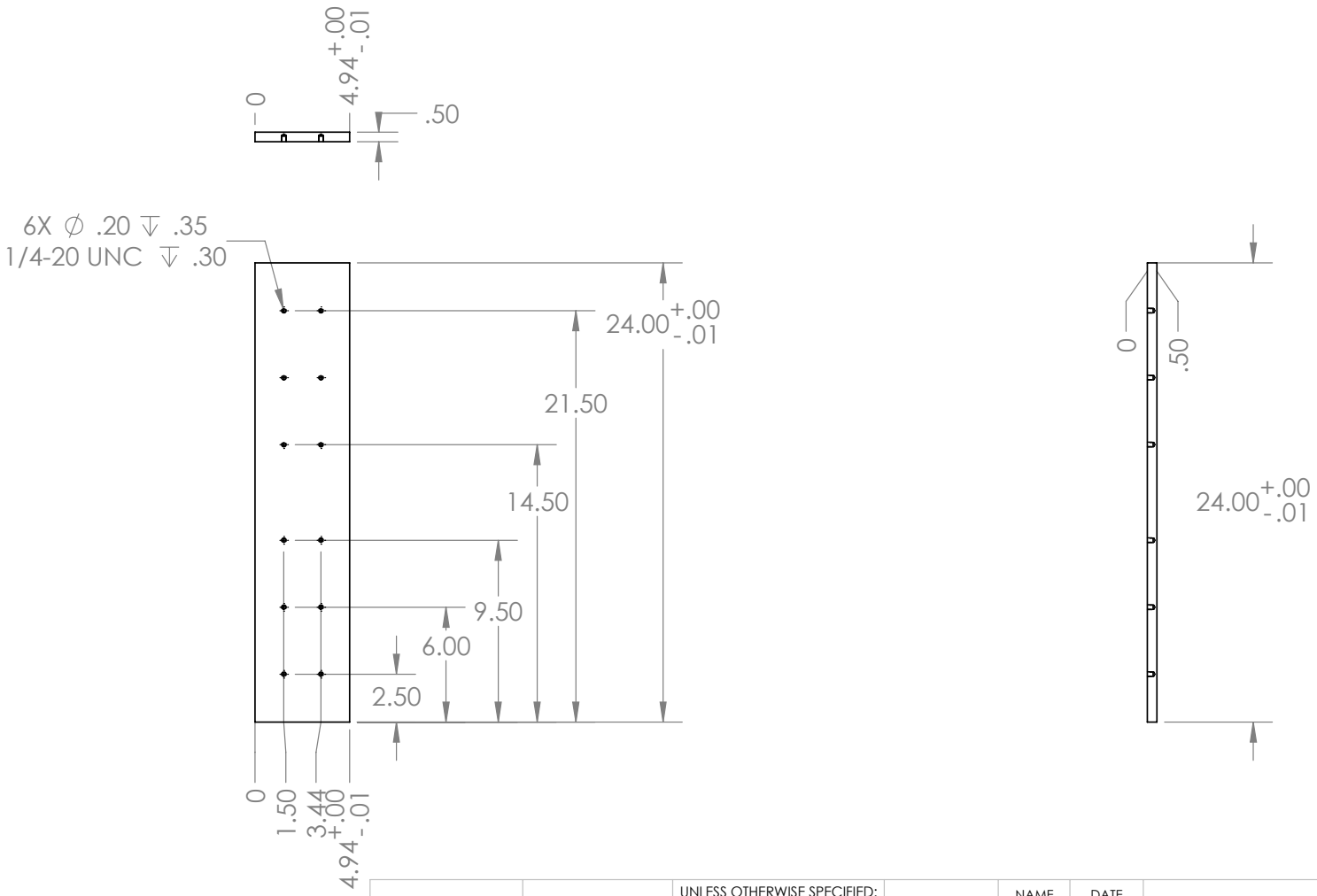

		UNLESS OTHERWISE SPECIFIED:		NAME	DATE
		DIMENSIONS ARE IN INCHES TOLERANCES: FRACTIONAL ± ANGULAR: MACH ± BEND ± TWO PLACE DECIMAL ± THREE PLACE DECIMAL ±	DRAWN		
			CHECKED		
			ENG APPR.		
			MFG APPR.		
		INTERPRET GEOMETRIC TOLERANCING PER:	Q.A.		
		MATERIAL	COMMENTS:		
NEXT ASSY	USED ON	FINISH			
APPLICATION		DO NOT SCALE DRAWING			

TITLE:

SIZE	DWG. NO.	REV
A	anerplate_face	
SCALE: 1:8	WEIGHT:	SHEET 1 OF 1

5 4 3 2 1

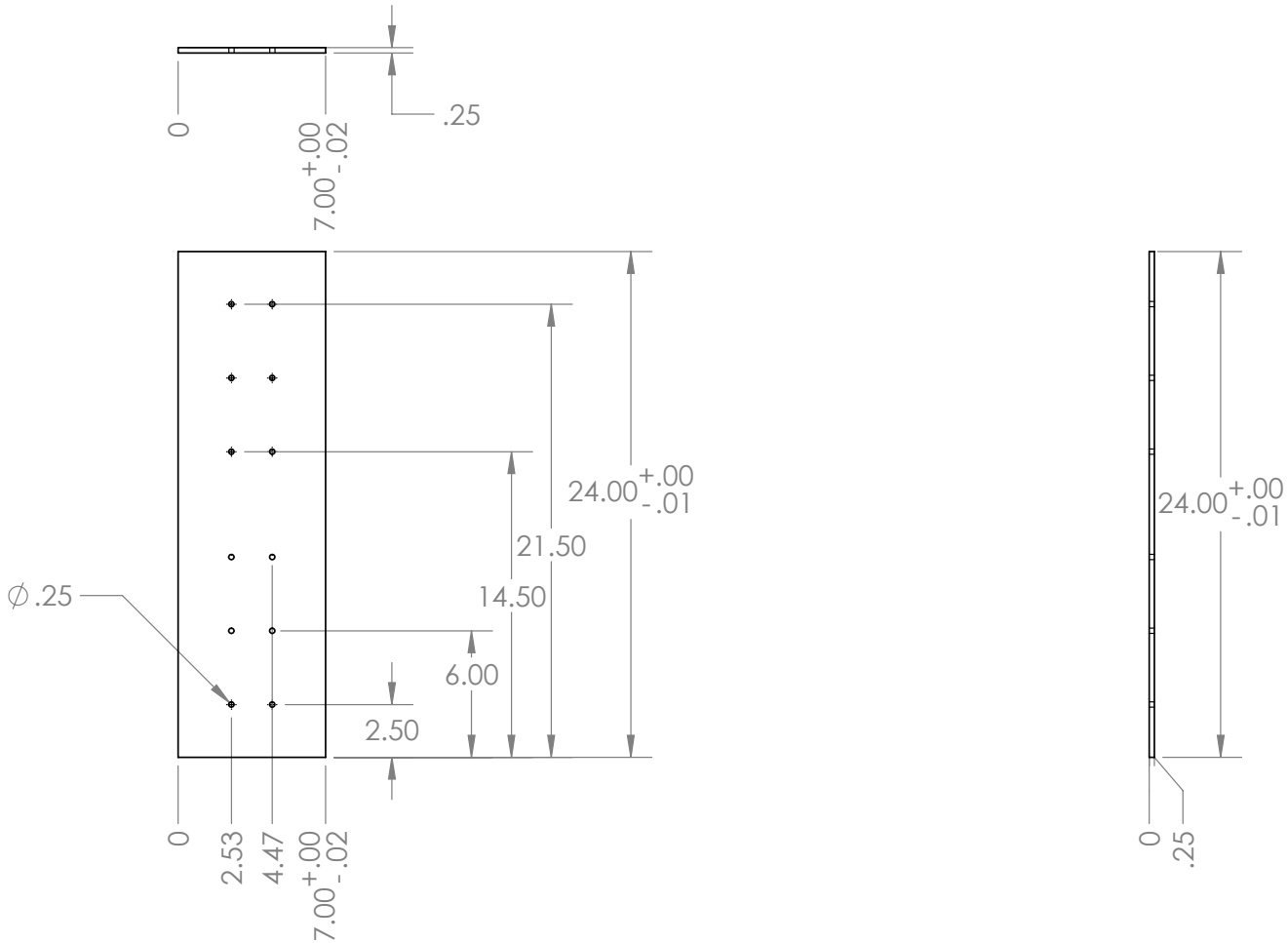

		UNLESS OTHERWISE SPECIFIED:		NAME	DATE
		DIMENSIONS ARE IN INCHES TOLERANCES: FRACTIONAL ± ANGULAR: MACH ± BEND ± TWO PLACE DECIMAL ± THREE PLACE DECIMAL ±	DRAWN		
			CHECKED		
			ENG APPR.		
			MFG APPR.		
		INTERPRET GEOMETRIC TOLERANCING PER:	Q.A.		
		MATERIAL	COMMENTS:		
NEXT ASSY	USED ON	FINISH			
APPLICATION		DO NOT SCALE DRAWING			

TITLE:

SIZE A | DWG. NO. inerplate_base | REV

SCALE: 1:8 | WEIGHT: | SHEET 1 OF 1

5 4 3 2 1

Appendix C

Ramjet – Standard Operating Procedures

C.1 Installing the SSWT Pressure Relief System

NOTE: Before doing any work on the Ramjet or the SSWT, ensure that the main valve to the SSWT is closed at the Air Tank.

NOTE: Ramjet will be configured for a Blank run, with a 15o wedge installed in the SSWT test section.

IN CASE OF EMERGENCY:

University Police Department #805756-2281

San Luis Obispo Police Department #911

C.1.1 Installing the SSWT Pressure Relief System

NOTE: Get Aluminum Tape Dimensions.

Removing the Test Section Plate

1. Ensure that the ramjet or SSWT have been removed from downstream of the test section
2. Remove the 7 hex key bolts from the top of the test section plate
3. Remove the 2 plates secured by the 7 bolts
4. Remove the 2 hex key bolts from the downstream side of the test section plate
5. Using a mallet or hammer and a block of wood, gently knock the test section plate out of its position

Installing the Test Section Plate

1. Ensure that the ramjet or SSWT have been removed from downstream of the test section
2. Using a mallet or hammer and a block of wood, gently knock the test section plate into position
3. Insert the 2 hex key bolts into the downstream side of the test section plate and get the threads started
4. Place the 2 plates above the test section plate into position
   – Note: one side has 3 holes and the other 4
5. Insert the 7 hex key bolts into the top of the test section and tighten down but not all the way.
6. Tighten down the 2 hex key bolts in the downstream side of the test section plate
7. Tighten down the 7 hex key bolts in the top of the test section

Installing the Relief system

1. Remove the test section plate
   – See section 1.1
2. Ensure that no tape remains from a previous broken relief system
3. Lay a single piece of Aluminum tape down over the hole from front to back covering the length of the plate.
4. Remove any excess tape that over hangs on the edges of the plate
5. Install the test section plate
   – See Section 1.2
6. Place a ping pong ball on top of the hole in the test section plate from the outside.
   – During tests, watch for the ping pong ball moving to determine if the pressure relief system broke. This indicates an over pressure situation has occurred
   – 1 Stop test if Ping Pong Ball moves
   – 2 Cross reference with collected Data to determine if it was a bad break or if the Ramjet was about to over pressurize once shut down is complete.

Installing the Calibration Wedge

1. Remove the test section plate
   – See section 1.1
2. Place the 15o wedge in position above the SSWT test section windows. – Ensure some of the wedge is visible for reference in the video
3. Install the test section plate – See Section 1.2

C.2 Assembling the Ramjet

C.2.1 Chassis Set Up

1. Place front brace (A), and the two middle braces (B and C) in their positions and bolt into place on the frame
2. Latch front brace to the SSWT
3. Remove 4 screws from the top bars of both mid braces (8 bolts total), set bars aside
4. Loosen the bolts on bottom cross bar of both mid braces, but do not remove
5. Set one of the outer plates into position on mid braces and the front brace
6. Place desired bottom inner plates into outer plate
   – See Sections C.2.3 through C.2.7 for specific test setup
7. Place the two walls into the gutters of the inner plates
8. Place desired top inner plates onto the walls
   – See Sections C.2.3 through C.2.7 for specific test setup
9. Place the remaining outer plate into position on top of inner plates
   – If the plate will not slide into the front plate, loosen the bolts holding the top bar of the front brace
10. Set the back brace into position onto the ramjet and bolt into place
11. Set the top bars of the mid braces back onto the ramjet and insert all 8 bolts
12. Tighten all bolts in the lab setup

13. Connect any instruments, fuel lines, or hoses as required for your setup
    – See Sections C.2.3 through C.2.7 for specific test setup

C.2.2 Chassis Tear Down

1. Disconnect any instruments, fuel lines, or hoses as required for your setup
   – See Sections C.2.8 through C.2.12 for specific test tear down
2. Remove 4 screws from the top bars of both mid braces (8 bolts total), set bars aside
3. Loosen the bolts on bottom cross bar of both mid braces, but do not remove
4. Unbolt the back brace from the support frame and remove from the test area
   – It is often helpful to loosen the bolts surrounding the rear face before removing
5. Remove the top outer plate from the assembly
   – If the plate is stuck, loosen the bolts holding the top bar of the front brace
6. Remove the top 3 inner plates
   – See Sections C.2.8 through C.2.12 for specific test tear down
7. Remove each wall
8. Remove the bottom 3 inner plates
   – See Sections C.2.8 through C.2.12 for specific test tear down
9. Remove the bottom outer plate
10. Set the top bars of the mid braces back into position and insert all 8 bolts
11. Unlatch the front brace
12. Unbolt the front brace and the two mid braces from the support frame and remove from the test area

C.2.3 Blank Setup

NOTE – The Blank setup has only blank plates. There should be no obstructions in the ramjet or any other inhibitors to the flow.

1. Before Proceeding, steps 1-5. from Section C.2.1 must be completed

2. Place the aluminum instrumentation plate onto the outer plate in the forward position
   – The pressure port is mounted 4 from the back of the plate and the plate should be place with the stagnation prongs pointed toward the SSWT
3. Place a blank aluminum plate onto the outer plate in the middle position
4. Place the stainless steel instrumentation plate onto the outer plate in the rear position
   – The pressure port is located 6 from the front of the plate and should be placed with the stagnation prongs pointed toward the SSWT
5. Complete step 7. from Section C.2.1
6. Place 3 Blank inner plates onto the walls
   – These plates do not have high temperature requirements so they can be made from Aluminum or stainless steel
7. Complete steps 10. – 12. from Section C.2.1
8. Connect the pressure transducers to the pressure ports
   – Check that the pressure transducers are wired to the DAQ and 10V DC power supply correctly (see Section 2.2.1)
   – 1. Fuel and ignition are not required for this test

C.2.4 Inlet Setup

NOTE – The Inlet setup has the inlet plate installed in the forward position

1. Before Proceeding, steps 1-5. from Section C.2.1 must be completed
2. Place the aluminum instrumentation plate onto the outer plate in the forward position
   – The pressure port is mounted 4 from the back of the plate and the plate should be place with the stagnation prongs pointed toward the SSWT
3. Place a blank aluminum plate onto the outer plate in the middle position
4. Place the stainless steel instrumentation plate onto the outer plate in the rear position
   – The pressure port is located 6 from the front of the plate and should be placed with the stagnation prongs pointed toward the SSWT

5. Complete step 7. from Section C.2.1

6. Place the Inlet plate onto the walls onto the forward position

7. Place 2 Blank inner plates onto the walls
   – These plates do not have high temperature requirements so they can be made from Aluminum or stainless steel

8. Complete steps 10. – 12. from Section C.2.1

9. Connect the pressure transducers to the pressure ports
   – Check that the pressure transducers are wired to the DAQ and 10V DC power supply correctly (see Section 2.2.1)

   – 1. Fuel and ignition are not required for this test

C.2.5 Inlet and Nozzle Setup

NOTE – The Inlet and nozzle setup has the inlet plate installed in the forward position and the nozzle plate in the rear position

1. Before Proceeding, steps 1-5. from Section C.2.1 must be completed

2. Place the aluminum instrumentation plate onto the outer plate in the forward position
   – The pressure port is mounted 4 from the back of the plate and the plate should be place with the stagnation prongs pointed toward the SSWT

3. Place a blank aluminum plate onto the outer plate in the middle position

4. Place the stainless steel instrumentation plate onto the outer plate in the rear position
   – The pressure port is located 6 from the front of the plate and should be placed with the stagnation prongs pointed toward the SSWT

5. Complete step 7. from Section C.2.1

6. Place the Inlet plate onto the walls in the forward position

7. Place 1 Blank inner plate onto the walls in the middle position
   – This plate does not have high temperature requirements so it can be made from Aluminum or stainless steel

8. Place the nozzle plate onto the walls in the rear position

9. Complete steps 10. – 12. from Section C.2.1

10. Connect the pressure transducers to the pressure ports

    – Check that the pressure transducers are wired to the DAQ and 10V DC power supply correctly (see Section 2.2.1)

    – 1. Fuel and ignition are not required for this test

C.2.6 Full Setup – Cold

NOTE – The full cold setup has ramps, a fuel injector, and a baffle inside the ramjet.

1. Before Proceeding, steps 1-5. from Section C.2.1 must be completed

2. Place the aluminum instrumentation plate onto the outer plate in the forward position

   – The pressure port is mounted 4 from the back of the plate and the plate should be place with the stagnation prongs pointed toward the SSWT

3. Place the stainless steel instrumentation plate onto the outer plate in the rear position

   – The pressure port is located 6 from the front of the plate and should be placed with the stagnation prongs pointed toward the SSWT

4. Disconnect the baffle track from the stainless steel combustor plate with the fuel injector.

5. Place the fuel injector combustor plate into the outer plate in the middle position

   – The fuel injector should be pointed with the tallest tube pointed upstream, rotate fuel injector to align with desired placement

6. Complete steps 7. from Section C.2.1

7. Place the igniter combustor plate onto the walls in the middle position

   – The igniter port from the plate must be mounted in the upstream position

   – Rotate the lower rail to allow for proper alignment with the fuel injector

8. Bolt down the rail to the lower plate

9. Place the inlet plate onto the walls in the forward position

10. Place the nozzle plate onto the walls in the rear position

11. Complete steps 10. – 12. from Section C.2.1

12. Connect the pressure transducers to the pressure ports

    – Check that the pressure transducers are wired to the DAQ and 10V DC power supply correctly (see Section 2.2.1)

C.2.7 Full Setup – Hot

Warning: Jet A is flammable; avoid heat, sparks, and flames

IN CASE OF EMERGENCY:

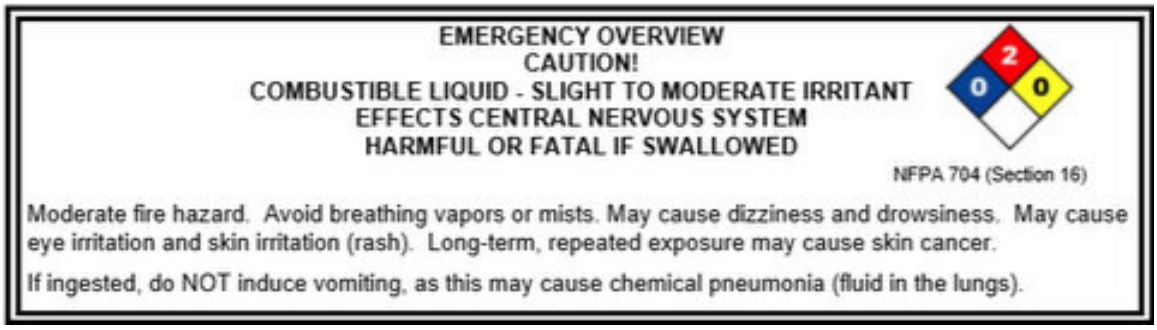

University Police Department #805756-2281

San Luis Obispo Police Department #911

NOTE – The full setup has ramps, a fuel injector, an ignition source and a baffle inside the ramjet. There will be burning fuel during a successful test and proper equipment must be accessible.

1. Before Proceeding, steps 1-5. from Section C.2.1 must be completed

2. Place the aluminum instrumentation plate onto the outer plate in the forward position

   – The pressure port is mounted 4 from the back of the plate and the plate should be place with the stagnation prongs pointed toward the SSWT

3. Place the stainless steel instrumentation plate onto the outer plate in the rear position

   – The pressure port is located 6 from the front of the plate and should be placed with the stagnation prongs pointed toward the SSWT

4. Disconnect the baffle track from the stainless steel combustor plate with the fuel injector.

5. Place the fuel injector combustor plate into the outer plate in the middle position

   – The fuel injector should be pointed with the tallest tube pointed upstream, rotate fuel

injector to align with desired placement

6. Complete steps 7. from Section C.2.1

7. Place the igniter combustor plate onto the walls in the middle position
   – The igniter port from the plate must be mounted in the upstream position
   – Rotate the lower rail to allow for proper alignment with the fuel injector

8. Bolt down the rail to the lower plate

9. Place the inlet plate onto the walls in the forward position

10. Place the nozzle plate onto the walls in the rear position

11. Complete steps 10. – 12. from Section C.2.1

12. Connect the pressure transducers to the pressure ports
    – Check that the pressure transducers are wired to the DAQ and 10V DC power supply correctly (see Section 2.2.1)

13. Connect the igniter to the MSD box and the ground

14. Connect the fuel system to the fuel injector
    – Insure that the fuel solenoid valve vertical once installed

15. In the control room, ensure the control box switches are all turned off and connect the power wiring harness connection to the control box

16. Plug in the control box to the wall outlet and the 12V DC leads to the 12V DC power source

C.2.8 Blank Tear Down

1. Before proceeding, complete step 1. in section C.2.2

2. If Pressure data was collected follow these steps:
   – Disconnect the leads in the DAQ.
   – Disconnect the pressure transducers from the pressure ports

3. Complete steps 2 – 5. in section C.2.2

4. Remove the two instrument plates and the blank plate

5. Complete step 7. in section C.2.2

6. Remove the three blank plates from the lower outer plate

7. Complete steps 9. – 12. in section C.2.2

C.2.9 Inlet Tear Down

1. Before proceeding, complete step 1. in section C.2.2

2. If Pressure data was collected follow these steps:
   – Disconnect the leads in the DAQ.
   – Disconnect the pressure transducers from the pressure ports

3. Complete steps 2 – 5. in section C.2.2

4. remove the inlet plate from the walls

5. Remove the two blank plates from walls

6. Complete step 7. in section C.2.2

7. Remove the two instrument plates and the blank plate from the lower outer plate

8. Complete steps 9. – 12. in section C.2.2

C.2.10 Inlet and Nozzle Tear Down

1. Before proceeding, complete step 1. in section C.2.2

2. If Pressure data was collected follow these steps:
   – Disconnect the leads in the DAQ.
   – Disconnect the pressure transducers from the pressure ports

3. Complete steps 2 – 5. in section C.2.2

4. Remove the inlet plate from the walls

5. Remove the nozzle plate from the walls

6. Remove the blank plate from walls

7. Complete step 7. in section C.2.2

8. Remove the two instrument plates and the blank plate from the lower outer plate

9. Complete steps 9. – 12. in section C.2.2

C.2.11 Full Tear Down – Cold

1. Before proceeding, complete step 1. in section C.2.2

2. If Pressure data was collected follow these steps:
   – Disconnect the leads in the DAQ.
   – Disconnect the pressure transducers from the pressure ports

3. Complete steps 2 – 5. in section C.2.2

4. Remove the nozzle plate from the rear position and the inlet from the forward position.

5. Disconnect the baffle track from the lower stainless steel combustor plate with the fuel injector.

6. Remove the upper combustor plate and the track assembly

7. Complete step 7. in section C.2.2

8. Remove the two instrumentation plates and the lower combustor plate

9. Reconnect the combustor plate to the track assembly

10. Complete steps 9. – 12. in section C.2.2

C.2.12 Full Tear Down – Hot

1. Before proceeding, complete step 1. in section C.2.2

2. Disconnect the control box from the wall outlet, and from the 12V DC power supply

3. Ensure the control box switches are turned off and disconnect the power wiring harness connection at the control box

4. Disconnect the fuel system from the fuel injector

5. If Pressure data was collected follow these steps:
   – Disconnect the leads in the DAQ.
   – Disconnect the pressure transducers from the pressure ports

6. Complete steps 2 – 5. in section C.2.2
7. Remove the nozzle plate from the rear position and the inlet from the forward position.
8. Disconnect the baffle track from the lower stainless steel combustor plate with the fuel injector.
9. Remove the upper combustor plate and the track assembly
10. Complete step 7. in section C.2.2
11. Remove the two instrumentation plates and the lower combustor plate
12. Reconnect the combustor plate to the track assembly
13. Complete steps 9. – 12. in section C.2.2

C.3 Running the Ramjet – COLD FLOW

CAUTION – Ensure that all power sources are turned off. Always check the power supply is off before beginning test procedures

IN CASE OF EMERGENCY:

University Police Department #805756-2281

San Luis Obispo Police Department #911

C.3.1 Job Descriptions

1. **Safety Controller** – Inside the control room with door shut during test, responsible for ensuring all the steps in the procedure are done. Responsible for accurate placement of all personnel such that they are behind the protective barrier of the SSWT hard walls. Also responsible for turning on the data recording in LabView, opening the pressure valve to the Electro pneumatic valve. Will remain in the control room until all clear is given.
2. **Manual Valve Operator** – Opens the manual valve and then stands behind the Air tank in sight of the Parking Lot Signal person. Will not move until given the close valve signal, then will return position behind the Air tank until all clear is given.

3. **Parking Lot Relay** – Stands on the corner of the building, alerts the Manual valve operator when to open or close the valve, alerts the Safety Controller when the valve is open or closed. Also must alert people of test who approach in their vehicles. Will not move until all clear is given.

4. **Stairs Signal Person** – stands on top of the stairs in view of the Parking Lot Signal Person to warn people of the upcoming test. Will not move until all clear is given.

5. **Electro-pneumatic valve Operator** – Inside the control room with door shut during test, responsible for turning on and off the electro pneumatic valve. Responsible for watching the ping pong ball that indicates an over pressure emergency, and the dial gage on the plenum. Will remain in the control room until all clear is given.

C.3.2 Hand Signals

1. "Success/Confirm task completion" – thumbs-up
2. "Stop run" – slash finger across throat
3. "All clear" – both arms straight up over shoulders
4. "Open Manual Valve" – Reverse alligator arm motion
5. "Close Manual valve" – Alligator arm motion

C.3.3 Emergency Shutdown Procedures

WARNING: No one is to leave positions until the all-clear is given
NOTE: Any test team member can shut down/call for shut down of the test at any time. Brief these procedures before each run and do not run unless everyone understands the emergency procedures

1. Determine that the test run must be stopped while in progress for an off-nominal reason. Depending on location, use the following procedures to indicate the test shut down
    - Inside the Control Room (Safety Controller or Electro Pneumatic Valve Operator)
        - 1 Use the electro-pneumatic valve to stop the run
        - 2 Safety Controller uses the "stop run" hand signal to indicate to the Parking Lot Relay to stop the run

- 3 Parking Lot Relay uses the "stop run" hand signal to indicate to the Manual Valve Operator to stop the run
- 4 Manual Valve Operator closes the manual valve and indicates success to the Parking Lot Relay
- 5 Parking Lot Relay indicates success to Safety Controller

- At the Manual Valve
  - 1. Manual Valve Operator closes the Manual Valve to stop the run
  - 2. Manual Valve Operator uses the "stop run" hand signal to indicate to the Parking Lot Relay to stop the run
  - 3. Parking Lot Relay uses the "stop run" hand signal to indicate to the Safety Controller to stop the run
  - 4. Safety Controller indicates to the electro-pneumatic valve operator to use the electro-pneumatic valve controller to close the electro-pneumatic valve and indicates success to the Parking Lot Relay
  - 5. Parking Lot Relay indicates success to Manual Valve Operator
- Support Personnel
  - 1. Personnel use the "stop run" hand signal to indicate to the Parking Lot Relay to stop the run
  - 2. Parking Lot Relay uses the "stop run" hand signal to indicate to the Manual Valve Operator to stop the run
  - 3. Manual Valve Operator closes the manual valve and indicates success to the Parking Lot Relay
  - 4. Parking Lot Relay uses the "stop run" hand signal to indicate to Safety Controller to stop the run
  - 5. Safety Controller indicates to the electro-pneumatic valve operator to use the electro-pneumatic valve controller to close the electro-pneumatic valve and indicates success to the Parking Lot Relay
  - 6. Parking Lot Relay indicates success to Manual Valve Operator

2. Safety Controller monitors pressure readings in test chamber and verifies pressures go to 0 psig

3. Safety Controller removes ear protection to listen for any indication of continued off-nominal behavior

4. Assuming pressure readings go to 0 psig and no off-nominal sounds are heard, Safety Controller indicates "All Clear" to Parking Lot Relay

5. Parking Lot Relay indicates "All Clear" to Manual Valve Operator and Supporting Personnel
   NOTE: If Pressure does not approach zero, or off nominal indications continue, Safety Controller should approach the window and indicate to Parking Lot Relay that they need to talk

C.3.4 Cold Flow Blank Run Procedures

WARNING: No one is to leave positions until the all-clear is given.

1. Ensure that the manual valve for the SSWT is closed.

2. Ensure that the Electro-Pneumatic valve for the SSWT is closed.
   WARNING: The Electro-Pneumatic valve can get stuck slightly open. To fix, perform step 34 and then slowly cycle the power switch in step 39, until the valve closes completely.

3. Ensure plenum pressure valve is open

4. Ramjet should be in the Blank Setup
   – See section C.2.3

5. Place ping pong ball on top of the pressure relief valve
   – Movement of the ping pong ball indicates a burst pressure disc and an over-pressure emergency

6. Ensure that the latches on the front brace of the ramjet and the SSWT are secured.

7. Place warning signs in the parking lot and at the top of stairs.
   – If applicable have someone near the signs to help people past the test setup.

8. Distribute protective eye wear and earmuffs

9. If instrumentation data is required for this run, complete the following steps.
   – Turn on the computer and open up LabView.

- Turn the 10v power supply to on.
- Start up the DAQ and allow LabView to register.

10. Ensure the area behind the Ramjet is clear.
11. Ensure all personnel are inside the control room or at their posts away from the test.
12. Ensure protective eye wear and earmuffs are worn form this point on.
13. Alert Team Members of the beginning of the test.
    - Receive confirmation from:
    - 1. Manual Valve Operator
    - 2. Electro-pneumatic valve Operator
    - 3. Parking Lot Sign Person
    - 4. Stairs Sign Person
14. Safety Controller checks completion of steps 1 – 25.
15. Review procedure sequence, hand signals, and personnel duties.
    - Ensure a charged cell phone is available
    - University Police Department #(805)756-2281
    - San Luis Obispo Police Department #911.
16. Safety Controller allows continuation of test.
17. Safety Controller opens the Electro-pneumatic airline located in the control room.
18. *If applicable* – Begin collecting Data on LabView.
19. Alert the Manual Valve Operator to open the SSWT valve.
    - Wait for confirmation.
20. Alert the Electro-pneumatic Valve Operator to flip switch from OFF to ON.
21. Start Timer.
    - Electro Pneumatic Operator is in control of keeping test time.
22. Let run until plenum pressure begins to drop rapidly, 10 seconds.
    - If test requires longer run, continue for required time frame.
    - Alert Safety Controller of time.

23. Alert the Electro-pneumatic Valve Operator to flip switch from ON to OFF.
    – Wait for confirmation.

    CAUTION Electro-pneumatic Valve has a delay when closing, confirm only that the switch was thrown before continuing.

24. Alert the Manual Valve Operator to close the SSWT valve.
    – Wait for confirmation.

25. Give "All Clear" Signal

26. Remove and collect protective eye wear and earmuffs.

27. *If Applicable* - Stop collecting data on LabView.
    – Turn off LabView
    – Turn off the Power Supply
    – Disconnect the DAQ
    – Turn off Computer

28. Remove signs from parking lot and stairs.

29. Remove the flame chute from behind the Ramjet

30. Tear down the Ramjet
    – See Section C.2.8.

C.3.5 Cold Flow Inlet Run Procedures

WARNING: No one is to leave positions until the all-clear is given.

1. Ensure that the manual valve for the SSWT is closed.

2. Ensure that the Electro-Pneumatic valve for the SSWT is closed.
   WARNING: The Electro-Pneumatic valve can get stuck slightly open. To fix, perform step 34 and then slowly cycle the power switch in step 39, until the valve closes completely.

3. Ensure plenum pressure valve is open

4. Ramjet should be in the Inlet Setup
   – See section C.2.4

5. Place ping pong ball on top of the pressure relief valve
   – Movement of the ping pong ball indicates a burst pressure disc and an over-pressure emergency
6. Ensure that the latches on the front brace of the ramjet and the SSWT are secured.
7. Place warning signs in the parking lot and at the top of stairs.
   – If applicable have someone near the signs to help people past the test setup.
8. Distribute protective eye wear and earmuffs
9. If instrumentation data is required for this run, complete the following steps.
   – Turn on the computer and open up LabView.
   – Turn the 10v power supply to on.
   – Start up the DAQ and allow LabView to register.
10. Ensure the area behind the Ramjet is clear.
11. Ensure all personnel are inside the control room or at their posts away from the test.
12. Ensure protective eye wear and earmuffs are worn form this point on.
13. Alert Team Members of the beginning of the test.
   – Receive confirmation from:
   – 1. Manual Valve Operator
   – 2. Electro-pneumatic valve Operator
   – 3. Parking Lot Sign Person
   – 4. Stairs Sign Person
14. Safety Controller checks completion of steps 1 – 13.
15. Review procedure sequence, hand signals, and personnel duties.
   – Ensure a charged cell phone is available
   – University Police Department #(805)756-2281
   – San Luis Obispo Police Department #911.
16. Safety Controller allows continuation of test.
17. Safety Controller opens the Electro-pneumatic airline located in the control room.

18. *If applicable* – Begin collecting Data on LabView.

19. Alert the Manual Valve Operator to open the SSWT valve.
    – Wait for confirmation.

20. Alert the Electro-pneumatic Valve Operator to flip switch from OFF to ON.

21. Start Timer.
    – Electro Pneumatic Operator is in control of keeping test time.

22. Let run until plenum pressure begins to drop rapidly, 10 seconds.
    – If test requires longer run, continue for required time frame.
    – Alert Safety Controller of time.

23. Alert the Electro-pneumatic Valve Operator to flip switch from ON to OFF.
    – Wait for confirmation.
    CAUTION Electro-pneumatic Valve has a delay when closing, confirm only that the switch was thrown before continuing.

24. Alert the Manual Valve Operator to close the SSWT valve.
    – Wait for confirmation.

25. Give “All Clear” Signal

26. Remove and collect protective eye wear and earmuffs.

27. *If Applicable* - Stop collecting data on LabView.
    – Turn off LabView
    – Turn off the Power Supply
    – Disconnect the DAQ
    – Turn off Computer

28. Remove signs from parking lot and stairs.

29. Remove the flame chute from behind the Ramjet

30. Tear down the Ramjet
    – See Section C.2.9.

C.3.6 Cold Flow Inlet and Nozzle Run Procedures

WARNING: No one is to leave positions until the all-clear is given.

1. Ensure that the manual valve for the SSWT is closed.
2. Ensure that the Electro-Pneumatic valve for the SSWT is closed.

   WARNING: The Electro-Pneumatic valve can get stuck slightly open. To fix, perform step 34 and then slowly cycle the power switch in step 39, until the valve closes completely.
3. Ensure plenum pressure valve is open
4. Ramjet should be in the Inlet and Nozzle Setup

   – See section C.2.5
5. Place ping pong ball on top of the pressure relief valve

   – Movement of the ping pong ball indicates a burst pressure disc and an over-pressure emergency
6. Ensure that the latches on the front brace of the ramjet and the SSWT are secured.
7. Place warning signs in the parking lot and at the top of stairs.

   – If applicable have someone near the signs to help people past the test setup.
8. Distribute protective eye wear and earmuffs
9. If instrumentation data is required for this run, complete the following steps.

   – Turn on the computer and open up LabView.

   – Turn the 10v power supply to on.

   – Start up the DAQ and allow LabView to register.
10. Ensure the area behind the Ramjet is clear.
11. Ensure all personnel are inside the control room or at their posts away from the test.
12. Ensure protective eye wear and earmuffs are worn form this point on.
13. Alert Team Members of the beginning of the test.

    – Receive confirmation from:

- 1. Manual Valve Operator
- 2. Electro-pneumatic valve Operator
- 3. Parking Lot Sign Person
- 4. Stairs Sign Person

14. Safety Controller checks completion of steps 1 – 13.
15. Review procedure sequence, hand signals, and personnel duties.
    - Ensure a charged cell phone is available
    - University Police Department #(805)756-2281
    - San Luis Obispo Police Department #911.
16. Safety Controller allows continuation of test.
17. Safety Controller opens the Electro-pneumatic airline located in the control room.
18. *If applicable* – Begin collecting Data on LabView.
19. Alert the Manual Valve Operator to open the SSWT valve.
    - Wait for confirmation.
20. Alert the Electro-pneumatic Valve Operator to flip switch from OFF to ON.
21. Start Timer.
    - Electro Pneumatic Operator is in control of keeping test time.
22. Let run until plenum pressure begins to drop rapidly, 10 seconds.
    - If test requires longer run, continue for required time frame.
    - Alert Safety Controller of time.
23. Alert the Electro-pneumatic Valve Operator to flip switch from ON to OFF.
    - Wait for confirmation.

    CAUTION Electro-pneumatic Valve has a delay when closing, confirm only that the switch was thrown before continuing.
24. Alert the Manual Valve Operator to close the SSWT valve.
    - Wait for confirmation.
25. Give “All Clear” Signal

26. Remove and collect protective eye wear and earmuffs.

27. *If Applicable* - Stop collecting data on LabView.
    – Turn off LabView
    – Turn off the Power Supply
    – Disconnect the DAQ
    – Turn off Computer

28. Remove signs from parking lot and stairs.

29. Remove the flame chute from behind the Ramjet

30. Tear down the Ramjet
    – See Section C.2.10.

C.3.7 Cold Flow Full Setup Run Procedures

WARNING: No one is to leave positions until the all-clear is given.

1. Ensure that the manual valve for the SSWT is closed.

2. Ensure that the Electro-Pneumatic valve for the SSWT is closed.
   WARNING: The Electro-Pneumatic valve can get stuck slightly open. To fix, perform step 34 and then slowly cycle the power switch in step 39, until the valve closes completely.

3. Ensure plenum pressure valve is open

4. Ramjet should be in the full – cold Setup
   – See section C.2.6

5. Place ping pong ball on top of the pressure relief valve
   – Movement of the ping pong ball indicates a burst pressure disc and an over-pressure emergency

6. Ensure that the latches on the front brace of the ramjet and the SSWT are secured.

7. Place warning signs in the parking lot and at the top of stairs.
   – If applicable have someone near the signs to help people past the test setup.

8. Distribute protective eye wear and earmuffs

9. If instrumentation data is required for this run, complete the following steps.
   - Turn on the computer and open up LabView.
   - Turn the 10v power supply to on.
   - Start up the DAQ and allow LabView to register.
10. Ensure the area behind the Ramjet is clear.
11. Ensure all personnel are inside the control room or at their posts away from the test.
12. Ensure protective eye wear and earmuffs are worn form this point on.
13. Alert Team Members of the beginning of the test.
    - Receive confirmation from:
    - 1. Manual Valve Operator
    - 2. Electro-pneumatic valve Operator
    - 3. Parking Lot Sign Person
    - 4. Stairs Sign Person
14. Safety Controller checks completion of steps 1 – 13.
15. Review procedure sequence, hand signals, and personnel duties.
    - Ensure a charged cell phone is available
    - University Police Department #(805)756-2281
    - San Luis Obispo Police Department #911.
16. Safety Controller allows continuation of test.
17. Safety Controller opens the Electro-pneumatic airline located in the control room.
18. *If applicable* – Begin collecting Data on LabView.
19. Alert the Manual Valve Operator to open the SSWT valve.
    - Wait for confirmation.
20. Alert the Electro-pneumatic Valve Operator to flip switch from OFF to ON.
21. Start Timer.
    - Electro Pneumatic Operator is in control of keeping test time.

22. Let run until plenum pressure begins to drop rapidly, 10 seconds.
    - If test requires longer run, continue for required time frame.
    - Alert Safety Controller of time.
23. Alert the Electro-pneumatic Valve Operator to flip switch from ON to OFF.
    - Wait for confirmation.

    CAUTION Electro-pneumatic Valve has a delay when closing, confirm only that the switch was thrown before continuing.
24. Alert the Manual Valve Operator to close the SSWT valve.
    - Wait for confirmation.
25. Give "All Clear" Signal
26. Remove and collect protective eye wear and earmuffs.
27. *If Applicable* - Stop collecting data on LabView.
    - Turn off LabView
    - Turn off the Power Supply
    - Disconnect the DAQ
    - Turn off Computer
28. Remove signs from parking lot and stairs.
29. Remove the flame chute from behind the Ramjet
30. Tear down the Ramjet
    - See Section C.2.11.

C.4 Running the Ramjet – Hot Fire Run (Untested)

Warning: Jet A is flammable; avoid heat, sparks, and flames, for more information see Apendix D.

IN CASE OF EMERGENCY:

University Police Department #805756-2281

San Luis Obispo Police Department #911

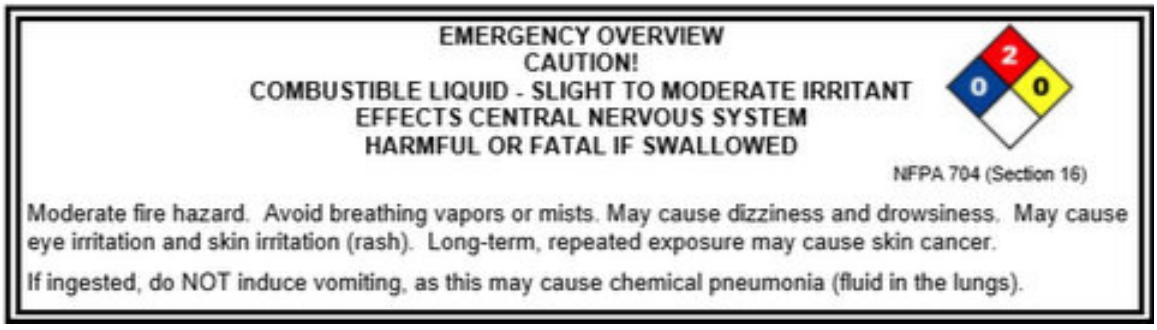

WARNING: No one is to leave positions until the all-clear is given

CAUTION – Ensure that all power sources are turned off

C.4.1 Job Descriptions

1. **Safety Controller** – Inside the control room with door shut during test, responsible for ensuring all the steps in the procedure are done. Responsible for accurate placement of all personnel such that they are behind the protective barrier of the SSWT hard walls. Also responsible for turning on the data recording in LabView, opening the pressure valve to the Electro pneumatic valve, and starting fuel and ignition systems. Will remain in the control room until all clear is given.

2. **Manual Valve Operator** – Opens the manual valve and then stands behind the Air tank in sight of the Parking Lot Signal person. Will not move until given the close valve signal, then will return position behind the Air tank until all clear is given.

3. **Parking Lot Relay** – Stands on the corner of the building, alerts the Manual valve operator when to open or close the valve, alerts the Safety Controller when the valve is open or closed. Also must alert people of test who approach in their vehicles. Will not move until all clear is given.

4. **Stairs Signal Person** – stands on top of the stairs in view of the Parking Lot Signal Person to warn people of the upcoming test. Will not move until all clear is given.

5. **Electro-pneumatic valve Operator** – Inside the control room with door shut during test, responsible for turning on and off the electro pneumatic valve. Responsible for watching the ping pong ball that indicates an over pressure emergency, and the dial gage on the plenum. Will remain in the control room until all clear is given.

C.4.2 Hand Signals

1. “Success/Confirm task completion” – thumbs-up
2. “Stop run” – slash finger across throat
3. “All clear” – both arms straight up over shoulders
4. “Open Manual Valve” – Reverse alligator arm motion
5. “Close Manual valve” – Alligator arm motion

C.4.3 Emergency Shutdown Procedures

WARNING: No one is to leave positions until the all-clear is given
NOTE: Any test team member can shut down/call for shut down of the test at any time. Brief these procedures before each run and do not run unless everyone understands the emergency procedures

1. Determine that the test run must be stopped while in progress for an off-nominal reason. Depending on location, use the following procedures to indicate the test shut down
    - Inside the Control Room (Safety Controller or Electro Pneumatic Valve Operator)
        - 1 Use the electro-pneumatic valve to stop the run
        - 2 Safety Controller uses the ”stop run” hand signal to indicate to the Parking Lot Relay to stop the run
        - 3 Parking Lot Relay uses the ”stop run” hand signal to indicate to the Manual Valve Operator to stop the run
        - 4 Manual Valve Operator closes the manual valve and indicates success to the Parking Lot Relay
        - 5 Parking Lot Relay indicates success to Safety Controller
    - At the Manual Valve
        - 1. Manual Valve Operator closes the Manual Valve to stop the run
        - 2. Manual Valve Operator uses the ”stop run” hand signal to indicate to the Parking Lot Relay to stop the run
        - 3. Parking Lot Relay uses the ”stop run” hand signal to indicate to the Safety Controller to stop the run

- 4. Safety Controller indicates to the electro-pneumatic valve operator to use the electro-pneumatic valve controller to close the electro-pneumatic valve and indicates success to the Parking Lot Relay
- 5. Parking Lot Relay indicates success to Manual Valve Operator

- Support Personnel
  - 1. Personnel use the "stop run" hand signal to indicate to the Parking Lot Relay to stop the run
  - 2. Parking Lot Relay uses the "stop run" hand signal to indicate to the Manual Valve Operator to stop the run
  - 3. Manual Valve Operator closes the manual valve and indicates success to the Parking Lot Relay
  - 4. Parking Lot Relay uses the "stop run" hand signal to indicate to Safety Controller to stop the run
  - 5. Safety Controller indicates to the electro-pneumatic valve operator to use the electro-pneumatic valve controller to close the electro-pneumatic valve and indicates success to the Parking Lot Relay
  - 6. Parking Lot Relay indicates success to Manual Valve Operator

2. Safety Controller monitors pressure readings in test chamber and verifies pressures go to 0 psig
3. Safety Controller removes ear protection to listen for any indication of continued off-nominal behavior
4. Assuming pressure readings go to 0 psig and no off-nominal sounds are heard, Safety Controller indicates "All Clear" to Parking Lot Relay
5. Parking Lot Relay indicates "All Clear" to Manual Valve Operator and Supporting Personnel NOTE: If Pressure does not approach zero, or off nominal indications continue, Safety Controller should approach the window and indicate to Parking Lot Relay that they need to talk

C.4.4 Hot Fire Run Procedures

WARNING: No one is to leave positions until the all-clear is given.

1. Ensure that the manual valve for the SSWT is closed.
2. Ensure that the Electro-Pneumatic valve for the SSWT is closed.

   WARNING: The Electro-Pneumatic valve can get stuck slightly open. To fix, perform step 34 and then slowly cycle the power switch in step 39, until the valve closes completely.
3. Ensure plenum pressure valve is open
4. Ramjet should be in the Full Setup
   – See section C.2.7
5. Place ping pong ball on top of the pressure relief valve
   – Movement of the ping pong ball indicates a burst pressure disc and an over-pressure emergency
6. Move Nitrogen bottle outside and place inside bottle stand
7. Ensure all fuel check valves are closed
8. Ensure that the latches on the front brace of the ramjet and the SSWT are secured.
9. Place warning signs in the parking lot and at the top of stairs.
   – If applicable have someone near the signs to help people past the test setup.
10. Distribute protective eye wear and earmuffs
11. If instrumentation data is required for this run, complete the following steps.
    – Turn on the computer and open up LabView.
    – Add Hot to the supplied save file name in LabView.
    – Turn the 10v power supply to on.
    – Turn the 12v power supply to on.
    – Start up the DAQ and allow LabView to register.
12. Ensure the area behind the Ramjet is clear.
13. Ensure all personnel are inside the control room or at their posts away from the test.
14. Ensure protective eye wear and earmuffs are worn form this point on.
15. Fill the large beaker with 1-liter of Jet-A

    Caution: Jet-A is flammable. Avoid ignition sources

16. Open check valve above fuel tank and pour Jet-A inside.
    - Pour slowly to avoid spills
17. Close check valve
18. Set the Nitrogen pressure regulator to 215psig
19. Ensure all switches on the control box are in the off position.
20. Connect the control box to the test
    - The power plug is inserted into a wall socket
    - The quick plug is connected to the ignition and fuel system wiring harness
    - The blue wire is connected to the 12 volt power supply positive terminal
    - The white wire is connected to the 12 volt power supply negative terminal
21. Ensure the fuel system is connected to the fuel injector
22. Ensure ignition system is connected
    - All colors and numbers on the test stand match the ignition and fuel system wiring harness
23. Open all check valves in the fuel system
    - Do not open the valve for filling the fuel tank or the purge valve
    - Should be opened in order, starting at the nitrogen tank
24. Alert Team Members of the beginning of the test.
    - Receive confirmation from:
    - 1. Manual Valve Operator
    - 2. Electro-pneumatic valve Operator
    - 3. Parking Lot Sign Person
    - 4. Stairs Sign Person
25. Spray down the hill behind the ramjet with water.
26. Safety Controller checks completion of steps 1 – 25.
27. Review procedure sequence, hand signals, and personnel duties.
    - Ensure a charged cell phone is available
    - University Police Department #(805)756-2281
    - San Luis Obispo Police Department #911

28. Place fire extinguisher by door of control room.

29. Safety Controller allows continuation of test.

30. Safety Controller opens the Electro-pneumatic airline located in the control room.

31. *If applicable* – Begin collecting Data on LabView.

32. Alert the Manual Valve Operator to open the SSWT valve.
    – Wait for confirmation.

33. Flip the switch labeled METH to ON

34. Flip the "MAIN" switch on the control box to ON

35. Alert the Electro-pneumatic Valve Operator to flip switch from OFF to ON.

36. On the control box, turn the "FIRE" switch to ON
    – Press and hold ignite button

37. Start Timer.
    – Electro Pneumatic Operator is in control of keeping test time.

38. Let run until plenum pressure begins to drop rapidly, 10 seconds.
    – If test requires longer run, continue for required time frame.
    – Alert Safety Controller of time.

39. Release ignition button.

40. Turn all switches off on the control box.

41. Alert the Electro-pneumatic Valve Operator to flip switch from ON to OFF.
    – Wait for confirmation.
    CAUTION – Electro-pneumatic Valve has a delay when closing, confirm only that the switch was thrown before continuing.

42. Alert the Manual Valve Operator to close the SSWT valve.
    – Wait for confirmation.

43. Remove and collect protective eye wear and earmuffs.

44. *If Applicable* – Stop collecting data on LabView.
    - Turn off LabView
    - Turn off the Power Supply
    - Disconnect the DAQ
    - Turn off Computer
45. Remove signs from parking lot and stairs.
46. Remove the flame chute from behind the Ramjet
47. Tear down the Ramjet
    - See Section C.2.12

Appendix D

Jet-A Fuel Specifications

EMERGENCY OVERVIEW
CAUTION!
COMBUSTIBLE LIQUID - SLIGHT TO MODERATE IRRITANT
EFFECTS CENTRAL NERVOUS SYSTEM
HARMFUL OR FATAL IF SWALLOWED

NFPA 704 (Section 16)

Moderate fire hazard. Avoid breathing vapors or mists. May cause dizziness and drowsiness. May cause eye irritation and skin irritation (rash). Long-term, repeated exposure may cause skin cancer.

If ingested, do NOT induce vomiting, as this may cause chemical pneumonia (fluid in the lungs).

1. CHEMICAL PRODUCT and COMPANY INFORMATION

HOVENSA LLC
1 Estate Hope
Christiansted, VI 00820-5652

EMERGENCY TELEPHONE NUMBER (24 hrs): **CHEMTREC (800)424-9300**
COMPANY CONTACT (business hours): **(340) 692-3000**

SYNONYMS: Aviation Kerosene; Aviation Turbine Fuel Jet A; Jet A; Jet A –1; JP – 1; Military Aviation Jet Fuel JP –1

See Section 16 for abbreviations and acronyms.

2. COMPOSITION and INFORMATION ON INGREDIENTS

INGREDIENT NAME (CAS No.)	CONCENTRATION PERCENT BY WEIGHT
Kerosene (8008-20-6)	100
Naphthalene (91-20-3)	Typically 0.04

A complex combination of hydrocarbons including naphthenes, paraffins, and aromatics.

3. HAZARDS IDENTIFICATION

EYES
Contact with eyes may cause mild to moderate irritation.

SKIN
May cause skin irritation with prolonged or repeated contact. Practically non-toxic if absorbed following acute (single) exposure. Liquid may be absorbed through the skin in toxic amounts if large areas of skin are repeatedly exposed.

INGESTION

The major health threat of ingestion occurs from the danger of aspiration (breathing) of liquid drops into the lungs, particularly from vomiting. Aspiration may result in chemical pneumonia (fluid in the lungs), severe lung damage, respiratory failure and even death.

Ingestion may cause gastrointestinal disturbances, including irritation, nausea, vomiting and diarrhea, and central nervous system (brain) effects similar to alcohol intoxication. In severe cases, tremors, convulsions, loss of consciousness, coma, respiratory arrest, and death may occur.

INHALATION
Excessive exposure may cause irritation to the nose, throat, lungs and respiratory tract. Central nervous system (brain) effects may include headache, dizziness, loss of balance and coordination, unconsciousness, coma, respiratory failure, and death.

HOVENSA
MATERIAL SAFETY DATA SHEET
Jet Fuel A / A-1 **MSDS No. 1787**

WARNING: the burning of any hydrocarbon as a fuel in an area without adequate ventilation may result in hazardous levels of combustion products, including carbon monoxide, and inadequate oxygen levels, which may cause unconsciousness, suffocation, and death.

CHRONIC EFFECTS and CARCINOGENICITY
Similar products produced skin cancer and systemic toxicity in laboratory animals following repeated applications. The significance of these results to human exposures has not been determined - see Section 11 Toxicological Information.

MEDICAL CONDITIONS AGGRAVATED BY EXPOSURE
Irritation from skin exposure may aggravate existing open wounds, skin disorders, and dermatitis (rash).

4. FIRST AID MEASURES

EYES
In case of contact with eyes, immediately flush with clean, low-pressure water for at least 15 min. Hold eyelids open to ensure adequate flushing. Seek medical attention.

SKIN
Remove contaminated clothing. Wash contaminated areas thoroughly with soap and water or waterless hand cleanser. Obtain medical attention if irritation or redness develops. Thermal burns require immediate medical attention depending on the severity and the area of the body burned.

INGESTION
DO NOT INDUCE VOMITING. Do not give liquids. Obtain immediate medical attention. If spontaneous vomiting occurs, lean victim forward to reduce the risk of aspiration. Monitor for breathing difficulties. Small amounts of material which enter the mouth should be rinsed out until the taste is dissipated.

INHALATION
Remove person to fresh air. If person is not breathing provide artificial respiration. If necessary, provide additional oxygen once breathing is restored if trained to do so. Seek medical attention immediately.

5. FIRE FIGHTING MEASURES

FLAMMABLE PROPERTIES:

FLASH POINT:	> 100 °F (38 °C) TCC
AUTOIGNITION POINT:	410 °F (210 °C)
OSHA/NFPA FLAMMABILITY CLASS:	2 (COMBUSTIBLE) (see Section 14 for transportation classification)
LOWER EXPLOSIVE LIMIT (%):	0.7
UPPER EXPLOSIVE LIMIT (%):	5.0

FIRE AND EXPLOSION HAZARDS
Vapors may be ignited rapidly when exposed to heat, spark, open flame or other source of ignition. When mixed with air and exposed to an ignition source, flammable vapors can burn in the open or explode in confined spaces. Being heavier than air, vapors may travel long distances to an ignition source and flash back. Runoff to sewer may cause fire or explosion hazard.

EXTINGUISHING MEDIA
SMALL FIRES: Any extinguisher suitable for Class B fires, dry chemical, CO2, water spray, fire fighting foam, or Halon.

LARGE FIRES: Water spray, fog or fire fighting foam. Water may be ineffective for fighting the fire, but may be used to cool fire-exposed containers.

FIRE FIGHTING INSTRUCTIONS
Small fires in the incipient (beginning) stage may typically be extinguished using handheld portable fire extinguishers and other fire fighting equipment.

HOVENSA
MATERIAL SAFETY DATA SHEET
Jet Fuel A / A-1 **MSDS No. 1787**

Firefighting activities that may result in potential exposure to high heat, smoke or toxic by-products of combustion should require NIOSH/MSHA- approved pressure-demand self-contained breathing apparatus with full facepiece and full protective clothing.

Isolate area around container involved in fire. Cool tanks, shells, and containers exposed to fire and excessive heat with water. For massive fires the use of unmanned hose holders or monitor nozzles may be advantageous to further minimize personnel exposure. Major fires may require withdrawal, allowing the tank to burn. Large storage tank fires typically require specially trained personnel and equipment to extinguish the fire, often including the need for properly applied fire fighting foam.

See Section 16 for the NFPA 704 Hazard Rating.

6. ACCIDENTAL RELEASE MEASURES

ACTIVATE FACILITY'S SPILL CONTINGENCY OR EMERGENCY RESPONSE PLAN.

Evacuate nonessential personnel and remove or secure all ignition sources. Consider wind direction; stay upwind and uphill, if possible. Evaluate the direction of product travel, diking, sewers, etc. to confirm spill areas. Spills may infiltrate subsurface soil and groundwater; professional assistance may be necessary to determine the extent of subsurface impact.

Carefully contain and stop the source of the spill, if safe to do so. Protect bodies of water by diking, absorbents, or absorbent boom, if possible. Do not flush down sewer or drainage systems, unless system is designed and permitted to handle such material. The use of fire fighting foam may be useful in certain situations to reduce vapors. The proper use of water spray may effectively disperse product vapors or the liquid itself, preventing contact with ignition sources or areas/equipment that require protection.

Take up with sand or other oil absorbing materials. Carefully shovel, scoop or sweep up into a waste container for reclamation or disposal - caution, flammable vapors may accumulate in closed containers. Response and clean-up crews must be properly trained and must utilize proper protective equipment (see Section 8).

7. HANDLING and STORAGE

HANDLING PRECAUTIONS
Handle as a combustible liquid. Keep away from heat, sparks, and open flame! Electrical equipment should be approved for classified area. Bond and ground containers during product transfer to reduce the possibility of static-initiated fire or explosion.

Special slow load procedures for "switch loading" must be followed to avoid the static ignition hazard that can exist when higher flash point material (such as fuel oil) is loaded into tanks previously containing low flash point products (such as this product) - see API Publication 2003, "Protection Against Ignitions Arising Out Of Static, Lightning and Stray Currents.

STORAGE PRECAUTIONS
Keep away from flame, sparks, excessive temperatures and open flame. Use approved vented containers. Keep containers closed and clearly labeled. Empty product containers or vessels may contain explosive vapors. Do not pressurize, cut, heat, weld or expose such containers to sources of ignition.

Store in a well-ventilated area. This storage area should comply with NFPA 30 "Flammable and Combustible Liquid Code". Avoid storage near incompatible materials. The cleaning of tanks previously containing this product should follow API Recommended Practice (RP) 2013 "Cleaning Mobile Tanks In Flammable and Combustible Liquid Service" and API RP 2015 "Cleaning Petroleum Storage Tanks".

WORK/HYGIENIC PRACTICES
Emergency eye wash capability should be available in the near proximity to operations presenting a potential splash exposure. Use good personal hygiene practices. Avoid repeated and/or prolonged skin exposure. Wash hands before eating, drinking, smoking, or using toilet facilities. Do not use as a cleaning solvent on the skin. Do not use gasoline or solvents (naphtha, kerosene, etc.) for washing this

HOVENSA
MATERIAL SAFETY DATA SHEET
Jet Fuel A / A-1 **MSDS No. 1787**

product from exposed skin areas. Waterless hand cleaners are effective. Promptly remove contaminated clothing and launder before reuse. Use care when laundering to prevent the formation of flammable vapors which could ignite via washer or dryer. Consider the need to discard contaminated leather shoes and gloves.

8. EXPOSURE CONTROLS and PERSONAL PROTECTION

EXPOSURE LIMITS

		Exposure Limits	
Components (CAS No.)	Source	TWA/STEL	Note
Kerosene (8008-20-6)	OSHA	5 mg/m³ as mineral oil mist	
	ACGIH	100 mg/m³ TWA	A3
Naphthalene (91-20-3)	OSHA	10 ppm	
	ACGIH	10 ppm TWA/ 15 ppm STEL	A4

ENGINEERING CONTROLS
Use adequate ventilation to keep vapor concentrations of this product below occupational exposure and flammability limits, particularly in confined spaces.

EYE/FACE PROTECTION
Safety glasses or goggles are recommended where there is a possibility of splashing or spraying

SKIN PROTECTION
Gloves constructed of nitrile, neoprene, or PVC are recommended. Chemical protective clothing such as of E.I. DuPont Tyvek QC®, Saranex®, TyChem® or equivalent recommended based on degree of exposure. Note: The resistance of specific material may vary from product to product as well as with degree of exposure. Consult manufacturer specifications for further information

RESPIRATORY PROTECTION
A NIOSH/MSHA-approved air-purifying respirator with organic vapor cartridges or canister may be permissible under certain circumstances where airborne concentrations are or may be expected to exceed exposure limits or for odor or irritation. Protection provided by air-purifying respirators is limited. Refer to OSHA 29 CFR 1910.134, ANSI Z88.2-1992, NIOSH Respirator Decision Logic, and the manufacturer for additional guidance on respiratory protection selection.

Use a positive pressure, air-supplied respirator if there is a potential for uncontrolled release, exposure levels are not known, in oxygen-deficient atmospheres, or any other circumstance where an air-purifying respirator may not provide adequate protection.

WORK/HYGIENIC PRACTICES
Emergency eye wash capability should be available in the near proximity to operations presenting a potential splash exposure. Use good personal hygiene practices. Avoid repeated and/or prolonged skin exposure. Wash hands before eating, drinking, smoking, or using toilet facilities. Do not use as a cleaning solvent on the skin. Do not use gasoline or solvents (naphtha, kerosene, etc.) for washing this product from exposed skin areas. Waterless hand cleaners are effective. Promptly remove contaminated clothing and launder before reuse. Use care when laundering to prevent the formation of flammable vapors which could ignite via washer or dryer. Consider the need to discard contaminated leather shoes and gloves.

9. PHYSICAL and CHEMICAL PROPERTIES

APPEARANCE
Pale yellow to water-white liquid

ODOR
Characteristic petroleum distillate odor

BASIC PHYSICAL PROPERTIES

BOILING RANGE:	280 to 572 °F (140 to 300 °C)
VAPOR PRESSURE:	0.029 psia @ 100 °F (38 °C)
VAPOR DENSITY (air = 1):	AP 4.5
SPECIFIC GRAVITY (H_2O = 1):	0.75 - 0.80
PERCENT VOLATILES:	100 %
EVAPORATION RATE:	Slow; varies with conditions
SOLUBILITY (H_2O):	Negligible

10. STABILITY and REACTIVITY

STABILITY: Stable. Hazardous polymerization will not occur.

CONDITIONS TO AVOID and INCOMPATIBLE MATERIALS

Avoid high temperatures, open flames, sparks, welding, smoking and other ignition sources. Keep away from strong oxidizers such as nitric and sulfuric acids.

HAZARDOUS DECOMPOSITION PRODUCTS:

Carbon monoxide, carbon dioxide and non-combusted hydrocarbons (smoke).

11. TOXICOLOGICAL PROPERTIES

CHRONIC EFFECTS AND CARCINOGENICITY

Carcinogenicity: OSHA: NO IARC: NO NTP: NO ACGIH: 1997 NOIC: A3
Dermal carcinogenicity: positive (mice)

ACUTE TOXICITY

Acute dermal LD50 (rabbits): > 5 g/kg
Acute oral LD50 (rats): > 25 g/kg
Primary dermal irritation: mildly irritating (rabbits)
Primary eye irritation: mildly irritating (rabbits)
Guinea pig sensitization: negative

Studies have shown that similar products produce skin cancer or skin tumors in laboratory animals following repeated applications without washing or removal. The significance of this finding to human exposure has not been determined. Other studies with active skin carcinogens have shown that washing the animal's skin with soap and water between applications reduced tumor formation.

12. ECOLOGICAL INFORMATION

Keep out of sewers, drainage and waterways. Report spills and releases, as applicable, under Federal and State regulations.

13. DISPOSAL CONSIDERATIONS

Consult federal, state and local waste regulations to determine appropriate disposal options.

14. TRANSPORTATION INFORMATION

DOT PROPER SHIPPING NAME:	Fuel, Aviation, Turbine Engine
DOT HAZARD CLASS and PACKING GROUP:	3, PG II
DOT IDENTIFICATION NUMBER:	UN 1863
DOT SHIPPING LABEL:	FLAMMABLE LIQUID

PLACARD:

May be reclassified for transportation as a COMBUSTIBLE LIQUID under conditions of DOT 49 CFR 173.120(b)(2).

HOVENSA
MATERIAL SAFETY DATA SHEET
Jet Fuel A / A-1 **MSDS No. 1787**

15. REGULATORY INFORMATION

U.S. FEDERAL, STATE, and LOCAL REGULATORY INFORMATION

This product and its constituents listed herein are on the EPA TSCA Inventory. Any spill or uncontrolled release of this product, including any substantial threat of release, may be subject to federal, state and/or local reporting requirements. This product and/or its constituents may also be subject to other regulations at the state and/or local level. Consult those regulations applicable to your facility/operation.

CLEAN WATER ACT (OIL SPILLS)

Any spill or release of this product to "navigable waters" (essentially any surface water, including certain wetlands) or adjoining shorelines sufficient to cause a visible sheen or deposit of a sludge or emulsion must be reported immediately to the National Response Center (1-800-424-8802) or, if not practical, the U.S. Coast Guard with follow-up to the National Response Center, as required by U.S. Federal Law. Also contact appropriate state and local regulatory agencies as required.

CERCLA SECTION 103 and SARA SECTION 304 (RELEASE TO THE ENVIRONMENT)

The CERCLA definition of hazardous substances contains a "petroleum exclusion" clause which exempts crude oil, refined, and unrefined petroleum products and any indigenous components of such. However, other federal reporting requirements (e.g., SARA Section 304 as well as the Clean Water Act if the spill occurs on navigable waters) may still apply.

SARA SECTION 311/312 - HAZARD CLASSES

ACUTE HEALTH	CHRONIC HEALTH	FIRE	SUDDEN RELEASE OF PRESSURE	REACTIVE
X	X	X	--	--

SARA SECTION 313 - SUPPLIER NOTIFICATION

This product may contain listed chemicals below the *de minimis* levels which therefore are not subject to the supplier notification requirements of Section 313 of the Emergency Planning and Community Right-To-Know Act (EPCRA) of 1986 and of 40 CFR 372. If you may be required to report releases of chemicals listed in 40 CFR 372.28, you may contact Hess Corporate Safety if you require additional information regarding this product.

CANADIAN REGULATORY INFORMATION (WHMIS)

Class B, Division 3 (Combustible Liquid) Class D, Division 2, Subdivision B (Toxic by other means)

CALIFORNIA PROPOSITON 65 LIST OF CHEMICALS

This product contains the following chemicals that are included on the Proposition 65 "List of Chemicals" required by the California Safe Drinking Water and Toxic Enforcement Act of 1986:

INGREDIENT NAME (CAS NUMBER)	Date Listed
Naphthalene	04/19/2002

16. OTHER INFORMATION

NFPA® HAZARD RATING	HEALTH:	0	
	FIRE:	2	
	REACTIVITY:	0	

Refer to NJPA 704 "Identification of the Fire Hazards of Materials" for further information

HMIS® HAZARD RATING	HEALTH:	1*	Slight
	FIRE:	2	Moderate
	PHYSICAL:	0	Negligible
			*Chronic

HOVENSA
MATERIAL SAFETY DATA SHEET
Jet Fuel A / A-1 **MSDS No. 1787**

SUPERSEDES MSDS DATED: 9/30/98

ABBREVIATIONS:

AP = Approximately	< = Less than	> = Greater than
N/A = Not Applicable	N/D = Not Determined	ppm = parts per million

ACRONYMS:

ACGIH	American Conference of Governmental Industrial Hygienists	NTP	National Toxicology Program
AIHA	American Industrial Hygiene Association	OPA	Oil Pollution Act of 1990
ANSI	American National Standards Institute (212)642-4900	OSHA	U.S. Occupational Safety & Health Administration
API	American Petroleum Institute (202)682-8000	PEL	Permissible Exposure Limit (OSHA)
CERCLA	Comprehensive Emergency Response, Compensation, and Liability Act	RCRA	Resource Conservation and Recovery Act
DOT	U.S. Department of Transportation [General info: (800)467-4922]	REL	Recommended Exposure Limit (NIOSH)
EPA	U.S. Environmental Protection Agency	SARA	Superfund Amendments and Reauthorization Act of 1986 Title III
HMIS	Hazardous Materials Information System	SCBA	Self-Contained Breathing Apparatus
IARC	International Agency For Research On Cancer	SPCC	Spill Prevention, Control, and Countermeasures
MSHA	Mine Safety and Health Administration	STEL	Short-Term Exposure Limit (generally 15 minutes)
NFPA	National Fire Protection Association (617)770-3000	TLV	Threshold Limit Value (ACGIH)
NIOSH	National Institute of Occupational Safety and Health	TSCA	Toxic Substances Control Act
NOIC	Notice of Intended Change (proposed change to ACGIH TLV)	TWA	Time Weighted Average (8 hr.)
		WEEL	Workplace Environmental Exposure Level (AIHA)
		WHMIS	Canadian Workplace Hazardous Materials Information System

Appendix E

Structure Study

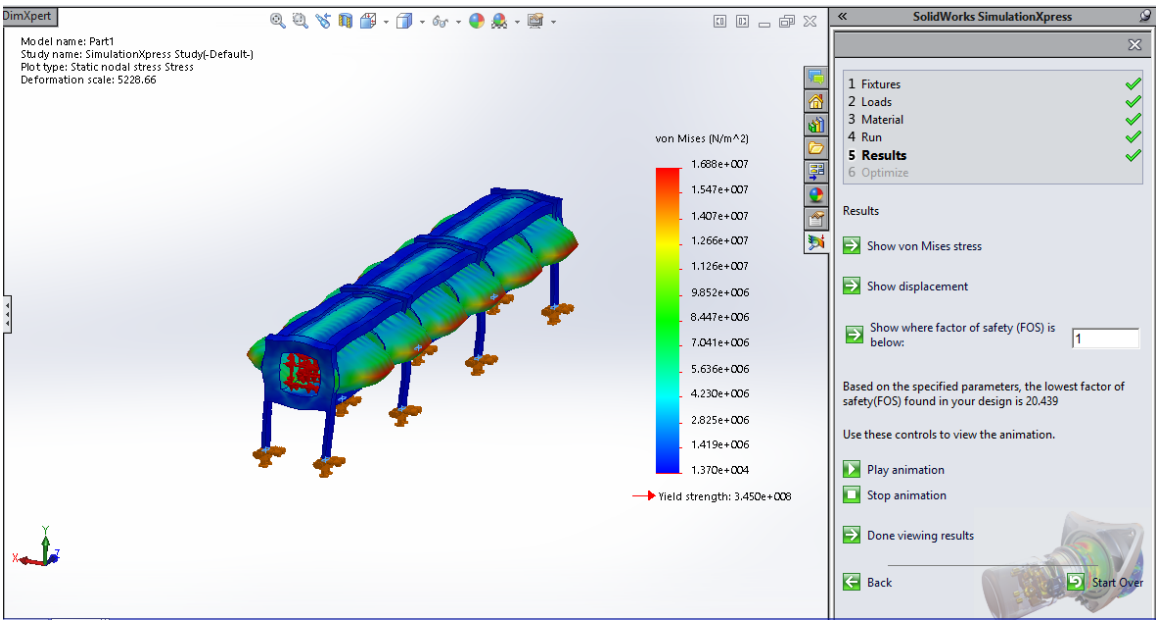

Figure E.1: Simulation Reults: Full Ramjet AL

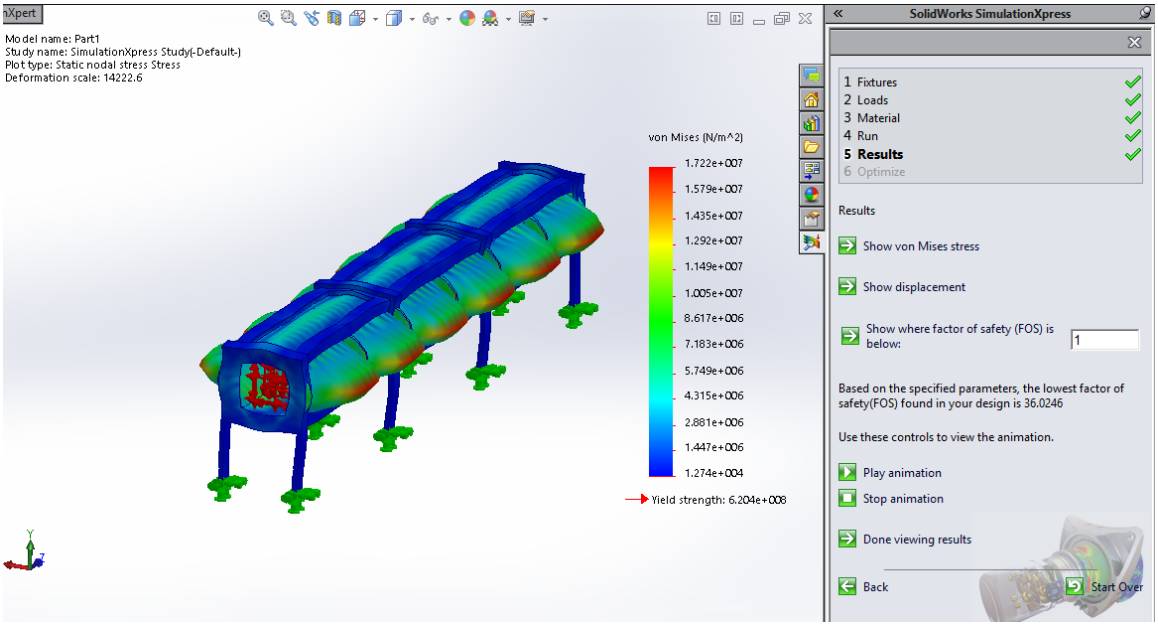

Figure E.2: Simulation Reults: Full Ramjet Alloy Steel

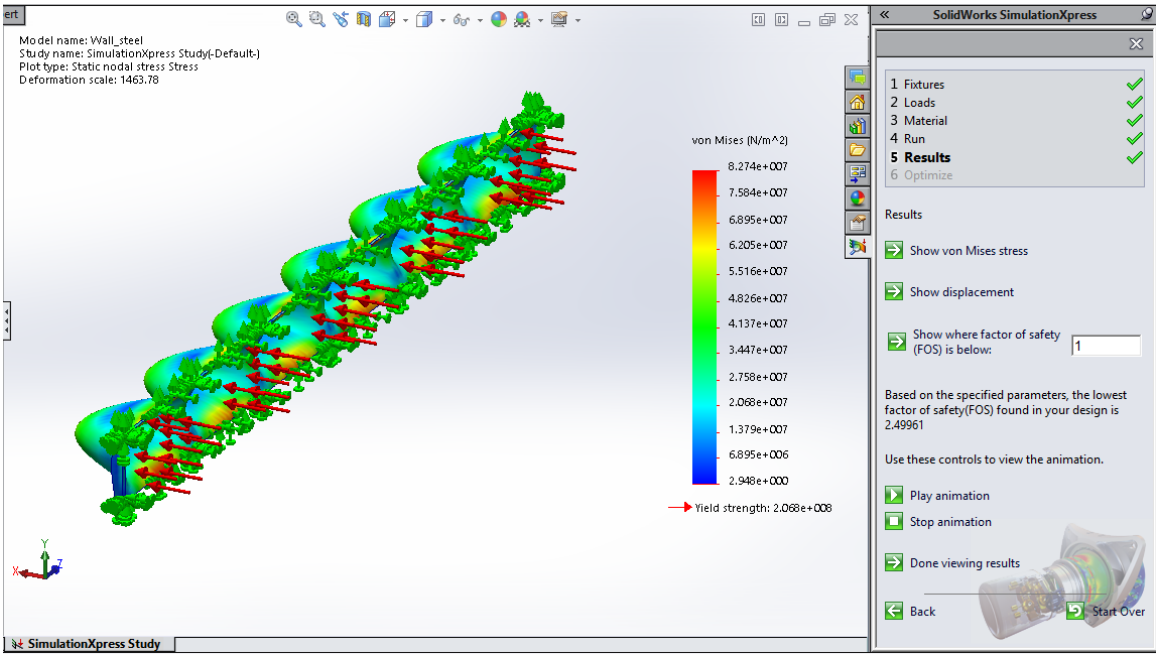

Figure E.3: Simulation Reults: 304SS Wall

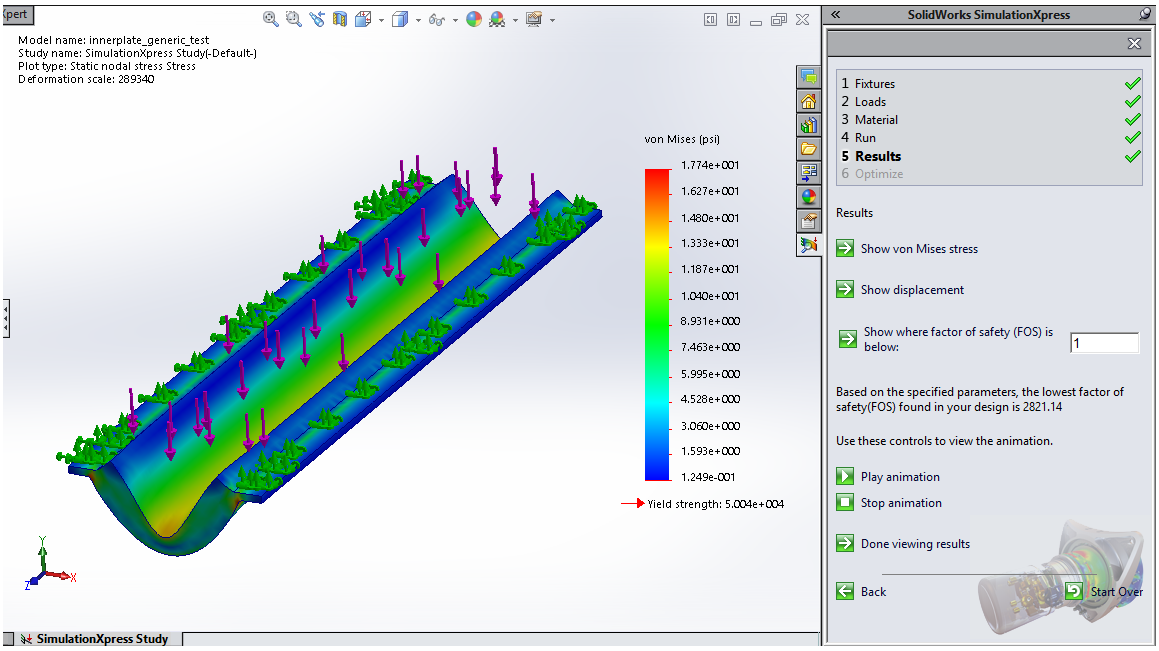

Figure E.4: Simulation Reults: Inner Plate A

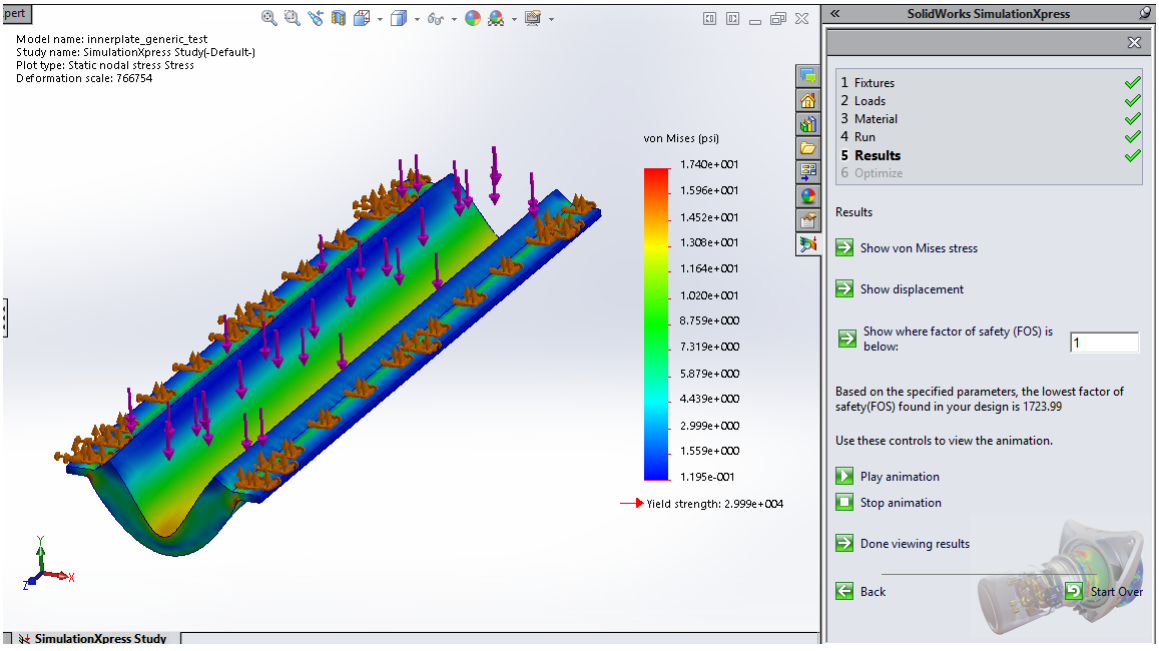

Figure E.5: Simulation Reults: Inner Plate 304SS

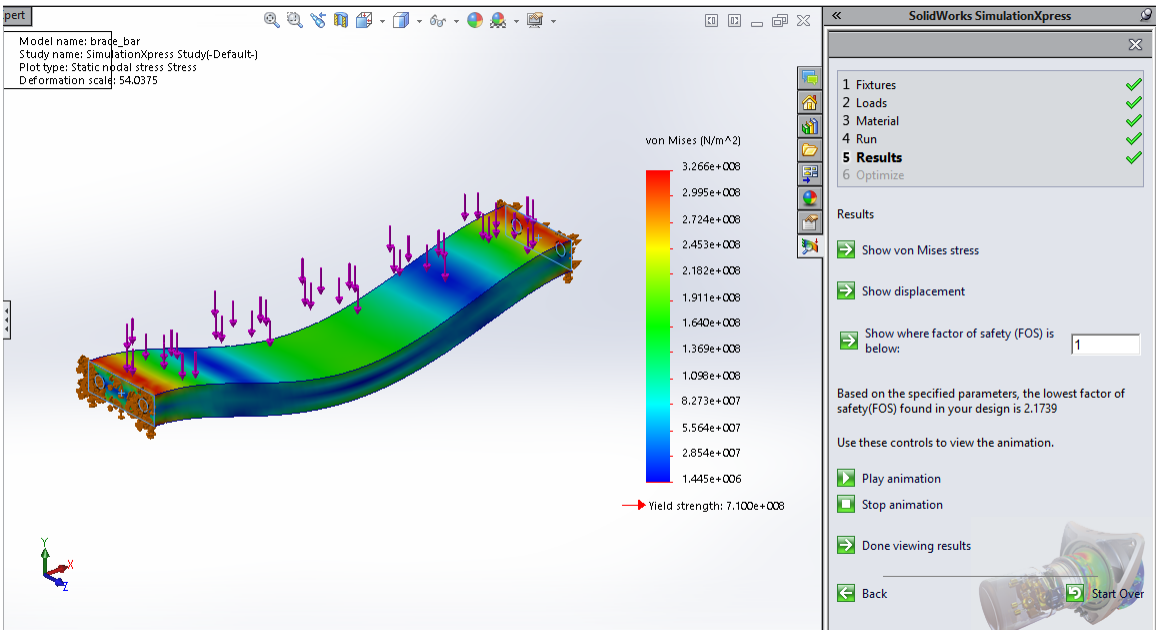

Figure E.6: Simulation Reults: Brace Cross Bar